Modulating Rice Grain Phenylalanine: Effects of Foliar Biostimulant Application

Parastoo Daryadel[1], Seyedeh Batool Hassani[1], Morteza Nasiri[2], Mohammad Reza Ghalamboran[1*]

Received: 2025-08-05 Accepted: 2025-10-08

Abstract

Phenylketonuria (PKU) requires a strict low-phenylalanine diet to prevent harmful accumulation in the body. Current dietary options, largely reliant on processed foods, are often unpalatable, expensive, and inaccessible in developing countries. This study aimed to naturally develop a rice strain with reduced phenylalanine levels, avoiding genetic modification, andoptimize biological stimulants for modulating phenylalanine biosynthesis. Field trials involved foliar application of cinnamic acid (0, 0.5, 1, and 1.5 g/L) and phenylalanine (0, 0.25, 0.5, and 1 g/L) on two local rice cultivars (Helal and Keshvari) during seed formation and filling, using a randomized complete block design with three replications. Key molecular traits measured included total protein content, phenylalanine ammonia-lyase (PAL) enzyme activity, and expression of genes involved in phenylalanine biosynthesis and catabolism (*phenylpyruvate aminotransferase*, *arogenate dehydratase*, and *PAL*). Results showed that phenylalanine application increased *PAL* gene expression, while cinnamic acid suppressed it. Although both stimulants significantly downregulated phenylalanine biosynthesis genes and reduced total protein content for both treatments, a decrease in total protein content occurred at the highest applied concentration. Notably, cinnamic acid significantly decreased phenylalanine levels in Keshvari (1 and 1.5 g/L), while increasing tyrosine and tryptophan concentrations at higher dosages. In addition, phenylalanine treatments at concentrations of 0.5 and 1 g/L led to decreased expression of the *arogenate dehydratase* gene. Moreover, the application of phenylalanine at 0.5 and 1 g/L reduced the expression of the *phenylpyruvate aminotransferase* gene in both rice cultivars studied. Cinnamic acid treatment can reduce phenylalanine in rice, offering a natural strategy for PKU-friendly diets.

Keywords Biostimulants, Phenylketonuria, Phenylalanine, Cinnamic acid, Rice

Introduction

Rice (*Oryza sativa L.*) is one of the oldest and most widely consumed cereal crops worldwide. It serves not only as a staple food for more than half of the global pop-

1- Department of Plant Sciences and Biotechnology, Faculty of Life Sciences and Biotechnology, Shahid Beheshti University, Tehran, Iran
2- Rice Research Institute of Amol, Amol, Iran
*Corresponding author email address: m_ghalamboran@sbu.ac.ir
Doi: 10.48308/PAE.2026.242182.1127

ulation but also as a key contributor to the economies of rice-producing countries. With the global population projected to reach 9.7 billion by 2050, the demand for rice and other staple crops is expected to rise substantially. To address this challenge, various strategies, including modern biotechnological approaches and breeding programs, are being developed to enhance rice productivity and sustainability (Mohidem, 2022). Beyond its nutritional and economic value, rice also holds significant cultural importance; in many societies, it symbolizes prosperity, abundance, and well-being, and is commonly featured in traditional ceremonies and rituals. Owing to its adaptability to diverse environments and its central role in food security, rice remains an indispensable crop, particularly in Asia and other developing regions (Mohidem, 2022).

From another aspect, phenylketonuria (PKU) is an autosomal recessive disorder caused by mutations in the phenylalanine hydroxylase gene, impairing the metabolism of phenylalanine (Phe) and leading to its accumulation in the liver and urine (Van Spronsen, 2021). Phe, an essential amino acid, is also a precursor for tyrosine synthesis. In PKU patients, defective hydroxylation of Phe results in low tyrosine levels, causing symptoms like developmental delays, vomiting, poor growth, hypopigmentation, and seizures. As they age, affected individuals may show a smaller head size compared to peers, hyperactivity, attention deficits, repetitive movements, and intellectual disability (Blau, 2016; Ashe, 2019; Ali, 2021). Since Phe is an essential amino acid that must be obtained from food, PKU patients require a strict diet low in Phe, under medical supervision, to prevent adverse effects. Due to the importance, complexity, and cost of producing specialized foods for PKU, their diet is particularly expensive, especially in underdeveloped countries. Currently, the main approach involves hydrolyzing food and combining it with pseudo-foods such as stimulants and vitamins to create semi-medicated products (Soltanizadeh, 2014). However, this method has major drawbacks, including high costs, reduced food quality due to hydrolysis, limited food variety, high perishability, spoilage, and the frequent use of artificial sweeteners like aspartame to improve taste (Chattopadhyay, 2014). Despite current drawbacks, alternative methods are needed to safely and naturally reduce Phe content in foods for PKU patients. A simpler, cost-effective approach that maintains food quality and avoids hydrolysis is essential. A recent study by Ghalamboran (Ghalamboran, 2023) introduced a novel strategy using chitosan nanoparticles as elicitors during rice growth. This method enhances phenylalanine ammonia lyase (PAL) activity and reduces total protein content, leading to lower Phe levels in rice grains. Previous studies on various plants, including soybean, *Lactuca sativa L*., and rice, using elicitors like phenolic acids, cinnamic acid (CA), and chitosan have reported increased PAL activity and reduced Phe and total protein content (Baziramakenga, 1997; Hussain, 2011; Cheng, 2015; Ghalamboran, 2023). The current study examined the impact of spraying biological elicitors on developing rice grains to regulate Phe metabolism. Given its high nutritional value and wide-

spread consumption, especially in Eastern countries, rice is a dietary staple for PKU patients (Huke, 1982). The Phe biosynthetic pathway in plants begins with the shikimic acid pathway, which produces chorismate, a precursor for aromatic amino acids like Phe, tyrosine, and tryptophan. These amino acids are essential for synthesizing secondary metabolites involved in plant biological functions. Enzymes in the shikimic acid pathway can be inhibited, potentially blocking chorismate production and disrupting the organism's biological processes (Zulet-González, 2020). Chorismate, the final product of the shikimic acid pathway, enters the phenylpropanoid pathway and acts as the main precursor for Phe production in both the plastid and cytosol of plant cells. In plastids, chorismate is converted to prephenate by chorismate mutase (CM1), then to arogenate via prephenate aminotransferase. Arogenate can either be converted to tyrosine by arogenate dehydrogenase (ADH) or to Phe by arogenate dehydratase (ADT); thus, *ADT* gene expression indicates Phe synthesis in plastids. In the cytosol, chorismate is also converted to prephenate by CM2. Prephenate is then transformed into phenylpyruvate by prephenate dehydratase and finally into Phe by phenylpyruvate aminotransferase (PPY-AT). Measuring *PPY-AT* gene expression helps assess the effects of foliar elicitor sprays on Phe production (Qian, 2019).

Phe levels in plants are influenced not only

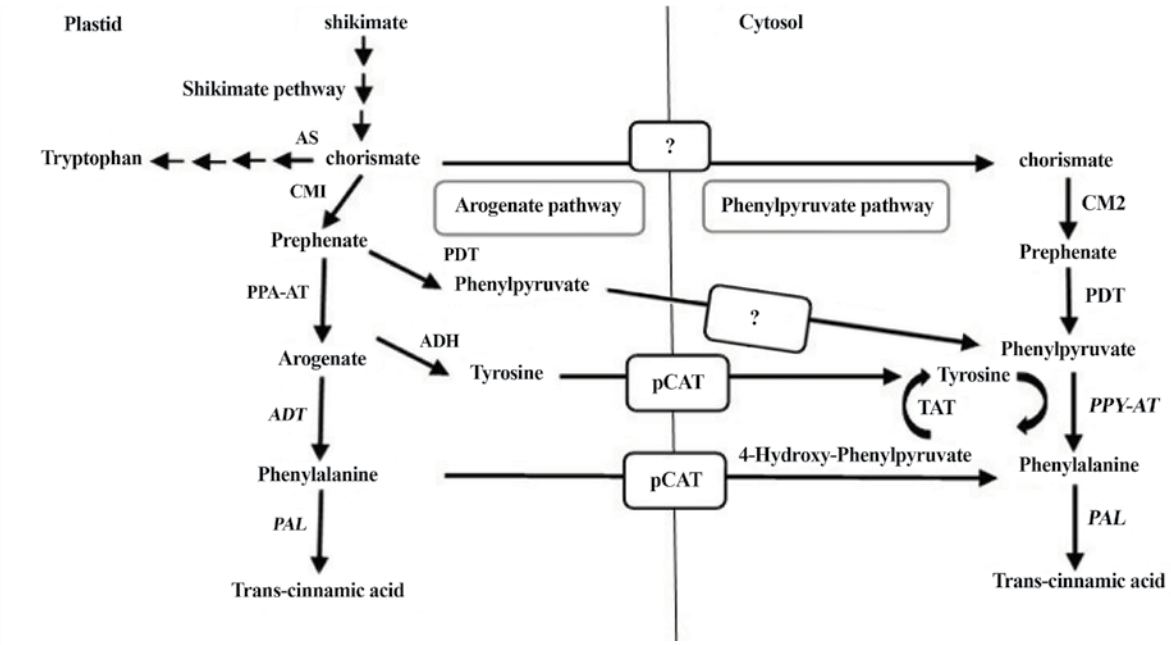

Fig. 1. Schema of Phe biosynthetic pathways in plant cells. Enzymes whose gene expression was measured are bolded. Paths and enzymes whose processes are unknown are grayed out. Abbreviations: AS - anthranilate synthesis, ADH - arogenate dehydrogenase, *ADT* - *arogenate dehydratase*, pCAT - plastidial cationic amino acid transporter, CM - chorismate mutase, PDT - prephenate dehydratase, PPA-AT - prephenate aminotransferase, *PPY-AT- phenylpyruvate aminotransferase*, TAT - tyrosine aminotransferase, *PAL - phenylalanine ammonia lyase* (Qian, 2019).

by the expression of biosynthetic genes and related enzyme activity but also by its catabolism. PAL is the key enzyme in Phe catabolism, converting Phe into CA, a precursor of various secondary metabolites such as flavonoids, isoflavonoids, tannins, anthocyanins, coumarins, lignin, and flavonols. Measuring *PAL* gene expression and enzyme activity provides insight into the extent of Phe catabolism and its conversion into secondary metabolites in plant cells. This study focused on two physiological strategies, inhibition and stimulation, to control Phe production in rice. The goal was to reduce Phe content in rice grains while maintaining other key qualities. The effectiveness of these strategies in altering gene expression and their impact on Phe biosynthesis and catabolism were investigated. Two local rice cultivars, Helal and Keshvari, were used to explore the genetic potential for Phe reduction. Foliar spraying with two biological elicitors, Phe and CA, at different concentrations was tested during four growth stages. Key variables such as total protein, PAL enzyme activity, and the gene expression of *PPY-AT*, *ADT*, and *PAL* were examined. This approach highlights the potential of science and technology in addressing medical and food-related challenges in the future.

Material and methods

Preparation of rice seeds

The rice seeds (*Oryza sativa L*., cultivars Helal and Keshvari) were obtained from Amol Rice Research Institute (Amol, Iran). The cultivars Helal and Keshvari were selected because rice cultivation in our region is traditionally based on local landraces, and it is essential to utilize the genetic potential of these regionally adapted varieties. At the same time, the methodology employed in this study is not limited to these specific cultivars; rather, it can be applied to any rice variety worldwide, making the findings broadly relevant and transferable.

Experimental design

The data presented is a composite analysis derived from three consecutive years, i.e., 2019, 2020, and 2021. The method used for planting rice in this research was a local method. The rice seeds of both cultivars were soaked in water for 3 days. Then, the germinated seeds (Figure 2A) were placed in a flooded soil bed soaked in a large amount of water and covered with nylon (Figure 2B). After 31 days, the seedlings (Figure 2C) were transplanted by hand to the rice paddies (plots) (Figure 2D). In the main field, the division was done in such a way that the cultivated land was divided into plots with an area of 5 x 6 square meters. To prevent interference between treatments, a distance of 50 cm was maintained between the plots. Each plot included 16 planting holes, in which 4 seedlings were planted. The distance between the holes was 30 cm. The water in the test plots was kept at a level of 5 cm during the plant growth period, and the soil bed was dried 10 days before rice harvesting. The project area has the coordinates of latitude 36 degrees and 28 minutes east and longitude 52 degrees and 23 minutes north, with an elevation of 29.8 meters above sea level.

Preparation of experimental treatments

Elicitors of CA and Phe were prepared using Merck brand (Germany) at various concen-

trations: 0, 0.5, 1, and 1.5 g/L for CA, and 0, 0.25, 0.5, and 1 g/L for Phe. Foliar spraying of rice spikes was done in 4 periods of rice physiological growth (spike onset, pre-flowering, flowering onset, and milky onset of grain) during sunset on the aerial parts (Figure 2D). Safety measures were taken during foliar application to avoid interference with the efficacy of different concentrations of functional elicitors. The selection of CA and Phe concentrations was guided by three considerations. First, previous studies indicated that within this concentration range, these compounds influence the biosynthetic pathway of Phe in rice and other cereal grains. Second, the chosen concentrations were optimized to activate the biosynthesis pathway while avoiding toxic or adverse effects on grain development, thereby ensuring plant health and maintaining optimal yield. Third, employing multiple concentration levels enables the evaluation of dose–response relationships and facilitates the identification of the most effective concentration for enhancing Phe biosynthesis (Fatahi Siahkamary, 2025).

Sampling time

Sampling was done after complete ripening of rice seeds (Helal variety after 67 days and Keshvari variety after 97 days). Furthermore, samples were taken from the sampling line, which was the bushes in the middle of the plots, in order to minimize testing errors. Rice seeds, along with their hulls, were placed in liquid nitrogen upon harvesting from the clusters and transferred to a -80°C freezer for further analysis.

Gene expression analysis

In order to study the expression levels of genes that are effective in Phe biosynthesis

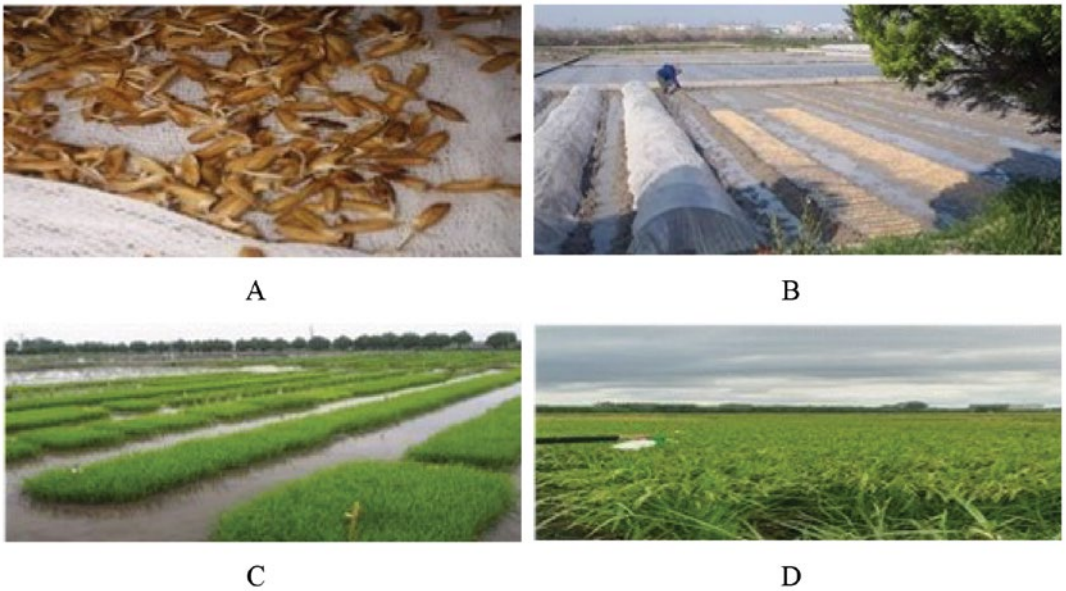

Fig. 2. A. The stage of soaking the seeds before placing them in the main field. B- Transferring the germinated seeds to the main field. C- Growing the germinated seeds in beds (a special farm that is very small and very fertile, suitable for seedling growth) and preparing for transfer to the main land. D- Spraying the growing bushes at predetermined stages.

and catabolism, the quantitative real-time PCR (qRT-PCR) technique was used. RNA extraction from rice seeds stored at -80°C was performed using the RNSOL Reagent kit (Rojetechnologies, Iran) with 3 repetitions for each sample. The qualitative analysis of the extracted RNAs was conducted using gel electrophoresis. cDNA synthesis was performed using the Pars Tous kit (Pars Tous, Iran). The sequences of the studied genes (*Arogenate dehydratase* (*ADT*), *Phenylalanine ammonia-lyase* (*PAL*), *Phenylpyruvate aminotransferase* (*PPY-AT*), *Ubiquitin 10*) were obtained from the NCBI website. The primers for the target genes were designed using Oligo 7 software (Table1). Furthermore, the Ubiquitin 10 gene was also considered as an internal reference gene in the current study. Quantitative expression of genes was performed using the qRT-PCR technique and an ABI device (Step One Plus system, Thermo Fisher Scientific, Inc., Waltham, MA, USA) according to a specific temperature and time schedule (95°C for 5 minutes, followed by 35 cycles at 95°C for 15 seconds, 60°C for 20 seconds, and 72°C for 30 seconds, with a final extension at 72°C for 5 minutes). The cycle threshold (CT) samples were examined by Step One software, and CTs with better melt curves and amplification plots were selected. The relative expression of each gene was analyzed using the $2^{-\Delta\Delta CT}$ method (Pfaffl, 2001).

Determination of amino acids

To determine amino acids in rice kernels, a modified method by Yang Zhang (Yang, 2016) was employed. To process each experimental treatment, 100 mg of powdered rice kernel was first measured and mixed with 1 ml of 80% ethanol. The samples were then stored at 4°C. They were subsequently placed in a thermomixer for one hour at 80°C and 700 rpm before allowing them to cool down to ambient temperature. The samples were then centrifuged at 14,000 rpm for 5 min at 4°C, and the supernatant was carefully transferred into a new tube. These tubes were sealed with paraffin and placed in a freeze-dryer overnight for complete lyophilization. Upon completion, the samples were stored at -20°C. The next step involved adding 1 ml of distilled water to each tube and filtering the contents through 0.22 µm syringe filters. Afterwards, 250 µl of the samples were transferred to a new tube, followed by the addition of 200 µl of borate buffer and 100 µl of ortho-phthalate dihydrate (OPD). The samples were vortexed for 120 s to ensure proper mixing. Subsequently, 50 µl of 0.5 mM HCl was added to each sample and vortexed for an additional 15 s to dissolve the mixture. Finally, the samples were loaded into the HPLC instrument equipped with a HALO 5 µm, C18 column for further analysis. The chromatographic separation

Table 1 Primers used for qRT-PCR in this study

Gene	Acc. No	Forward primer(5`to3`)	Reverse primer(5` to 3`)
ADT	NM_001403279.1	GAGCTATCCTACCGATGTCAG	CTGCTATCGGTGCTTCCAAG
PAL	NM_001401906.1	ACTGCCTCAAGGAGTGGAAC	CTCCTCTCCTCCTCGATGA
Ubiquitin 10	AK101547.1	GACTACAACATCCAGAAGGAG	CAGGCACATCGGCAGCTC
PPY-AT	AC087182.12	GAAGCTGCGTTGGTTGCGT	CAGTAAGCACCTGAAGGATGA

was performed using a reversed-phase C18 column (150 × 4.6 mm, 5 μm) maintained at 30 ± 2 °C. The mobile phases consisted of mobile phase A: 10 mM ammonium acetate (pH adjusted to 4.8 with acetic acid) and mobile phase B: HPLC-grade acetonitrile. The flow rate was set to 1.0 mL·min^{-1}, and the injection volume was 10 μL. Detection was carried out using a UV detector at a primary wavelength of 258 nm. A calibration curve was generated using phenylalanine standards prepared by serial dilution to obtain seven concentration levels (1, 5, 10, 25, 50, 100, and 200 μM), which were used to ensure accurate quantification. The total run time for each sample was 12–18 min (Haghighi, 2015).

Determination of the PAL

The PAL activity was determined according to Aydas' method (Aydas, 2013). The PAL activity was measured by the rate of conversion of Phe to trans-CA. One unit of PAL activity is equivalent to one micromole of CA produced per minute.

Determination of the total protein

The total protein in rice kernel was measured by standard Bradford essay (Kruger, 2009), and bovine serum albumin was used as a standard material to check the protein content in each extract.

Statistical analysis

The effect of treatments (CA and Phe and cultivars) was investigated in a factorial experiment (4×4×2) using a randomized complete block design (RCBD) with three replications. Each treatment had 3 plots with dimensions of 5 × 6 square meters. The experimental data obtained from different methods were normalized using the Kolmogorov-Smirnov test and then statistically analyzed using SPSS software version 2016. Comparisons of treatment averages were performed with Duncan's test at a 95% probability level, and the data were also plotted using Excel.

Assessment of yield and grain quality parameters

Spikelet fertility

Spikelet fertility was calculated as the ratio of filled spikelets to the total number of spikelets per panicle, expressed as a percentage. At maturity, five representative panicles from each treatment were sampled, and the numbers of filled and unfilled spikelets were recorded. The following formula was used:

$$\text{Spikelet fertility (\%)} = \frac{\text{Number of filled spikelets}}{\text{Total number of spikelets}} \times 100$$

This method follows the standard procedure described by the International Rice Research Institute (IRRI, 1996).

Thousand grain weight

Thousand grain weight was measured by counting and weighing 1,000 fully matured and air-dried grains from each treatment. The grains were cleaned, dehulled, and adjusted to a standard moisture content of 14% before weighing to ensure accuracy. The average weight was expressed in grams (g). The procedure followed the guidelines described in the Standard Evaluation System for Rice (IRRI, 1996).

Milling recovery

Milling recovery was determined as the percentage of total milled rice obtained from a given weight of rough rice after dehusking and polishing. Approximately 150 g of

paddy rice from each treatment were dehulled using a laboratory husker, and the resulting brown rice was polished using a rice polisher. The weight of the milled rice was recorded and expressed as a percentage of the original paddy weight. This procedure was performed according to the method described by the International Rice Research Institute (IRRI, 1996).

Determination of grain yield

Grain yield was determined at physiological maturity by harvesting the central rows of each plot to avoid border effects. The harvested panicles were threshed, cleaned, and air-dried to a constant weight, and the yield was expressed as the weight of dehulled rice per plant (or per square meter) after adjusting to 14% moisture content. The procedure followed the standard guidelines provided by the International Rice Research Institute (IRRI, 1996).

Results

Foliar elicitors alter Phe pathway gene Expression in rice cultivars

The data illustrated in Figure 3 clearly demonstrate that foliar application of Phe and CA on immature rice spikes significantly influenced the expression of *PAL*, *ADT*, and *PPY-AT* genes in rice seeds. According to the bar chart, CA treatment in the Helal variety (at all three concentrations) led to a substantial reduction in *PAL* gene expression. However, in the Keshvari variety, a decrease in *PAL* expression was only observed at the 1.5 g/L concentration (Figure 3A). In contrast, across both cultivars, *PAL* gene expression markedly increased in response to all Phe concentrations (Figure 3B). *ADT* gene expression showed a consistent and significant decrease in both varieties under all concentrations of CA foliar spray. Notably, this reduction appeared to be concentration-independent in the Keshvari variety (Figure 3C). Additionally, Phe application resulted in a significant reduction of *ADT* expression in the Helal variety at 0.5 and 1 g/L, with no notable effect observed at 0.25 g/L. In contrast, all three concentrations led to a marked decline in *ADT* expression in the Keshvari variety (Figure 3D).

Furthermore, CA exerted a pronounced impact on *PPY-AT* gene expression, precipitating a steep decline in both cultivars (Figure 3F). While the lowest concentration applied (0.5 g/L) did not cause any significant change compared to the control, the higher concentrations (1 and 1.5 g/L) notably widened the gap between treated and control samples. Indeed, the modulation of *PPY-AT* gene expression was clearly dependent on the applied concentration (Figure 3F). On the other hand, Phe treatment also led to a decrease in *PPY-AT* gene expression. In this case, both cultivars exhibited reduced gene expression at higher concentrations (1 and 0.5 g/L) (Figure 3F). Overall, the CA elicitor at a concentration of 1 g/L appeared to be optimal, particularly in the Keshvari variety. Not only did it maintain *PAL* gene expression, but it also effectively reduced the expression of the biosynthetic genes *ADT* and *PPY-AT* in both cultivars.

The grouping of treatments in the graphs was based on cultivars rather than treatment concentrations within a single cultivar in order to facilitate the comparison of genotypic responses. Since the objective of this

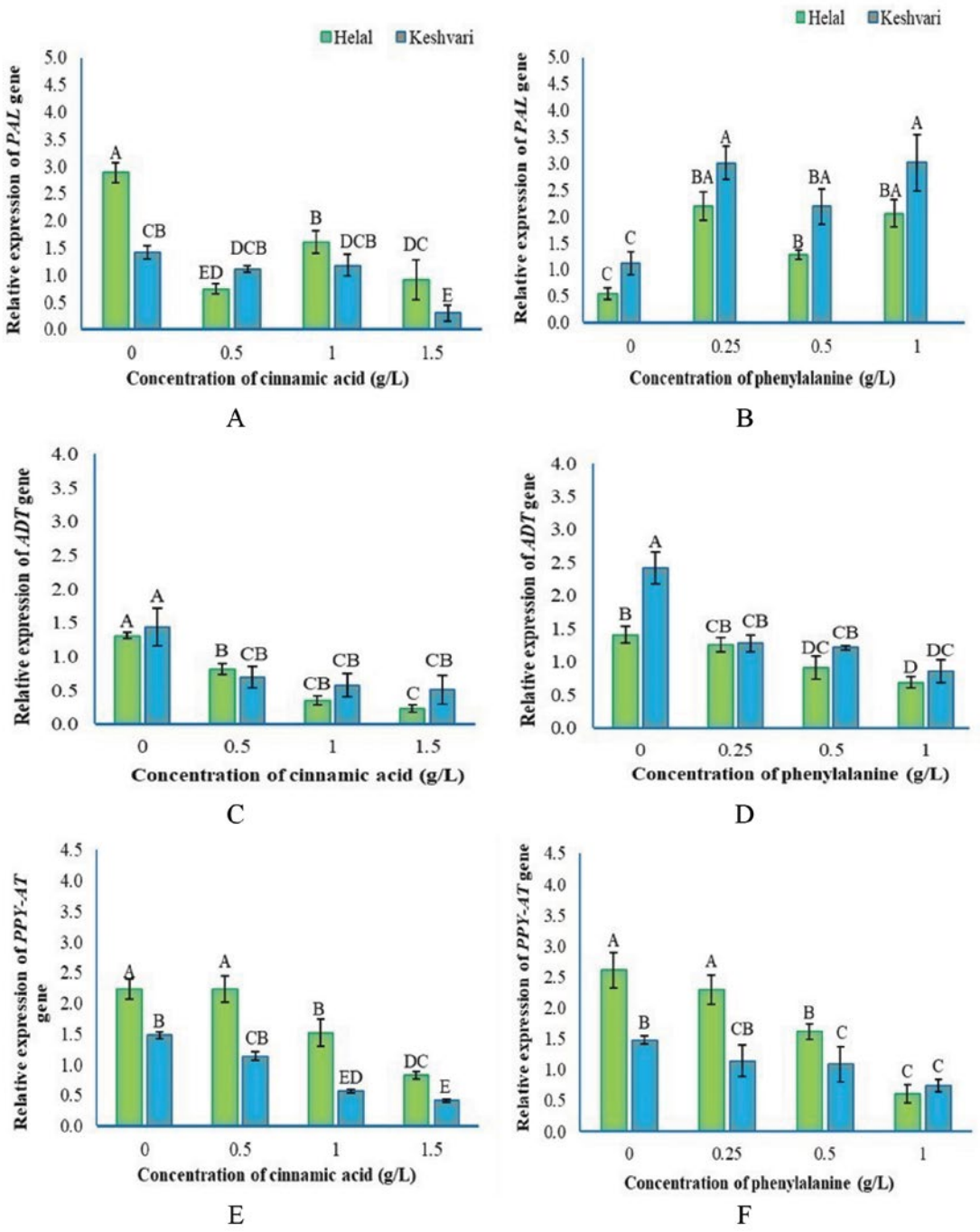

Fig. 3. Relative expression levels of enzymes involved in Phe amino acid biosynthesis and catabolism in rice kernels of the Helal (Green) and Keshvari (Blue) cultivars, treated with various concentrations of CA and Phe spraying. The figure in divided into the following panels: (A) Comparison of PAL gene expression under different CA concentrations, (B) Comparison of PAL gene expression under different Phe concentrations, (C) Comparison of ADT gene expression under different CA concentrations, (D) Comparison of ADT gene expression under different Phe concentrations, (E) Comparison of PPY-AT gene expression under different CA concentrations, (F) Comparison of PPY-AT gene expression under different Phe concentrations. Data are presented as mean values from at least three replicates ± standard error. Significant differences between means are indicated by alphabet mismatches at the probability level of $P \leq 0.05$, according to Duncan's test.

study was not only to assess the effects of Phe and CA treatments but also to evaluate the variability in response between the local rice cultivars, presenting the data by cultivar allowed for a clearer visualization of inter-cultivar differences. Nevertheless, the statistical analyses were performed across both factors (cultivar and treatment concentration), ensuring that the effects of treatment levels within each cultivar were also considered.

PAL activity in rice cultivars is regulated by CA and Phe concentrations

A detailed analysis of the data reveals a profound impact on PAL enzyme activity following the foliar application of biological stimulants (Figure 4). The 1.5 g/L concentration of CA induced the most significant metabolic response in the applied cultivars. Specifically, PAL activity decreased across all concentrations of CA in the Helal variety, whereas in the Keshvari variety, a decrease was observed only at the 1.5 g/L concentration of this stimulant (Figure 4A). In contrast, foliar application of Phe at all three concentrations led to a notable increase in PAL activity in both cultivars (Figure 4B).

Regulatory effects of CA and Phe on protein accumulation in rice seeds

As shown in Figure 5, the total protein content in rice kernels was affected by the CA and Phe foliar spray applications. A downward trend in total protein content was observed under the CA foliar application, with a notable decrease in both cultivars (Helal and Keshvari). Specifically, this indicator significantly decreased at a concentration of 1.5 g/L of the CA stimulant. However, other concentrations of this stimulant did not cause noteworthy changes in the desired factor and acted as an inert substance (Figure 5A). Hence, the concentration of 1 g/L of CA stands out as optimal, as it not only preserved total protein content, gene ex-

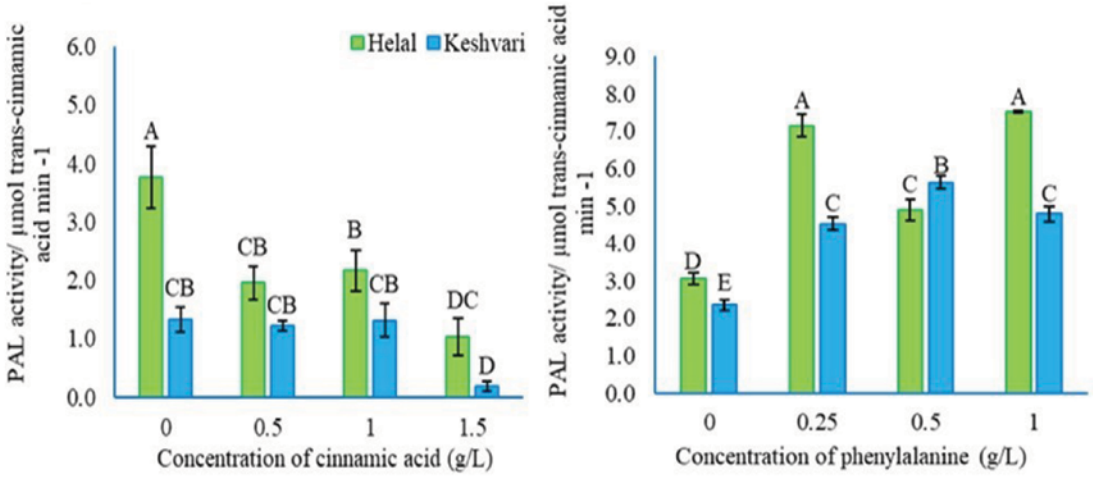

Figure 4. Effect of various concentrations of CA and Phe on PAL enzyme activity in rice kernels from the Helal (Green) and Keshvari (Blue) cultivars. Panels are as follows: (A) PAL enzyme activity under different concentrations of CA, (B) PAL enzyme activity under different concentrations of Phe. Data are presented as mean values from at least three replicates ± standard error. Significant differences between means are indicated by different letters ($P \leq 0.05$), according to Duncan's test.

pression, and PAL enzyme activity but also exerted a suppressive effect on Phe biosynthetic genes (*ADT* and *PPY-AT*). The stimulatory effect of Phe was also significant at the highest applied concentration (1 g/L), resulting in a decrease in total protein. Indeed, the trend remained steady up to the 1 g/L concentration of Phe (Figure 5B). Therefore, the significant consequence observed at this concentration is consistent in both cultivars.

The Phe content in rice Kernel

The lack of a detectable effect of Phe on the analyzed amino acids in Figure 6 can is related to the fact that, although Phe altered the expression of genes associated with its biosynthetic and catabolic pathways, these transcriptional changes did not lead to statistically significant variations in the concentrations of Phe, tryptophan, or tyrosine when compared with the control. In other words, the observed gene expression shifts were not reflected in measurable changes in amino acid levels. Moreover, neither of the rice cultivars displayed a significant alteration in amino acid content under Phe treatment. Likewise, treatment with CA in the Helal cultivar did not produce statistically meaningful differences in amino acid levels. Given that the results were not statistically significant, the related data and graphs were excluded from Figure 6 for the sake of emphasizing on statistically relevant outcomes. Additionally, in this study, Phe content was measured in dehulled and polished rice grains (milled rice) rather than whole kernels with husk and bran, as the aim was to assess the nutritional and biochemical status of the edible portion commonly consumed.

Regarding the figure allocated to the Phe content, it is clear that spraying with the CA elicitor led to a significant response and a substantial reduction in Phe amino acid lev-

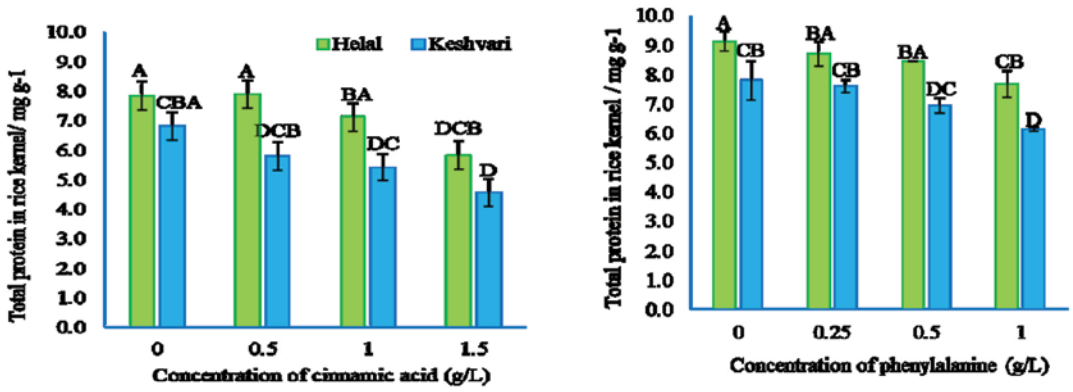

Fig. 5. Impact of varying concentrations of CA and Phe on total protein content in rice kernels from Helal (Green) and Keshvari (Blue) cultivars. The figure is divided into: (A) Total protein content in response to different concentrations of CA, (B) Total protein content in response to different concentrations of Phe. Data are expressed as mean values from a minimum of three replicates ± standard error. Significant differences between means are denoted by different letters ($P \leq 0.05$), as determined by Duncan's test.

els (Figure 6A). Ironically, all concentrations (0.5, 1, and 1.5 g/L) resulted in a significant decrease in Phe levels. Interestingly, while the lowest concentration (0.5 g/L) did not cause a noteworthy increase in tryptophan and tyrosine amino acids, higher concentrations (1 and 1.5 g/L) showed a remarkable decline in Phe levels, along with a notable rise in tryptophan and tyrosine. Therefore, as Phe levels decreased with higher concentrations, an increase in other amino acids occurred. There was no substantial difference between the increase in tyrosine levels at concentrations of 1 and 1.5 g/L, indicating that both concentrations led to the same increase in tyrosine, with a similar experience in tryptophan.

Evaluation of agronomic and grain Quality traits

The analysis of spikelet fertility under CA treatment revealed no statistically significant differences among the tested rice cultivars compared with the control. Although a slight decreasing trend was observed in the Helal cultivar at higher concentration (1.5 g/L), this change was not statistically significant (Fig 7, A). Similarly, the response of Helal and Keshvari cultivars to Phe treatment indicated a relative increase in spikelet fertility; however, these variations were not significant when compared to the control (Fig 7, B).

Examination of Figure 7(C, D) indicates that CA and Phe treatments did not cause any statistically significant increase or decrease in the thousand grain weight of the Helal and Keshvari cultivars, and the inherent grain quality of these cultivars was maintained. The analysis of milling recovery showed that the slight reduction observed under CA treatment at 0.5 g/L in the Keshvari cultivar was not statistically significant compared with the control (figure 7, E). Likewise, foliar application of the elicitor Phe did not induce any significant response in this trait (figure 7, F). Finally, the evaluation of He-

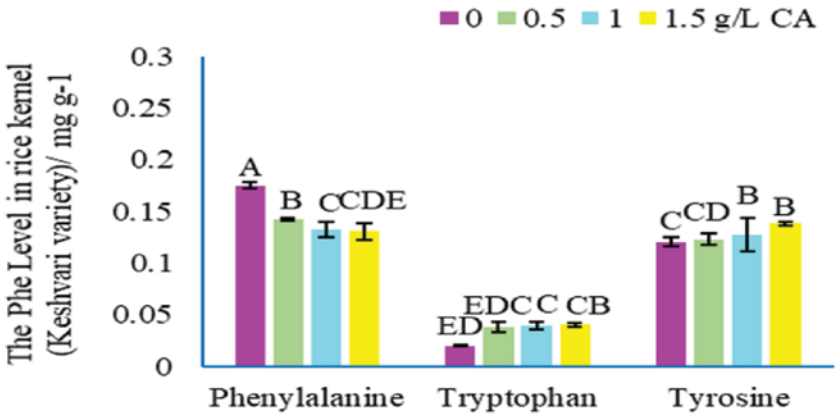

Fig. 6. Impact of varying concentrations of CA on Phe content in rice kernels from Keshvari cultivar. Figure (A) Phe content in response to different concentrations of CA. Data are expressed as mean values from a minimum of three replicates ± standard error. Significant differences between means are denoted by different letters ($P \leq 0.05$), as determined by Duncan's test.

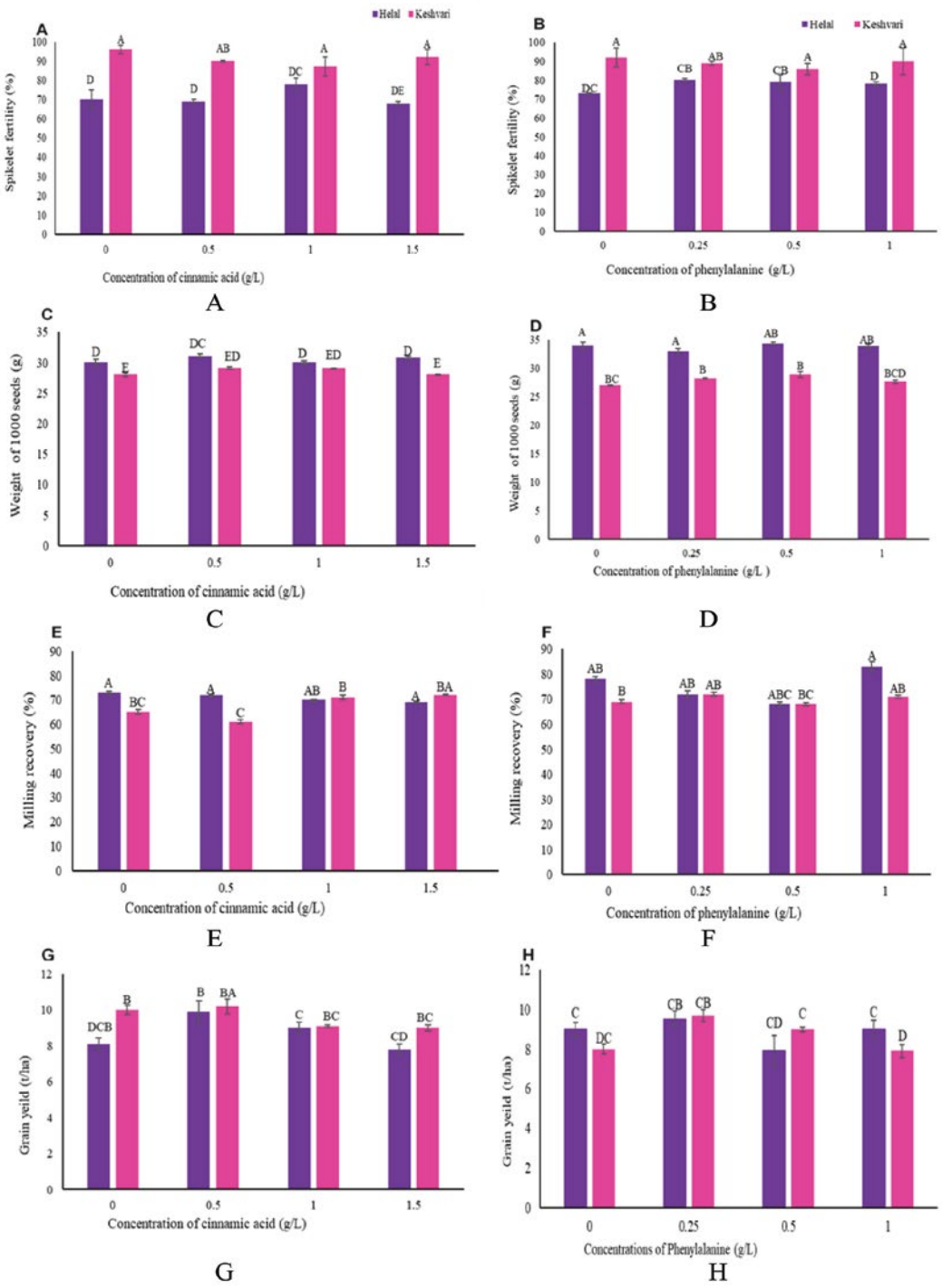

Fig. 7. Evaluation of agronomic and grain quality traits in Helal and Keshvari cultivars under the foliar application of CA and Phe biostimulants; (A) percentage of spikelet fertility under different concentrations of CA, (B) percentage of spikelet fertility under different concentrations of Phe, (C) comparison of thousand-seed weight in consumption varieties treated with CA, (D) comparison of thousand-seed weight in consumption varieties treated with Phe, (E) comparison of milling recovery percentage in Helal and Keshvari cultivars under foliar spraying of CA, (F) comparison of milling recovery percentage in Helal and Keshvari cultivars under foliar spraying of Phe, (G) investigation of grain yield index under CA foliar spraying, (H) investigation of grain yield index under Phe foliar spraying. Data are presented as mean values from at least three replicates ± standard error. Significant differences between means are indicated by alphabet mismatches at the probability level of $P \leq 0.05$, according to Duncan's test.

lal and Keshvari cultivars under the applied treatments indicated that foliar application of these elicitors did not result in any significant increase or decrease in grain yield (figure 7 G, H).

Discussion

There are two schools of thought when it comes to reducing Phe levels in plants. One approach involves inhibiting the expression of genes responsible for its biosynthesis, such as *ADT* and *PPY-AT*, while the other focuses on stimulating catabolic pathways by enhancing *PAL* gene expression and activity. In line with these perspectives, the present study investigated the expression of genes involved in Phe biosynthesis using both inhibitory and stimulatory strategies. Inhibition targeted the suppression of Phe biosynthesis enzymes (*ADT*, *PPY-AT*) in the plastids and cytosol, while stimulation aimed to enhance *PAL* gene expression and activity. In this regard, it was assumed that supplementing with Phe led to its accumulation in plant cells, particularly during specific growth stages, resulting in higher Phe levels for limit interval. Additionally, Phe influenced the synthesis of various compounds, redirecting the pathway to boost tyrosine and tryptophan production. Ultimately, the Phe foliar spray may elevate substrate levels, shifting the arogenate pathway to enhance tyrosine synthesis. The increase in tyrosine production results from altering Phe's metabolic pathway. Elevated substrate levels stimulate PAL activity and enhance its gene expression, while also redirecting the biosynthetic pathway towards tryptophan production. Foliar spraying of Phe acts as a stimulant, reducing Phe content in plant cells and making the plant less dependent on Phe synthesis during growth. This independence is driven by increased substrate levels. After Phe catabolism during seed filling and aging, when amino acid production slows, the amino acids in the seeds are hydrolyzed and used for various metabolic processes. Thus, foliar-applied Phe is catabolized during plant growth, especially during senescence, contributing to metabolic needs. In contrast, in this study, Phe spraying, despite significantly reducing the expression of the *ADT* and *PPY-AT* genes, did not lead to a decrease in Phe content in any of the examined cultivars. Analysis of this factor revealed no significant differences between treated and control samples across any of the consumption varieties over three consecutive years.

The study highlights the effectiveness of foliar Phe application during rice seed growth, reducing Phe biosynthetic gene expression (*ADT* and *PPY-AT*) while significantly increasing *PAL* gene expression, approximately fourfold in Helal and threefold in Keshvari. In comparison, Feduraev (Feduraev, 2020) reported a twofold increase in PAL enzyme activity and a slight rise in gene expression in wheat following external Phe application. Similarly, Peng (Peng, 2023) observed a 53% increase in PAL activity and gene expression in Tartary buckwheat, while Wen (Wen, 2005) found a 1.87-fold increase in PAL activity and gene expression in grape berry after salicylic acid treatment. These findings align with other studies, highlighting the impact of elicitor treatments on PAL regulation. Foliar application of Phe during

the growth stage, before grain ripening, led to a significant reduction in *ADT* gene expression in both rice cultivars. This reduction became more pronounced with higher Phe concentrations. The observed decrease in gene expression, and the potential impact on Phe content, may be influenced by factors such as the timing and concentration of elicitor application, as well as the genetic potential of the cultivars used. In Keshvari, Phe application led to a 1.5-fold reduction in *ADT* expression, while in Helal, *ADT* expression dropped by nearly 50%. This reduction may be due to increased Phe content in the plastid, the primary site of Phe biosynthesis, which can overwhelm its export capacity and cause intermittent accumulation. This feedback regulation reduces carbon flow toward the plastid Phe pathway, inhibiting *ADT* gene expression. Previous studies (Cho et al., 2007; Yamada et al., 2008) suggest that Phe content regulates *ADT* expression, and feedback mechanisms, potentially controlled by redox processes in photosynthesis, also contribute to downregulating biosynthetic genes like *ADT* (Wakasa, 2009).

CA, used as a pseudo-hormone and elicitor, can have dual effects in plants. It was expected to increase PAL activity and gene expression while downregulating Phe biosynthesis genes (*PPY-AT*, *ADT*). However, CA treatment resulted in a surprising decrease in both *PAL* gene expression and activity, as well as reduced expression of Phe biosynthesizing genes. This outcome suggests that CA did not enhance PAL performance as anticipated. However, despite not enhancing gene expression or PAL enzyme activity, it significantly reduced Phe content in the Keshvari cultivar. Additionally, its impact on reducing total protein content and nitrate reductase activity indicates that reduced nitrogen levels may decrease enzyme activities, including those involved in amino acid biosynthesis (Singh, 2013). However, in the present study, CA increased the levels of the amino acids tryptophan and tyrosine. This suggests that it may have acted specifically by enhancing the expression of genes encoding enzymes involved in the biosynthesis of these amino acids, leading to their elevated levels in the harvested samples. The lowered expression of *PPY-AT* and *ADT* genes suggests a reduction in Phe biosynthesis in both plastids and cytosol. Additionally, the decrease in PAL activity may be linked to reduced Phe levels, its substrate. What is more, the effects of CA during the spike filling period may vary due to factors such as genetic potential, elicitor efficacy, and application site. CA and Phe influence Phe catabolism by disrupting biosynthetic pathways and altering key enzymatic processes. Differences in responses across cultivars may result from genetic variation, environmental factors (pH, soil moisture, temperature), plant growth stage, and stimulant concentration.

In addition, this study investigated the cytosolic pathway of Phe biosynthesis, mediated by the *PPY-AT* gene, which serves as an alternative to the plastid pathway (MacDonald 2007). The flux of this pathway increases when entry into the arogenate pathway is restricted (Yoo, 2013; Corea, 2012; Maeda, 2010). Data from qRT-PCR analysis showed that stimulant consumption affected

PPY-AT expression, with higher concentrations eliciting stronger responses. In the Helal cultivar, Phe and CA treatments led to nearly identical metabolic responses, reducing *PPY-AT* expression by about 75%, while Keshvari showed a 50% decrease. The cytosolic chorismate mutase directs carbon flux toward cytosolic Phe production through the phenylpyruvate pathway (Qian, 2019).

Another finding of this study is the significant increase in PAL activity in rice seeds following Phe stimulation. However, this increase was not sufficient to reduce the overall Phe content. Data analysis revealed a strong correlation between *PAL* gene expression and enzyme activity across both cultivars and all tested Phe concentrations. These results are consistent with previous studies, such as (Singh, 2010), which reported enhanced PAL activity in crops like *Pisum sativum* following foliar application of Phe. Plants accumulate phenolic compounds as a defense mechanism or in response to stress or stimulants (Singh, 2003; Singh, 2002; Vermerriset, 2006), with Phe content playing a central role in regulating this accumulation. What is more, PAL activity can be influenced by secondary metabolite content (Jan, 2021; Waterman, 2019). Studies show that foliar spraying with amino acids, such as Phe, boosts defense enzyme activity and resistance to pathogens in plants like Arabidopsis, tomato, and petunia (Oliva, 2020). Moreover, Bahadur (Bahadur, 2012) reported a near doubling of PAL activity in pea leaves with Phe spray, while Ghalamboran (Ghalamboran, 2023) observed a 2.5-fold increase in rice grains using chitosan nanoparticles. In this study, Phe foliar spray resulted in a 4.5-fold increase in PAL activity in the Helal variety and a nearly 2.5-fold increase in Keshvari, compared to controls.

Analysis reveals that reduced *ADT* and *PPY-AT* gene expression correlates with a decrease in total protein content, particularly at the highest concentrations of elicitors. At this concentration, both cultivars exhibited similar responses, thereby triggering a significant metabolic shift. This observation aligns with studies supporting the role of amino acid foliar sprays in enhancing photosynthesis and cell division, ultimately leading to improved plant growth (Levitt, 1980; Reham, 2016; Ping, 2023). Nevertheless, these benefits appear to plateau or reverse at excessive levels, as excessive amino acid uptake can reduce protein content. In support of this, research by Ghalamboran (Ghalamboran, 2023) demonstrated a 2.5-fold reduction in rice seed protein content following chitosan nanoparticle application, which was directly linked to decreased Phe levels.

As previously highlighted, CA application was expected to enhance *PAL* gene expression; however, contrary to expectations, it markedly reduced *PAL* expression in both Helal and Keshvari cultivars. This unexpected reduction may be attributed to suppressed nitrate reductase activity, which in turn leads to decreased nitrogen and amino acid content. Given that *PAL* expression is dependent on Phe availability, it is likely that the decline in substrate contributed to the observed reduction in gene expression. This is further supported by quantitative results, showing a six-fold reduction in *PAL* expression in He-

lal and a 75% decrease in Keshvari, thereby underscoring CA's strong inhibitory effect. In line with these findings, CA elicitor consumption reduces *PAL* gene expression and enzyme activity by disrupting Phecatabolism, as CA acts as a feedback modulator (Zhang, 2015). This inhibitory role is consistent with previous findings, such as those by Blount (Blount, 2000), who observed similar effects in tobacco, and Yuan (Yuan, 2023), who reported reduced PAL activity in taro treated with peppermint extracts rich in p-coumaric acid. In addition to affecting PAL, our results also show that CA reduces the expression of Phe biosynthesis genes, including *ADT* and *PPY-AT*. Interestingly, while CA decreased *ADT* expression in the Helal variety, the Keshvari variety did not exhibit a dose-dependent response, instead maintaining consistently reduced expression levels.

ADT gene expression in Arabidopsis thaliana is regulated by free Phe levels via an allosteric feedback mechanism (Chen, 2016). Though research is limited, evidence suggests a strong link between phenylpropanoid content and *ADT* expression. El-Azaz (El-Azaz, 2020) found a correlation between ADT regulation and lignin content in conifers, indicating secondary metabolites influence enzyme gene expression. Accordingly, CA may directly modulate *ADT* expression and promote lignin biosynthesis which is stems from Phe in monocots (Bubna, 2011). As a matter of fact, the study aimed to investigate gene expression levels related to Phe biosynthesis, focusing on both the plastidial and cytosolic pathways. As mentioned previously, the cytosolic pathway, an alternative to the arogenate (plastidial) pathway, increases in flux when the latter is limited (Yoo, 2021; Corea, 2012; Maeda, 2010). qRT-PCR data showed that certain concentrations of consumptive stimulants significantly affected gene expression. In the Helal variety, *PPY-AT* expression decreased, especially at higher concentrations. Unlike (Qian, 2019), this study found the cytosolic phenylpyruvate pathway is subject to feedback regulation. CA foliar application reduced both *PPY-AT* expression and PAL activity by limiting substrate availability. To further explain, the reduced expression of the *PPY-AT* gene, along with the decreased expression and activity of the PAL enzyme, is due to the availability of the product resulting from the catabolism of the amino acid Phe. This is because the presence of CA indicates an enhanced antioxidant system in the plant, reducing the need for further synthesis of Phe. Therefore, based on the data from amino acid content measurements, it can be concluded that due to the availability of CA, the cytosolic and plastidial pathways for Phe biosynthesis are redirected toward the production of tyrosine and tryptophan, which are required for the synthesis of pigments and plant hormones. This shift occurs as the precursor for many antioxidant compounds is already available to the plant. This aligns with findings by (Blount, 2000; Rajaeian, 2015; Bahadur, 2012; Liu, 2024; Jorrín, 1990). However, Mohagheghian (Mohagheghian, 2021) reported increased PAL activity in tobacco under salinity stress due to CA.

Additionally, Yang (Yang, 2022) confirmed reduced PAL activity in faba beans exposed

to CA. Several studies report that CA diminishes plant protein content by disrupting nitrogen uptake and nitrate reductase activity (López-González, 2023; Hussain, 2011). In lettuce, external CA application decreased protein content, consistent with our findings. Mohagheghian (Mohagheghian, 2021) observed a 12% protein reduction in tobacco under CA treatment, while Singh (Singh, 2013) reported similar declines in maize due to phenolic acids inhibiting amino acid binding during protein synthesis. Since nitrogen is vital for protein formation and tissue growth, its disruption by CA is significant. Kapoor (Kapoor, 2021) showed that CA suppresses nitrate reductase activity, reducing nitrogen and protein levels in *Pisum sativum*. Likewise, Hussain (Hussain, 2017; Wisetkomolmat, 2023) found that high CA concentrations reduce protein content in *Solanum lycopersicum* through decreased synthesis and increased degradation.

Conclusion

The epitome of these discussions is ultimately reflected in the Phe levels, as illustrated below:

Foliar application of Phe suppresses Phe biosynthetic genes but does not affect actual Phe levels in Helal and Keshvari cultivars. Conversely, CA application significantly enhances the tyrosine biosynthetic pathway, increasing tyrosine production. This phenomenon is cultivar-dependent, as only the Keshvari cultivar exhibits reduced Phe content under CA treatment. The Helal cultivar maintains Phe levels despite reduced gene expression. The observed increase in tryptophan levels further confirms the biosynthetic pathway shift, attributed to the chorismate compound favoring tryptophan production. Therefore, foliar application of CA proved effective in two key aspects. The foliar application of CA with higher concentrations induced a shift in the biosynthetic pathway, prioritizing tyrosine production and enhancing tryptophan synthesis. This observation suggests a strong correlation between CA concentration and the alteration of enzyme activity within the amino acid biosynthetic pathway. Notably, the effect varies across different rice varieties, indicating that the species and genome can influence CA's efficacy and its concentration-dependent effects. Precisely, the response of different plant varieties to various concentrations of CA plays a crucial role in determining amino acid production levels and modulating their biosynthetic pathways, with no discernible impact on the quantitative traits. The broader implications of this study highlight the potential of foliar elicitor treatments as a practical, non-GM approach for nutritional biofortification of rice. By demonstrating that CA and Phe can modulate Phe biosynthesis, our findings suggest a feasible strategy for producing rice with reduced Phe content, which could benefit individuals affected by phenylketonuria (PKU). Importantly, preliminary evaluations of agronomic traits (e.g., panicle length, thousand-grain weight, and spikelet fertility) indicated no adverse effects, supporting the practical applicability of this method. Beyond medical nutrition, such treatments may also improve amino acid balance in rice, potentially enhancing its value for general consumers. Considering the limited accessibility of specialized

low-Phe foods in developing countries, integrating this approach into existing rice cultivation systems could provide a cost-effective and scalable solution to address both health-related and agricultural needs.

Author contribution statement

P.D. and M. R. GH. designed and supervised the project. P.D. carried out the experiments and wrote the original draft of the manuscript. M.N. performed cultivation of rice, P.D. and M. R. GH. data analysis, and P.D. and S. B. H. performed gene expression. P.D. and M. R. GH. were responsible for editing the manuscript. All authors agreed on the final version of the manuscript.

References

Ali, A., More, T.A. and Shaikh, Z., 2021. Artificial sweeteners and their health implications: a review. *Biosciences Biotechnology Research Asia*, 18(2), pp.227-237. Doi: http://dx.doi.org/10.13005/bbra/2910.

Ashe, K., Kelso, W., Farrand, S., Panetta, J., Fazio, T., De Jong, G. and Walterfang, M., 2019. Psychiatric and cognitive aspects of phenylketonuria: the limitations of diet and promise of new treatments. *Frontiers in psychiatry*, 10, p.561. Doi: https://doi.org/10.3389/fpsyt.2019.00561.

Aydaş, S.B., Ozturk, S. and Aslım, B., 2013. Phenylalanine ammonia lyase (PAL) enzyme activity and antioxidant properties of some cyanobacteria isolates. *Food Chemistry*, 136(1), pp.164-169. Doi: https://doi.org/10.1016/j.foodchem.2012.07.119.

Bahadur, A., Singh, D.P., Sarma, B.K. and Singh, U.P., 2012. Foliar application of l-phenylalanine and ferulic acids to pea plants: induced phenylalanine ammonia lyase activity and resistance against Erysiphe pisi. *Archives of Phytopathology and Plant Protection,* 45(4), pp.398-403. Doi: https://doi.org/10.1080/03235408.2011.587963.

Baziramakenga, R., Leroux, G.D., Simard, R.R. and Nadeau, P., 1997. Allelopathic effects of phenolic acids on nucleic acid and protein levels in soybean seedlings. *Canadian Journal of Botany*, *75*(3), pp.445-450.Doi: https://doi.org/10.1139/b97-047.

Blau, N., 2016. Genetics of phenylketonuria: then and now. *Human mutation*, *37*(6), pp.508-515. Doi: https://doi.org/10.1002/humu.22980.

Blount, J.W., Korth, K.L., Masoud, S.A., Rasmussen, S., Lamb, C. and Dixon, R.A., 2000. Altering expression of cinnamic acid 4-hydroxylase in transgenic plants provides evidence for a feedback loop at the entry point into the phenylpropanoid pathway. *Plant physiology*, *122*(1), pp.107-116. Doi: https://doi.org/10.1104/pp.122.1.107.

Bubna, G.A., Lima, R.B., Zanardo, D.Y.L., Dos Santos, W.D., Ferrarese, M.D.L.L. and Ferrarese-Filho, O., 2011. Exogenous caffeic acid inhibits the growth and enhances the lignification of the roots of soybean (Glycine max). *Journal of Plant Physiology*, 168(14), pp.1627-1633. Doi: https://doi.org/10.1016/j.jplph.2011.03.005.

Chattopadhyay, S., Raychaudhuri, U. and Chakraborty, R., 2014. Artificial

sweeteners–a review. *Journal of food science and technology*, *51*(4), pp.611-621. Doi: https://doi.org/10.1007/s13197-011-0571-1.

Chen, Q., Man, C., Li, D., Tan, H., Xie, Y. and Huang, J., 2016. Arogenate dehydratase isoforms differentially regulate anthocyanin biosynthesis in Arabidopsis thaliana. *Molecular plant*, *9*(12), pp.1609-1619. Doi: 10.1016/j.molp.2016.09.010 .

Cheng, F. and Cheng, Z., 2015. Research progress on the use of plant allelopathy in agriculture and the physiological and ecological mechanisms of allelopathy. *Frontiers in Plant Science*, *6*, p.1020. Doi: https://doi.org/10.3389/fpls.2015.01020.

Cho, M.H., Corea, O.R., Yang, H., Bedgar, D.L., Laskar, D.D., Anterola, A.M., Moog-Anterola, F.A., Hood, R.L., Kohalmi, S.E., Bernards, M.A. and Kang, C., 2007. Phenylalanine biosynthesis in Arabidopsis thaliana: identification and characterization of arogenate dehydratases. *Journal of Biological Chemistry*, *282*(42), pp.30827-30835. Doi: 10.1074/jbc.M702662200.

Corea, O.R., Ki, C., Cardenas, C.L., Kim, S.J., Brewer, S.E., Patten, A.M., Davin, L.B. and Lewis, N.G., 2012. Arogenate dehydratase isoenzymes profoundly and differentially modulate carbon flux into lignins. *Journal of Biological Chemistry*, *287*(14), pp.11446-11459. Doi: https://doi.org/10.1074/jbc.M111.322164.

El-Azaz, J., de la Torre, F., Pascual, M.B., Debille, S., Canlet, F., Harvengt, L., Trontin, J.F., Ávila, C. and Cánovas, F.M., 2020. Transcriptional analysis of arogenate dehydratase genes identifies a link between phenylalanine biosynthesis and lignin biosynthesis. *Journal of Experimental Botany*, *71*(10), pp.3080-3093. Doi: https://doi.org/10.1093/jxb/eraa099.

Fatahi Siahkamary, S., Rabiei, V., Shoor, M. and Nicola, S., 2025. Foliar application of L-phenylalanine, sodium selenate, and nitroxine biological fertilizer can improve antioxidant and phytochemical properties of goji berry (Lycium barbarum L.). *Journal of Horticulture and Postharvest Research*, pp.291-308. Doi: https://doi.org/10.22077/jhpr.2024.7895.1397.

Feduraev, P., Skrypnik, L., Riabova, A., Pungin, A., Tokupova, E., Maslennikov, P. and Chupakhina, G., 2020. Phenylalanine and tyrosine as exogenous precursors of wheat (Triticum aestivum L.) secondary metabolism through PAL-associated pathways. *Plants*, *9*(4), p.476. Doi: https://doi.org/10.3390/plants9040476.

Ghalamboran, M.R., Kohnavard, A. and Hassani, S.B., 2023. Phenylalanine response in rice kernel under chitosan nanoparticles spraying. *Acta Physiologiae Plantarum*, *45*(4), p.61. Doi: https://doi.org/10.1007/s11738-023-03538-3.

Haghighi, F., Talebpour, Z., Amini, V., Ahmadzadeh, A., & Farhadpour, M. (2015). A fast high performance liquid chromatographic (HPLC) analysis of amino acid phenylketonuria disorder in dried blood spots and serum samples, employing C18 monolithic silica columns and photo diode array detection. *Analytical Methods*, *7*(18), 7560-7567.Doi: https://doi.org/10.1039/

C5AY00745C.

Huke, R.E., 1982. *Rice area by type of culture: South, Southeast, and East Asia*. Int. Rice Res. Inst.

Hussain, I., Singh, N.B., Singh, A., Singh, H., Singh, S.C. and Yadav, V., 2017. Exogenous application of phytosynthesized nanoceria to alleviate ferulic acid stress in Solanum lycopersicum. *Scientia horticulturae*, *214*, pp.158-164. Doi: https://doi.org/10.1016/j.scienta.2016.11.032.

Hussain, M.I. and Reigosa, M.J., 2011. A chlorophyll fluorescence analysis of photosynthetic efficiency, quantum yield and photon energy dissipation in PSII antennae of Lactuca sativa L. leaves exposed to cinnamic acid. *Plant Physiology and Biochemistry*, *49*(11), pp.1290-1298. Doi: https://doi.org/10.1016/j.plaphy.2011.08.007.

IRRI, I., 2002. Standard evaluation system for rice. *International Rice Research Institute, Philippine*, pp.1-45.

Jan, R., Asaf, S., Numan, M., Lubna and Kim, K.M., 2021. Plant secondary metabolite biosynthesis and transcriptional regulation in response to biotic and abiotic stress conditions. *Agronomy*, *11*(5), p.968. Doi: https://doi.org/10.3390/agronomy11050968.

Jorrín, J., López-Valbuena, R. and Tena, M., 1990. L-phenylalanine ammonia-lyase from sunflower hypocotyls: Modulation by cinnamic acids. *Journal of plant Physiology*, *136*(4), pp.415-420. Doi: https://doi.org/10.1016/S0176-1617(11)80029-5.

Kapoor, R.T., Alyemeni, M.N. and Ahmad, P., 2021. Exogenously applied spermidine confers protection against cinnamic acid-mediated oxidative stress in Pisum sativum. *Saudi Journal of Biological Sciences*, *28*(5), pp.2619-2625.Doi: https://doi.org/10.1016/j.sjbs.2021.02.052.

Kruger, N.J., 2009. The Bradford method for protein quantitation. *The protein protocols handbook*, pp.17-24. Doi: https://doi.org/10.1007/978-1-59745-198-7_4.

Levitt, J., 1980. Responses of plants to environmental stresses. *Chilling, Freezing, and High Temperature Stress*, *1*, pp.345-447.Doi: https://doi.org/10.2503/jjshs.72.29.

Liu, J., Lefevere, H., Coussement, L., Delaere, I., De Meyer, T., Demeestere, K., Höfte, M., Gershenzon, J., Ullah, C. and Gheysen, G., 2024. The phenylalanine ammonia-lyase inhibitor AIP induces rice defence against the root-knot nematode Meloidogyne graminicola. *Molecular Plant Pathology*, *25*(1), p.e13424. Doi: https://doi.org/10.1111/mpp.13424.

López-González, D., Bruno, L., Díaz-Tielas, C., Lupini, A., Aci, M.M., Talarico, E., Madeo, M.L., Muto, A., Sánchez-Moreiras, A.M. and Araniti, F., 2023. Short-term effects of trans-cinnamic acid on the metabolism of Zea mays L. Roots. *Plants*, *12*(1), p.189. Doi: https://doi.org/10.3390/plants12010189.

MacDonald, M.J. and D'Cunha, G.B., 2007. A modern view of phenylalanine ammonia lyase. *Biochemistry and Cell Biology*, *85*(3), pp.273-282. Doi: https://doi.org/10.1139/O07-018.

Maeda, H., Shasany, A.K., Schnepp, J., Orlova, I., Taguchi, G., Cooper, B.R., Rhodes, D., Pichersky, E. and Dudareva, N., 2010. RNAi suppression of Arogenate Dehydratase1 reveals that phenylalanine is synthesized predominantly via the arogenate pathway in petunia petals. *The Plant Cell*, *22*(3), pp.832-849. Doi: https://doi.org/10.1105/tpc.109.073247.

Mohagheghian, E. and Ehsan Pour, A.A., 2021. Effect of Cinnamic acid on the activity of phenylalanine ammonialyase (PAL) and tyrosine ammonialyase (TAL) enzymes and some physiological characteristics of tobacco plant (Nicotiana rustica L.) under salinity stress in vitro calture. *Cell and Tissue Journal*, *12*(2), pp.88-102. Doi: https://doi.org/10.52547/JCT.12.2.88.

Mohidem, N.A., Hashim, N., Shamsudin, R. and Che Man, H., 2022. Rice for food security: Revisiting its production, diversity, rice milling process and nutrient content. *Agriculture*, *12*(6), p.741. Doi: https://doi.org/10.3390/agriculture12060741.

Oliva, M., Hatan, E., Kumar, V., Galsurker, O., Nisim-Levi, A., Ovadia, R., Galili, G., Lewinsohn, E., Elad, Y., Alkan, N. and Oren-Shamir, M., 2020. Increased phenylalanine levels in plant leaves reduces susceptibility to Botrytis cinerea. *Plant Science*, *290*, p.110289. Doi: https://doi.org/10.1016/j.plantsci.2019.110289.

Peng, W., Wang, N., Wang, S., Wang, J. and Bian, Z., 2023. Effect of co-treatment of microwave and exogenous l-phenylalanine on the enrichment of flavonoids in Tartary buckwheat sprouts. *Journal of the Science of Food and Agriculture*, *103*(4), pp.2014-2022. Doi: https://doi.org/10.1002/jsfa.12263.

Pfaffl, M.W., 2001. A new mathematical model for relative quantification in real-time RT–PCR. *Nucleic acids research*, *29*(9), pp.e45-e45. Doi: https://doi.org/10.1093/nar/29.9.e45.

Ping, H., Jie, M., Shujing, K., Sanfeng, L., Xianmei, W., Longjun, Z., Caolin, L., Rui, H., Huiying, H., Lianguang, S. and Yuchun, R., 2023. Chlorophyllide-a oxygenase 1 (OsCAO1) over-expression affects rice photosynthetic rate and grain yield. *Rice Science*, *30*(2), p.87. Doi: 10.1016/j.rsci.2022.05.006.

Qian, Y., Lynch, J.H., Guo, L., Rhodes, D., Morgan, J.A. and Dudareva, N., 2019. Completion of the cytosolic post-chorismate phenylalanine biosynthetic pathway in plants. *Nature communications*, *10*(1), p.15.Doi: https://doi.org/10.1038/s41467-018-07969-2.

Rajaeian, S., Ehsanpour, A.A., and Toghyani, M.A., 2015. Changes in phenolic compound, TAL, PAL activity of Nicotiana rustica triggered by ethanolamine pretreatment under in vitro salt stress condition. *Journal of Plant Biological Sciences*, *7*(26), pp.1-12.Doi: 20.1001.1.20088264.1394.7.26.2.4.

Reham, M.S., Khattab, M.E., Ahmed, S.S. and Kandil, M.A.M., 2016. Influence of foliar spray with phenylalanine and nickel on growth, yield quality and chemical composition of genoveser basil plant. *African Journal of Agricultural Research*, *11*(16), pp.1398-1410.Doi: https://doi.org/10.5897/AJAR2015.10699.

Singh, D.P., Bahadur, A., Sarma, B.K., Maurya, S., Singh, H.B. and Singh, U.P., 2010. Exogenous application of L-phenylalanine and ferulic acid enhance phenylalanine ammonia lyase activity and accumulation of phenolic acids in pea (*Pisum sativum*) to offer protection against Erysiphe pisi. *Archives Of Phytopathology and Plant Protection*, *43*(15), pp.1454-1462. Doi: https://doi.org/10.1080/03235400802536881.

Singh, P.K., Singh, R. and Singh, S., 2013. Cinnamic acid induced changes in reactive oxygen species scavenging enzymes and protein profile in maize (Zea mays L.) plants grown under salt stress. *Physiology and Molecular Biology of Plants*, *19*(1), pp.53-59. Doi: https://doi.org/10.1007/s12298-012-0126-6.

Singh, U.P., Sarma, B.K. and Singh, D.P., 2003. Effect of plant growth-promoting rhizobacteria and culture filtrate of *Sclerotium rolfsii* on phenolic and salicylic acid contents in chickpea (Cicer arietinum). *Current Microbiology*, *46*(2), pp.0131-0140. Doi: https://doi.org/10.1007/s00284-002-3834-2.

Singh, U.P., Sarma, B.K., Singh, D.P. and Bahadur, A., 2002. Plant growth-promoting rhizobacteria-mediated induction of phenolics in pea (Pisum sativum) after infection with Erysiphe pisi. *Current Microbiology*, *44*(6), pp.396-400. Doi: https://doi.org/10.1007/s00284-001-0007-7.

Soltanizadeh, N. and Mirmoghtadaie, L., 2014. Strategies used in production of phenylalanine-free foods for PKU management. *Comprehensive Reviews in Food Science and Food Safety*, *13*(3), pp.287-299. Doi: https://doi.org/10.1111/1541-4337.12057.

Van Spronsen, F.J., Blau, N., Harding, C., Burlina, A., Longo, N. and Bosch, A.M., 2021. Phenylketonuria. *Nature reviews Disease primers*, *7*(1), p.36. Doi: https://doi.org/10.1038/s41572-021-00267-0.

Vermerris, W. and Nicholson, R., 2008. The role of phenols in plant defense. In *Phenolic compound biochemistry* (pp. 211-234). Dordrecht: Springer Netherlands. Doi: https://doi.org/10.1007/978-1-4020-5164-7_6.

Wakasa, K. and Ishihara, A., 2009. Metabolic engineering of the tryptophan and phenylalanine biosynthetic pathways in rice. *Plant biotechnology*, *26*(5), pp.523-533. Doi: https://doi.org/10.5511/plantbiotechnology.26.523.

Waterman, P.G. and Mole, S., 2019. Extrinsic factors influencing production of secondary metabolites in plants. In *Insect-plant interactions* (pp. 107-134). CRC press.

Wen, P.F., Chen, J.Y., Kong, W.F., Pan, Q.H., Wan, S.B. and Huang, W.D., 2005. Salicylic acid induced the expression of phenylalanine ammonia-lyase gene in grape berry. *Plant Science*, *169*(5), pp.928-934. Doi: https://doi.org/10.1016/j.plantsci.2005.06.011.

Wisetkomolmat, J., Arjin, C., Hongsibsong, S., Ruksiriwanich, W., Niwat, C., Tiyayon, P., Jamjod, S., Yamuangmorn, S., Prom-U-Thai, C. and Sringarm, K., 2023. Antioxidant activities and characterization of polyphenols from selected Northern Thai rice husks:

Relation with seed attributes. *Rice Science*, *30*(2), pp.148-159. Doi: https://doi.org/10.1016/j.rsci.2023.01.007.

Yamada, T., Matsuda, F., Kasai, K., Fukuoka, S., Kitamura, K., Tozawa, Y., Miyagawa, H. and Wakasa, K., 2008. Mutation of a rice gene encoding a phenylalanine biosynthetic enzyme results in accumulation of phenylalanine and tryptophan. *The Plant Cell*, *20*(5), pp.1316-1329. Doi: https://doi.org/10.1105/tpc.107.057455.

Yang, Q.Q., Zhang, C.Q., Chan, M.L., Zhao, D.S., Chen, J.Z., Wang, Q., Li, Q.F., Yu, H.X., Gu, M.H., Sun, S.S.M. and Liu, Q.Q., 2016. Biofortification of rice with the essential amino acid lysine: molecular characterization, nutritional evaluation, and field performance. *Journal of Experimental Botany*, *67*(14), pp.4285-4296. Doi: https://doi.org/10.1093/jxb/erw209.

Yang, W., Li, Y., Zhao, Q., Guo, Y. and Dong, Y., 2022. Intercropping alleviated the phytotoxic effects of cinnamic acid on the root cell wall structural resistance of faba bean and reduced the occurrence of Fusarium wilt. *Physiologia Plantarum*, *174*(6), p.e13827. Doi: https://doi.org/10.1111/ppl.13827.

Yoo, H., Shrivastava, S., Lynch, J.H., Huang, X.Q., Widhalm, J.R., Guo, L., Carter, B.C., Qian, Y., Maeda, H.A., Ogas, J.P. and Morgan, J.A., 2021. Overexpression of arogenate dehydratase reveals an upstream point of metabolic control in phenylalanine biosynthesis. *The Plant Journal*, *108*(3), pp.737-751. Doi: https://doi.org/10.1111/tpj.15467.

Yoo, H., Widhalm, J.R., Qian, Y., Maeda, H., Cooper, B.R., Jannasch, A.S., Gonda, I., Lewinsohn, E., Rhodes, D. and Dudareva, N., 2013. An alternative pathway contributes to phenylalanine biosynthesis in plants via a cytosolic tyrosine: phenylpyruvate aminotransferase. *Nature communications*, *4*(1), p.2833. Doi: https://doi.org/10.1038/ncomms3833.

Yuan, X., Tang, B., Wang, Y., Jiang, Y., He, J., Wang, G., Yang, P. and Wang, B., 2023. Inhibitory effects of peppermint extracts on the browning of cold-stored fresh-cut taro and the phenolic compounds in extracts. *Frontiers in Sustainable Food Systems*, *7*, p.1191396. Doi: https://doi.org/10.3389/fsufs.2023.1191396.

Zhang, X. and Liu, C.J., 2015. Multifaceted regulations of gateway enzyme phenylalanine ammonia-lyase in the biosynthesis of phenylpropanoids. *Molecular Plant*, *8*(1), pp.17-27. Doi: 10.1016/j.molp.2014.11.001 .

Zulet-González, A., Barco-Antoñanzas, M., Gil-Monreal, M., Royuela, M. and Zabalza, A., 2020. Increased glyphosate-induced gene expression in the shikimate pathway is abolished in the presence of aromatic amino acids and mimicked by shikimate. *Frontiers in Plant Science*, *11*, p.459. Doi: https://doi.org/10.3389/fpls.2020.00459.

Morphological, Physiological, and Reproductive Influencing Factors of Yield in Native Iranian Fenugreek Based on Path Analysis

Mahdi Mohebodini[1*], Fatemah Mohammadzadeh[1], Asghar Ebadi[1], Karim Farman-pour-Kalalagh[2], Naser Sabaghnia[3*]

Received: 2025-09-12 Accepted: 2025-11-18

Abstract

Fenugreek is an important medicinal and nutritionally rich legume with significant potential for cultivation in semi-arid and marginal environments. Twenty-six native Iranian fenugreek populations were evaluated under field conditions through a randomized block scheme with three replications. A comprehensive set of vegetative, reproductive, and biochemical traits; including fresh and dry stem and root weights, leaf dimensions, pod and seed characteristics, and photosynthetic pigments, were recorded to assess their contribution to seed yield. Correlation analysis revealed strong positive associations among vegetative traits, such as stem biomass and leaf area, indicating coordinated plant growth. Reproductive traits, including thousand seed weight, number of pods per plant, and number of seeds per pod, were correlated with seed yield. Also, some negative correlations indicated trade-offs, particularly between root biomass and shoot branching, as well as between pod number and seed number per pod. Path analysis identified number of pods per plant (with coefficient 0.61), number of seeds per pod (0.37), and thousand seed weight (0.93), as the primary direct contributors to seed yield, whereas traits such as pod height, dry stem weight, leaf area, and carotenoid content exerted significant indirect effects through reproductive components. Bootstrap analysis with 2,000 resamples confirmed the stability and reliability of the path coefficients, highlighting the robustness of the model in accounting for multicollinearity among interrelated traits. These findings suggest that integrated selection strategies targeting both reproductive traits and supporting vegetative and physiological attributes can substantially improve seed yield in fenugreek. Genotypes combining vegetative growth, efficient photosynthetic machinery, and superior reproductive performance represent ideal candidates for breeding programs aimed at enhancing productivity.

Keywords: Correlations, Pods per plant, Seeds per pod, Thousand seed weight

1-Department of Horticultural Science, Faculty of Agricultural Science and Natural Resources, University of Mohaghegh Ardabili, Ardabil, Iran
2-Department of Horticultural Science, Faculty of Agriculture, Tarbiat Modares University, Tehran, Iran
3-Department of Plant Production and Genetics, Faculty of Agriculture, University of Maragheh, Maragheh, Iran
*Corresponding author email address: mohebodini@uma.ac.ir, sabaghnia@maragheh.ac.ir
Doi: 10.48308/PAE.2026.239699.1115

Introduction

As an annual herb belonging to the Fabaceae family, fenugreek (*Trigonella foenum-graecum* L.), has long been cultivated as a valuable medicinal and food plant in many other parts of the world. The leaves and seeds of fenugreek contain a variety of bioactive compounds, including alkaloids, saponins, trigonelline, choline, and several vitamins (Akhtar et al., 2025), which contribute to its therapeutic effects in the treatment of metabolic and digestive disorders and in lowering blood sugar and lipid levels (Syed et al., 2020). In addition to its medicinal importance, fenugreek is nutritionally rich, containing substantial amounts of protein, calcium, iron, phosphorus, and carotenoids (Tewari et al., 2024). The primary center of origin of fenugreek is believed to be the regions of North Africa and the eastern Mediterranean coast; however, historical and biogeographical evidence suggests that it was cultivated in Iran and later spread to various regions of Asia, Europe, and Africa (Seal et al., 2025). Currently, countries in the Indian subcontinent, China, Europe, and North Africa are recognized as major centers of cultivation and distribution of this species (Shahrajabian et al., 2021). The wide geographical range and environmental adaptability of fenugreek have resulted in considerable genetic diversity among its populations and ecotypes.

Because of its symbiotic association with nitrogen-fixing bacteria of the genus Rhizobium, fenugreek can meet part of its nitrogen requirement through biological fixation. Consequently, it serves as a drought-tolerant legume that can be incorporated into crop rotations to enhance soil fertility and contribute to the sustainability of agricultural systems (Mahfouz et al., 2017). Fenugreek is also relatively drought-tolerant, and traits such as root depth and branching help it withstand water limitation. The capacity for nodulation under water stress depends on both plant genotype and rhizobial strain compatibility, making selection of both host and symbiont important for improving performance in marginal environments (Sharma et al., 2021). The native populations of fenugreek exhibit high levels of variability in morphological and agronomic traits, which provides valuable potential for use in breeding programs and for selecting superior genotypes. To evaluate this diversity and identify the traits most closely related to yield performance, multivariate statistical approaches, such as path analysis, are widely applied, as they effectively explain the structural relationships among agronomic traits.

Previous studies on different species and ecotypes of legumes, including alfalfa and fenugreek, have shown that traits such as thousand-seed weight, seed weight per plant, harvest index, number of lateral branches, and chlorophyll content are among the most influential factors affecting seed yield (Camlica and Yaldiz, 2021; Azizi et al., 2025). Given the growing attention to the cultivation of native medicinal plants such as fenugreek, along with the need for efficient use of water and soil resources, identifying high-yielding and well-adapted genotypes and determining key traits contributing to yield improvement are of great importance. In addition, some investigations have report-

ed that traits related to photosynthetic efficiency, pod number per plant, and biomass accumulation are also strongly associated with yield potential under both optimal and stress conditions (Singh et al., 2025; Tilahun et al., 2025). These findings indicate that the coordination between source traits (e.g., chlorophyll concentration, leaf area index) and sink traits (e.g., pod and seed number, seed weight) is fundamental for yield determination in fenugreek and related legumes.

Given the increasing global and regional focus on sustainable agriculture and the growing demand for native medicinal crops, fenugreek is gaining renewed attention as a dual-purpose species valued for both its therapeutic and agronomic significance. Its adaptability to semi-arid and marginal environments, combined with its symbiotic nitrogen fixation capability, makes it an excellent candidate for inclusion in low-input and water-efficient cropping systems (Narayana et al., 2022). The selection of high-yielding genotypes is particularly critical due to increasing water scarcity and soil degradation in traditional cropping regions. Therefore, identifying superior genotypes and elucidating the key morphological and physiological traits that contribute most to yield improvement represent essential steps toward and productive fenugreek cultivars adapted to local environmental constraints. Despite extensive research on fenugreek's medicinal properties and general agronomic performance, important knowledge gaps remain regarding the relative contribution of morphological and physiological traits to seed yield under diverse environmental conditions. Most previous studies have focused on individual traits or simple correlations with yield, often under a single environment or management regime, which limits the ability to identify key traits with true causal effects on yield. Moreover, comparative evaluations of native fenugreek genotypes using multivariate approaches such as path analysis are scarce, particularly in semi-arid and marginal environments where water availability constrains productivity. The interaction between source-related traits (e.g., chlorophyll content and biomass accumulation) and sink-related traits (e.g., pod number and seed weight) has not been sufficiently quantified to determine their direct and indirect effects on yield formation. To address these gaps, the present study evaluates a diverse set of native fenugreek genotypes and applies multivariate statistical analyses, including path analysis, to disentangle the direct and indirect relationships among yield-related traits. By identifying the most influential morphological and physiological traits contributing to seed yield, this study provides a trait-based framework for selecting high-yielding and well-adapted fenugreek genotypes, thereby supporting breeding efforts and sustainable cultivation in water-limited environments.

Material and methods

Trial and traits

Twenty-six fenugreek populations were obtained from various areas of Iran (Table 1). A field trial was performed through a randomized block scheme with three replications. Following standard soil preparation (plowing and leveling) in April, plots measuring 50 × 80 cm were established. Uni-

form irrigation was applied throughout the growing season, and weeds were manually controlled. Fertilization followed local recommendations: 25 kg ha^{-1} N as starter, 60 kg ha^{-1} P, and 25 kg ha^{-1} K. Plots were regularly monitored for pests and diseases, and protective measures were applied as needed. At 50% flowering step, seven sample plants per plot were chosen randomly to measure the morphological and physiological traits, via standard instruments such as calipers, rulers, digital scales, and a leaf area meter (AM-3000, ADC BioScientific Ltd). They were weight of fresh stem (WFS), weight of fresh root (WFR), weight of dry stem (WDS), weight of dry root (WDR), nodes per plant (NP), number of leaves (NL), number of branches (NB), middle leaf length (MML), middle leaf width (MLW), middle leaf area (MLA), lateral leaf length (LLL), lateral leaf width (LLW), lateral leaf area (LLA), number of pods per plant (NPP), height of pods (HP), and number of seeds per pod (NSP). Chlorophyll-a (Chl.a), Chlorophyll-b (Chl.b), and Carotenoid (CAR), were quantified following Arnon's method (Rostami et al., 2022). After harvesting, seed yield (SY), was recorded and the thousand seed weight (TSW), was measured via three random samples.

Data analysis

The dataset was assessed for normality using the Shapiro-Wilk test, and phenotypic correlations among traits were calculated via Pearson's correlation coefficients. These correlations were subsequently partitioned into direct and indirect effects through path analysis. To determine the relative contribution of predictor variables to seed yield while mitigating multicollinearity, stepwise linear regression was conducted using SPSS version 26.0. Although, stepwise regression has been criticized for potential variable selection bias, it was employed in this study as an exploratory tool to identify the most influential yield-related traits from a relatively large set of intercorrelated morphological and physiological variables. Its use was justified by the primary objective of screening candidate predictors and reducing model complexity prior to path analysis, rather than for definitive causal inference. To minimize bias, stepwise regression was combined with correlation and path analyses, allowing cross-validation of selected variables through their direct and indirect effects on seed yield. This integrated analytical approach enhances the robustness of trait selection and supports biologically meaningful interpretation of yield determinants. Predictor variables were ranked based on their influence on yield variation and categorized into first-, second-, and third-order paths. Multicollinearity within each path was evaluated using tolerance; which represents the proportion of variability in a predictor not explained by other predictors, and the variance inflation factor (VIF), the reciprocal of tolerance, reflecting the degree to which a predictor's variance is inflated due to correlations with other variables. Tolerance values below 1.0 or VIF values exceeding 10 were considered indicative of significant multicollinearity. The coefficients of determination for each predictor were derived from the path coefficients, following conventional linear regression procedures. To assess the reliability of the

Table 1. Geographic characteristics of regions for the collected fenugreek (*Trigonella foenum-graecum* L.) genotypes

Code	Name	Coordinates	Rainfall	Code	Name	Coordinates	Rainfall
G1	Mashhad	36°19′N 59°32′E	250	G14	Kerman	30°15′N 57°03′E	142
G2	Gorgan	36°50′N 54°26′E	583	G15	Kashmar	35°14′N 58°27′E	237
G3	Bushehr	28°55′N 50°51′E	268	G16	Mughan-I	39°38′N 47°54′E	550
G4	Ardestan	33°22′N 52°22′E	112	G17	Jahrom	28°30′N 53°34′E	285
G5	Rezvanshahr	37°32′N 49°08′E	1800	G18	Mughan-II	39°38′N 47°54′E	550
G6	Sarab	37°56′N 47°32′E	295	G19	Ardabil	38°15′N 48°17′E	295
G7	Meshgin-I	38°23′N 47°40′E	373	G20	Urmia-II	37°32′N 45°03′E	338
G8	Tabriz-II	38°04′N 46°17′E	283	G21	Tabriz-III	38°04′N 46°17′E	283
G9	Tehran-II	35°41′N 51°23′E	231	G22	Tehran-I	35°41′N 51°23′E	231
G10	Urmia-I	37°32′N 45°03′E	338	G23	Rafsanjan	30°23′N 55°59′E	80
G11	Isfahan	32°39′N 51°40′E	130	G24	Meshgin-II	38°23′N 47°40′E	373
G12	Khansar	33°13′N 50°18′E	386	G25	Khalkhal	37°36′N 48°31′E	289
G13	Tabriz-I	38°04′N 46°17′E	283	G26	Kiashahr	37°25′N 49°56′E	1300

estimated path coefficients, standard errors were obtained through bootstrap analysis. Since breeders often require not only point estimates but also measures of variability and confidence intervals for true parameter values, resampling methods such as bootstrapping are particularly useful. In this study, the mean direct effects obtained from 2,000 bootstrap samples closely corresponded to the observed direct effects of the predictor variables.

Results and discussion

Correlation analysis (Table 2), indicated strong integration among stem, leaf, and root traits, reflecting coordinated vegetative growth in fenugreek. Positive associations between stem biomass (WFS and WDS), root weight, and leaf dimensions suggest that overall plant vigor is governed by common growth and resource-allocation processes. Rather than functioning independently, these organs develop in concert, allowing plants with greater structural biomass to support expanded photosynthetic surfaces and below-ground resource acquisition. The strong correlations between leaf size components (length, width, and area) further indicate that leaf expansion follows a coordinated developmental pattern. Larger leaves likely enhance light interception and carbon assimilation, thereby supporting greater dry matter accumulation and reproductive development. The positive association of dry stem weight with pod height and thousand-seed weight suggests that structural biomass acts as a critical source reservoir, facilitating assimilate translocation to devel-

oping seeds. Similar relationships between dry matter production and yield components have been reported in fenugreek and other legumes (Gurjar et al., 2016). Branch number showed positive relationships with leaf and pod numbers, highlighting its role in determining sink capacity. Increased branching expands the photosynthetic canopy and provides additional sites for pod formation, ultimately contributing to yield potential. This agrees with earlier findings that greater leaf area and branch number are key determinants of seed yield in fenugreek (Parmar et al., 2021). These results emphasize that yield formation in fenugreek is primarily driven by integrated vegetative vigor, where stem biomass, leaf development, and branching collectively enhance both source strength and sink capacity. Consequently, selection strategies targeting these interconnected traits may be more effective than focusing on single yield components in isolation.

Reproductive traits also demonstrated important associations, whereas seed yield (SY), was associated with dry stem weight (WDS), and thousand seed weight (TSW) (Table 2), thus plants with more vegetative growth potential tended to produce larger seeds and higher overall yield. This relationship reflects a strong source–sink linkage, in which greater stem biomass enhances assimilate storage and transport capacity, enabling more efficient partitioning of photoassimilates toward developing seeds. Consequently, plants with higher structural reserves and improved sink strength produce heavier seeds and achieve greater overall yield. Pod height (HP), was associated positively with the number of pods per plant (NPP), suggesting that taller pods may support higher pod numbers. This is in agreement with studies by Shakthi et al. (2020), who reported positive relations between yield and its attributing characters, including number of seeds per pod and 1000-seed weight. Additionally, chlorophyll pigments, Chl a and Chl b, were very strongly correlated (Table 2), reflecting coordinated photosynthetic pigment accumulation. This finding is consistent with the variability observed in chlorophyll content among fenugreek genotypes, as reported by Azizi et al. (2025), who found significant variation in chlorophyll content across different genotypes. Interestingly, some negative correlations revealed potential trade-offs in resource allocation. Dry root weight (WDR) was negatively correlated with nodes per plant (NP) and lateral leaf area (LLA), suggesting that increased root biomass may limit branching and leaf expansion, possibly reflecting resource allocation constraints. Similarly, the negative correlation between number of pods per plant (NPP), and number of seeds per pod (NSP) indicates a trade-off between pod number and seed size or number per pod, which is a classic reproductive allocation pattern in plants. Similar trade-offs have been reported in other studies, such as the one by Shakthi et al. (2020), who observed significant negative correlations between certain vegetative and reproductive traits. The observed correlations highlight that vegetative growth, leaf development, and reproductive performance are highly interdependent, while certain traits, particularly root biomass and pod-seed relationships, reflect trade-offs

that may influence ideotype selection. These findings can guide breeding programs by identifying key traits such as stem and leaf biomass that indirectly contribute to higher seed yield, as well as highlighting potential constraints due to negative associations between vegetative and reproductive allocation. Meena et al. (2021), reported the highest positive correlations among reproductive and yield components, like seed yield with pods per plant, seeds per pod, and seed yield per plot. The reproductive traits of fenugreek such as seeds per pod often load onto components separate from vegetative growth traits, indicating partly distinct genetic control (Roba and Mohammed, 2024). To examine the contribution of various traits to seed yield (SY), a regression model was fitted while accounting for multicollinearity (Table 3). Initially, all traits were included as first-order predictors, with SY as the target variable, and about half of traits exhibited high multicollinearity, so for addressing this issue, standardized coefficients were estimated using a stepwise regression strategy, which permitted identification of the most influential traits while minimizing multicollinearity effects.

Path analysis indicated that the stepwise model described almost all of SY variation, with NSP, NPP, and TSW identified as significant predictors and acceptable multicollinearity levels (Table 4). Identification of these traits as the main contributing components in seed yield of fenugreek, is verified in many field and vegetable crops like *Medicago sativa* (Sengul, 2006), *Glycine max* (Czopek et al., 2023), and *Nigella sativa* (Fikre et al., 2023). In the subsequent regression steps (Table 4), the number of pods per plant (NPP) was primarily driven by lateral leaf area (LLA) and carotenoid content (CAR), whereas dry root weight (WDR) exerted a negative effect, together explaining 63% of the variation. This pattern suggests that enhanced photosynthetic surface and pigment concentration increase reproductive sink formation, while excessive belowground biomass may divert assimilates away from pod development. Similarly, the number of seeds per pod (NSP) was positively associated with lateral leaf length (LLL) but negatively affected by LLA, indicating that leaf elongation rather than leaf expansion may be more efficient in supporting seed set, accounting for 54% of the variation. Thousand-seed weight (TSW) was positively influenced by dry stem weight (WDS) and negatively by leaf number (NL), explaining 47% of its variation. This implies that greater structural biomass supports assimilate storage and translocation to seeds, whereas excessive leaf proliferation may increase intra-plant competition for resources. Comparable relationships between leaf area, root biomass, and pod development have been reported in *Phaseolus vulgaris* and *Hibiscus sabdariffa*, reinforcing the biological relevance of these associations (Alemu et al., 2017; Fallahi et al., 2017). Further regression analysis revealed that variation in LLA was largely explained by leaf width traits, reflecting coordinated lateral leaf expansion, while WDR was positively associated with middle leaf length but negatively with pod number, supporting a trade-off between root biomass accumulation and reproductive output. Carotenoid content was strongly de-

Table 2. Pairwise correlation coefficients among morphological traits of fenugreek genotypes

	WFR	WDS	WDR	NP	NL	NB	MML	MLW	MLA	LLL	LLW	LLA	NPP	HP	NSP	TSW	Chl.a	Chl.b	CAR	SY
WFS	0.44	0.71	0.20	0.11	0.43	0.37	0.62	0.46	0.44	0.41	0.27	0.35	0.35	0.27	-0.03	0.22	0.49	0.52	0.52	0.40
WFR		0.04	0.23	-0.01	0.14	0.22	0.39	0.20	0.22	0.37	0.17	0.24	0.08	-0.19	-0.20	0.05	0.27	0.25	0.26	0.01
WDS			0.35	-0.05	0.32	0.26	0.57	0.54	0.52	0.42	0.23	0.43	0.20	0.53	0.04	0.55	0.37	0.43	0.40	0.65
WDR				-0.40	0.05	0.18	0.48	0.01	0.41	0.45	0.02	0.01	-0.39	-0.01	-0.11	0.47	0.33	0.39	0.34	0.15
NP					-0.20	0.18	-0.04	0.29	0.07	-0.08	0.27	0.35	0.56	0.39	0.23	-0.13	0.15	0.10	0.13	0.30
NL						0.52	0.23	0.26	0.08	0.17	0.39	0.25	0.36	0.09	0.08	-0.15	0.32	0.24	0.35	0.11
NB							0.41	0.48	0.53	0.57	0.63	0.54	0.38	0.23	0.04	-0.01	0.31	0.34	0.33	0.23
MML								0.51	0.70	0.50	0.22	0.41	0.11	0.04	-0.07	0.24	0.45	0.53	0.48	0.26
MLW									0.65	0.59	0.70	0.89	0.57	0.40	0.19	0.08	0.15	0.18	0.17	0.50
MLA										0.59	0.32	0.60	0.28	0.29	0.09	0.24	0.24	0.38	0.28	0.43
LLL											0.54	0.67	0.22	0.03	-0.17	0.14	0.18	0.22	0.17	0.22
LLW												0.78	0.52	0.42	0.12	-0.11	0.11	0.12	0.14	0.27
LLA													0.59	0.41	0.12	-0.02	0.01	0.01	0.02	0.40
NPP														0.34	0.44	-0.43	0.26	0.18	0.27	0.38
HP															0.36	0.39	0.21	0.21	0.23	0.71
NSP																-0.13	0.00	-0.12	0.00	0.52
TSW																	0.25	0.35	0.26	0.62
Chl.a																		0.94	0.99	0.37
Chl.b																			0.96	0.37
CAR																				0.39

Significant correlation coefficients at 24 degrees of freedom (DF) were 0.39 and 0.50 at the 0.05 and 0.01 probability levels, respectively. Traits were weight of fresh stem (WFS), weight of fresh root (WFR), weight of dry stem (WDS), weight of dry root (WDR), nodes per plant (NP), number of leaves (NL), number of branches (NB), middle leaf length (MML), middle leaf width (MLW), middle leaf area (MLA), lateral leaf length (LLL), lateral leaf width (LLW), lateral leaf area (LLA), number of pods per plant (NPP), height of pods (HP), number of seeds per pod (NSP), chlorophyll-a (Chl.a), chlorophyll-b (Chl.b), carotenoid (CAR), seed yield (SY), and the thousand seed weight (TSW).

Table 3. Regression slope (b), standard error (Std. Error), standardized coefficient (Beta), t-test statistics (t), significance level (Sig.), and collinearity statistics (Tolerance and variance inflation factor, VIF) of fenugreek traits used to predict the response variable, sed yield (SY)

	b	Std. Error	Beta	t	Sig.	Tolerance	VIF
WFS	0.06	0.053	0.037	1.09	0.33	0.08	12.36
WFR	-1.36	0.774	-0.034	-1.75	0.14	0.25	4.04
WDS	-0.25	0.310	-0.034	-0.82	0.45	0.05	18.75
WDR	0.28	3.580	0.002	0.08	0.94	0.13	7.67
NP	-0.10	0.060	-0.050	-1.67	0.16	0.10	9.69
NL	-0.01	0.005	-0.045	-1.69	0.15	0.13	7.73
NB	0.07	0.059	0.028	1.11	0.32	0.14	6.99
MML	-0.01	0.022	-0.011	-0.49	0.65	0.17	5.79
MLW	-0.05	0.038	-0.045	-1.44	0.21	0.09	10.84
MLA	0.00	0.001	-0.075	-2.07	0.09	0.07	14.28
LLL	-0.01	0.043	-0.010	-0.28	0.79	0.07	14.38
LLW	-0.04	0.022	-0.068	-1.90	0.12	0.07	14.02
LLA	0.01	0.002	0.201	3.19	0.02	0.02	43.40
NPP	0.08	0.005	0.591	16.16	0.00	0.17	6.49
HP	-0.02	0.037	-0.012	-0.48	0.65	0.14	6.93
NSP	0.45	0.020	0.398	22.78	0.00	0.30	3.32
TSW	0.67	0.017	0.928	38.78	0.00	0.16	6.24
Chl.a	-0.30	0.127	-0.297	-2.36	0.06	0.01	171.59
Chl.b	0.10	0.337	0.025	0.31	0.77	0.01	73.12
CAR	1.70	0.959	0.322	1.77	0.14	0.00	359.62

Traits were weight of fresh stem (WFS), weight of fresh root (WFR), weight of dry stem (WDS), weight of dry root (WDR), nodes per plant (NP), number of leaves (NL), number of branches (NB), middle leaf length (MML), middle leaf width (MLW), middle leaf area (MLA), lateral leaf length (LLL), lateral leaf width (LLW), lateral leaf area (LLA), number of pods per plant (NPP), height of pods (HP), number of seeds per pod (NSP), chlorophyll-a (Chl a), chlorophyll-b (Chl b), carotenoid (CAR), seed yield (SY), and the thousand seed weight (TSW)

termined by chlorophyll a and b, consistent with the coordinated regulation of photosynthetic pigments and their sensitivity to developmental and environmental factors, as previously reported in fenugreek (Kadam et al., 2017). Lateral leaf length was mainly controlled by leaf width components, whereas dry stem weight was associated with fresh stem weight and pod number but negatively influenced by pod height. In addition, leaf number was directly related to branch number, highlighting the architectural control of canopy development. These resulted indicate that seed yield formation in fenugreek

Table 4. Coefficients of determination (CD), standardized coefficients (SC), and collinearity diagnostics (Tolerance and variance inflation factor, VIF) for fenugreek genotypes in the stepwise regression model applied to predict the target traits

Target	CD	Predictor	SC	Tol.	VIF	Target	CD	Predictor	SC	Tol.	VIF
SY	0.99	NPP	0.61	0.67	1.49	WDR	0.37	MML	0.46	1.00	1.00
		NSP	0.37	0.81	1.24			NP	-0.38	1.00	1.00
		TSW	0.93	0.81	1.23						
						CAR	0.95	Chl a	0.72	0.12	8.19
NPP	0.63	LLA	0.58	1.00	1.00			Chl b	0.29	0.12	8.19
		WDR	-0.55	0.88	1.13						
		CAR	0.44	0.88	1.13	LLL	0.53	MLA	0.53	0.87	1.15
								LLW	0.52	0.78	1.28
NSP	0.54	LLL	-0.45	0.55	1.83			HP	-0.35	0.79	1.26
		LLA	0.42	0.55	1.83						
						WDS	0.66	WFS	0.62	0.93	1.08
TSW	0.47	WDS	0.66	0.90	1.11			HP	0.48	0.79	1.26
		NL	-0.36	0.90	1.11			NP	-0.30	0.85	1.18
LLA	0.83	MLW	0.68	0.51	1.97	NL	0.52	NB	0.52	1.00	1.00
		LLW	0.30	0.51	1.97						

Traits were weight of fresh stem (WFS), weight of fresh root (WFR), weight of dry stem (WDS), weight of dry root (WDR), nodes per plant (NP), number of leaves (NL), number of branches (NB), middle leaf length (MML), middle leaf width (MLW), middle leaf area (MLA), lateral leaf length (LLL), lateral leaf width (LLW), lateral leaf area (LLA), number of pods per plant (NPP), height of pods (HP), number of seeds per pod (NSP), chlorophyll-a (Chl a), chlorophyll-b (Chl b), carotenoid (CAR), seed yield (SY), and the thousand seed weight (TSW).

is governed by a balance between photosynthetic capacity, biomass partitioning, and sink development, with lateral leaf traits, stem biomass, and pigment content playing central roles. The consistency of these relationships with path analysis outcomes supports their use as biologically meaningful selection criteria in fenugreek breeding programs.

Path analysis indicated indirect contributions to response variables, whereas in SY, the indirect impact of NPP via NSP was low, and via TSW was moderately negative (Table 5). The indirect impact of NSP via NPP was relatively low, and via TSW was negatively low. Also, the indirect impacts of TSW via NPP and NSP, were negatively low, thus the importance of direct impacts of NSP, NPP, and TSW traits on SY were more than the indirect impacts (Table 5). Evaluation of the indirect impacts of LLA, WDR, and CAR on NPP, as well as indirect impacts of MLA, LLW, and HP on LLL, and indirect impacts of WFS, HP, NP on WDS were less pronounced than the direct effects (Table 5). Path analysis (Table 5) revealed that most indirect effects among traits were weak to moderate, indicating that yield formation in fenugreek is driven primarily by a few key direct relationships, with secondary modulation through interconnected vegetative and physiological traits. For example, the reciprocal indirect effects between lateral leaf length (LLL) and lateral leaf area (LLA) on seeds per pod (NSP) were small and opposite in direction, suggesting that leaf size

Table 5. Indirect path coefficients among traits of fenugreek, presented outside the diagonal

	NPP	NSP	TSW
SY	0.61	0.16	-0.40
	0.27	0.37	-0.12
	-0.26	-0.05	0.93

	LLA	WDR	CAR
NPP	0.58	0.01	0.01
	0.01	-0.55	0.14
	0.01	-0.19	0.44

	MLA	LLW	HP
LLL	0.53	0.16	-0.10
	0.17	0.52	-0.15
	0.15	0.22	-0.35

	WFS	HP	NP
WDS	0.62	0.13	-0.03
	0.17	0.48	-0.12
	0.07	0.19	-0.30

	LLL	LLA
NSP	-0.45	0.28
	-0.30	0.42

	WDS	NL
TSW	0.66	-0.12
	0.21	-0.36

	MLW	LLW
LLA	0.68	0.21
	0.48	0.30

	MML	NP
WDR	0.46	0.02
	-0.02	-0.38

	Chl.a	Chl.b
CAR	0.72	0.27
	0.67	0.29

Traits were weight of fresh stem (WFS), weight of fresh root (WFR), weight of dry stem (WDS), weight of dry root (WDR), nodes per plant (NP), number of leaves (NL), number of branches (NB), middle leaf length (MML), middle leaf width (MLW), middle leaf area (MLA), lateral leaf length (LLL), lateral leaf width (LLW), lateral leaf area (LLA), number of pods per plant (NPP), height of pods (HP), number of seeds per pod (NSP), chlorophyll-a (Chl a), chlorophyll-b (Chl b), carotenoid (CAR), seed yield (SY), and the thousand seed weight (TSW)

components influence seed set in a nuanced manner rather than through strong cascading effects. This supports the idea that seed formation is more sensitive to specific aspects of leaf morphology than to overall leaf expansion alone. Similarly, the indirect effects of dry stem weight (WDS) and leaf number (NL) on thousand-seed weight (TSW) were weak and compensatory, reflecting a trade-off between structural biomass and canopy size in regulating assimilate allocation to seeds. Moderate indirect effects observed between leaf width traits (MLW and LLW) on lateral leaf area indicate coordinated leaf development, but their influence on yield components remains largely indirect. Biochemical traits showed a clearer hierarchical structure: carotenoid content (CAR) was strongly regulated by chlorophyll pigments, particularly chlorophyll b, confirming the tight physiological coupling among photosynthetic pigments. In contrast, indirect effects involving root biomass (WDR) and pod number (NP) were weak, reinforcing the notion that excessive allocation to roots may have limited influence on reproductive traits beyond direct effects. While indirect pathways contribute to trait integration, seed

yield in fenugreek is largely governed by strong direct effects of reproductive components such as pods per plant, seeds per pod, and thousand-seed weight, consistent with earlier findings (Meena et al., 2021). However, unlike more linear yield models reported previously (Singh et al., 2019), the present study demonstrates a multilayered trait network, in which vegetative architecture and biochemical efficiency subtly shape yield components through indirect interactions. This highlights the importance of balanced selection strategies that integrate reproductive, morphological, and physiological traits to optimize fenugreek performance across diverse environments.

Bootstrap analysis with 2,000 resamples confirmed the stability of path coefficients, with low standard errors and minimal biases for all direct effects (Table 6), demonstrating the robustness of the methodology even among highly interrelated traits. The use of stepwise regression model minimized multicollinearity by maintaining relative independence among predictors at each modeling stage. Structuring predictors into primary, secondary, and tertiary, categories have been successfully applied in previous studies on crops such as *Carthamus tinctorius* (Shekari et al., 2025), and *Nigella sativa* (Sabaghnia et al., 2025), supporting the effectiveness of this strategy for analyzing complex trait interactions in fenugreek.

Path analysis further identified the most efficient paths influencing SY in fenugreek, whereas the paths HP → WDS → TSW → SY, and Chl.b → CAR → NPP → SY, were the most effective, each associated with high seed yield performance (Fig. 1). These results suggest that increasing NPP, TSW, WDS, HP, Chl.b and CAR can enhance fenugreek seed yield. The above-mentioned paths were followed by NSP → LLA → LLW → SY, in the next step, so considering leaf properties and NSP can be useful in fenugreek breeding programs. Finally, paths Chl a → CAR → NPP → SY, and LLW → LLA → NPP → SY, were the other efficient paths in seed yield performance of fenugreek. The efficient trait paths identified in current research extend the findings of Sharma and Sastry (2008), who reported number of pods per plant, number of seeds per pod, and seed yield per plot as the main direct contributors to yield. In contrast, the current analysis indicated a more integrated and hierarchical network, where vegetative vigor (HP, WDS) and photosynthetic capacity (Chl a, Chl b, CAR) indirectly enhance yield through improvements in pod number, seed size, and weight. This broader perspective indicates that yield performance is influenced not only by direct reproductive efficiency but also by other factors controlling resource capability, assimilate partitioning, and pigment-driven photosynthesis (Buckley, 2021; Liang et al., 2023). Therefore, selection for genotypes combining strong vegetative growth, efficient photosynthetic machinery, and superior reproductive traits may provide a more robust breeding strategy for increasing seed yield potential, particularly under environments, whereas physiological efficiency and biomass partitioning play key roles.

Understanding the relationships among traits is essential for improving seed yield in fenugreek. The current research demonstrated that fenugreek has a significant di-

Table 6. Bootstrapped path coefficients for target traits and predictor traits (X) in fenugreek genotypes according to the stepwise regression model

Target	Predictor	Mean	Bias	Std. Error	Sig.	Lower	Upper
SY	NPP	0.613	0.000	0.02	0.00	0.58	0.64
	NSP	0.373	-0.004	0.02	0.00	0.33	0.40
	TSW	0.927	0.003	0.02	0.00	0.90	0.96
NPP	LLA	0.580	-0.013	0.16	0.00	0.26	0.89
	WDR	-0.551	-0.008	0.14	0.00	-0.88	-0.30
	CAR	0.444	0.010	0.11	0.00	0.26	0.69
NSP	LLL	-0.446	0.003	0.04	0.04	-1.17	0.21
	LLA	0.417	-0.046	0.04	0.03	-0.44	1.03
TSW	WDS	0.665	-0.002	0.13	0.00	0.41	0.89
	NL	-0.363	-0.004	0.16	0.03	-0.69	-0.05
LLA	MLW	0.680	-0.133	0.02	0.00	0.08	0.87
	LLW	0.303	0.198	0.03	0.04	0.12	1.18
WDR	MML	0.462	0.015	0.01	0.00	0.21	0.81
	NP	-0.380	-0.012	0.02	0.03	-0.78	-0.12
CAR	Chl.a	0.719	-0.001	0.06	0.00	0.60	0.84
	Chl.b	0.289	0.003	0.06	0.00	0.18	0.40
LLL	MLA	0.528	-0.002	0.02	0.01	0.18	0.87
	LLW	0.518	0.010	0.01	0.00	0.22	0.80
	HP	-0.346	-0.022	0.02	0.11	-0.81	0.00
WDS	WFS	0.619	0.021	0.18	0.01	0.31	1.09
	HP	0.476	-0.035	0.18	0.02	0.02	0.73
	NP	-0.303	-0.003	0.15	0.06	-0.60	-0.02
NL	NB	0.521	0.001	0.18	0.04	0.15	0.86

Traits were weight of fresh stem (WFS), weight of fresh root (WFR), weight of dry stem (WDS), weight of dry root (WDR), nodes per plant (NP), number of leaves (NL), number of branches (NB), middle leaf length (MML), middle leaf width (MLW), middle leaf area (MLA), lateral leaf length (LLL), lateral leaf width (LLW), lateral leaf area (LLA), number of pods per plant (NPP), height of pods (HP), number of seeds per pod (NSP), chlorophyll-a (Chl.a), chlorophyll-b (Chl.b), carotenoid (CAR), seed yield (SY), and the thousand seed weight (TSW)

versity in morphological, biochemical, and yield-related traits that can be used in breeding programs. Correlation analysis revealed that plants with more vigorous stems tended to accumulate biomass in multiple organs, supporting the notion that vegetative vigor is closely related to reproductive potential. Similar trends have been reported in *Brassica napus* and *Triticum aestivum*, where biomass-related traits were positively correlated with components of seed yield (Zhang and Flottmann, 2016; Shamuyarira et al., 2023). Leaf traits, including median and lateral leaf dimensions, were highly correlated with each other, suggesting that selection for larger leaves may indirectly increase photosynthetic capacity and overall biomass accumulation. These results highlight the functional integration of source traits, such as leaf area and pigment content, with sink traits, such as pod and seed production, which is critical for optimizing yield. Seed yield performance was related with stem dry weight, thousand seed weight, and pod height, suggesting that stronger vegetative growth supports higher reproductive output. Photosynthetic pigments, were highly correlated, indicating coordinated accumulation of pigments. Given that photosynthetic efficiency directly affects the availability of

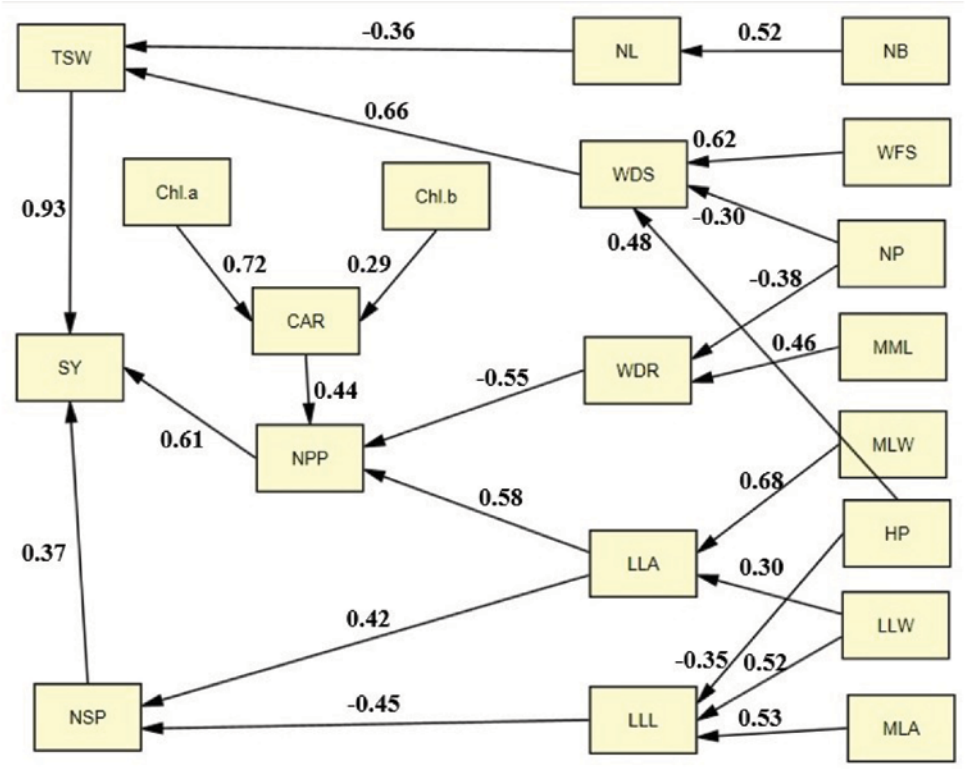

Fig. 1. Traits were weight of fresh stem (WFS), weight of fresh root (WFR), weight of dry stem (WDS), weight of dry root (WDR), nodes per plant (NP), number of leaves (NL), number of branches (NB), middle leaf length (MML), middle leaf width (MLW), middle leaf area (MLA), lateral leaf length (LLL), lateral leaf width (LLW), lateral leaf area (LLA), number of pods per plant (NPP), height of pods (HP), number of seeds per pod (NSP), chlorophyll-a (Chl.a), chlorophyll-b (Chl.b), carotenoid (CAR), seed yield (SY), and the thousand seed weight (TSW).

photosynthetic materials for reproductive development (Yaldiz and Camlica, 2022; Qiao et al., 2024), these findings emphasize the importance of considering physiological traits in addition to morphological characteristics to improve yield.

Some traits showed negative correlations, indicating potential exchange in resource allocation, whereas root dry weight was negatively correlated with node per plant and lateral leaf area, suggesting that increased root investment may limit branching or leaf expansion. Similarly, the negative correlation between pods per plant and seeds per pod suggests a reproductive exchange between pod number and size or seeds number. Such exchanges are common in legumes and reflect inherent physiological constraints, where resource allocation must balance vegetative growth, root development, and reproductive output. Understanding these trade-offs is important for ideal breeding, as it indicates that selection for one trait may affect other traits and potentially limit yield if not carefully balanced. Path analysis provided further insights into the hierarchical and dependent relationships between traits. Stepwise regression minimized multicollinearity and identified pods per plant, seeds per pod, and thousand seed weight, as the most effective predictors of grain yield. These traits collectively accounted for the majority of yield variation, supporting their use as key selection criteria in breeding programs. Path analysis revealed that vegetative and physiological traits indirectly contribute to yield by influencing reproductive components.

Conclusions

For effective fenugreek improvement, breeding programs should adopt a multi-trait selection strategy that integrates both reproductive and vegetative attributes. Prioritizing genotypes with high pods per plant, seeds per pod, and thousand-seed weight can directly enhance yield, while traits such as stem biomass, leaf area, and photosynthetic efficiency can indirectly support assimilate production and partitioning. Maintaining balanced root and shoot development is essential to avoid trade-offs between vegetative growth and reproductive output. This approach provides a practical framework for developing high-yielding, resilient fenugreek cultivars adapted to semi-arid and marginal environments, enabling more efficient and sustainable crop production.

References

Akhtar, H., Ali, Y.A., Wei, C.R., Albassam, R.S., Ahmed, F., Yasmin, A., and Ndagire, C.T. 2025. Bioactive Potential and Health Benefits of *Trigonella foenum-graecum* L.: A Comprehensive Review. *Food Science and Nutrition*, 13(9), pp. e70887. Doi: https://doi.org/10.1002/fsn3.70887.

Alemu, Y., Alamirew, S., and Dessalegn, L. 2017. Correlation and path analysis of green pod yield and its components in snap bean (*Phaseolus vulgaris* L.) genotypes. *International Journal of Research, 4,* pp. 30-36.

Azizi, M., Saeb, H., Nazari, M., Aroiee, H., and Morshedloo, M.R. 2025. Assessment of the phenotypic and physicochemical traits of nine Iranian endemic fenugreek

(*Trigonella foenum-graecum* L.). *Scientific Reports,* 15(1), pp. 3303. Doi: https://doi.org/10.1038/s41598-025-86947-3.

Buckley, T.N. (2021). Optimal carbon partitioning helps reconcile the apparent divergence between optimal and observed canopy profiles of photosynthetic capacity. *New Phytologist,* 230(6), pp. 2246-2260. Doi: https://doi.org/10.1111/nph.17199.

Camlica, M., and Yaldiz, G. 2021. Employing modern technologies in the cultivation and production of fenugreek (*Trigonella foenum-graecum* L.). In Fenugreek: Biology and applications (pp. 31-62). Singapore: Springer Singapore. Doi: https://doi.org/10.1007/978-981-16-1197-1_3.

Czopek, K., Staniak, M., Stępień-Warda, A., and Księżak, J. 2023. The effect of a superabsorbent as a soil amendment on seed yield and chemical composition of two soybean genotypes. *Archives of Agronomy and Soil Science,* 69(12), pp. 2443-2457. Doi: https://doi.org/10.1080/03650340.2022.2157408.

Fallahi, H.R., Ramazani, S. H.R., Ghorbany, M., and Aghhavani-Shajari, M. 2017. Path and factor analysis of roselle (*Hibiscus sabdariffa* L.) performance. *Journal of Applied Research on Medicinal and Aromatic Plants,* 6, pp. 119-125.

Fikre, D., Mengistu, F.G., Tsagaye, D., Ali, A., Fufa, N., and Wegayehu, G. 2023. Evaluation of black cumin (*Nigella sativa* L.) genotypes for yield and yield related parameters in potential growing areas of Ethiopia. *International Journal of Bio-resource and Stress Management, 14(7),* pp. 1037-1045.

Gurjar, M., Naruka, I.S., and Shaktawat, R.P.S. 2016. Variability and correlation analysis in fenugreek (*Trigonella foenum-graecum* L.). *Legume Research-An International Journal,* 39(3), pp. 459-465. Doi: https://doi.org/10.18805/lr.v0iOF.9286.

Kadam Vasant, B., Deore Sonali, V., and Kadam, U.B. 2017. Estimation of chlorophyll content in leaves of *Trigonella foenum-graecum* Linn. *World Journal of Pharmacy and Pharmaceutical Sciences, 6(3),* pp. 569-572. DOI:10.20959/wjpps2017.

Liang, X.G., Gao, Z., Fu, X.X., Chen, X.M., Shen, S., and Zhou, S.L. 2023. Coordination of carbon assimilation, allocation, and utilization for systemic improvement of cereal yield. *Frontiers in Plant Science, 14,* pp. 1206829. Doi: https://doi.org/10.3389/fpls.2023.1206829.

Mahfouz, S.A., Mohamed, M.A., Atteya, A.K., and Ibrahim, M.E. 2017. Impact of intercropping system on yield and quality of Lolium multiflorum and *Trigonella foenum-graecum* L. *International Journal of Pharmaceutical and Clinical Research, 9(4),* pp. 324-331.

Meena, R.S., Choudhary, S., Verma, A.K., Meena, N.K., and Mali, S.C. 2021. Estimates of genetic variability, divergence, correlation and path coefficient for morphological traits in fenugreek (*Trigonella foenum-graecum* L.) genotypes. *Legume Research,* 44(3), pp. 281-286.

Narayana, P.K., Bueno, E., Baur, A., Ahmed, S., von Wettberg, E.J.B. 2022. Fenugreek, A Legume Spice and Multiuse Crop Adapted to a Changing Climate.

In: Jha, U.C., Nayyar, H., Agrawal, S.K., Siddique, K.H.M. (eds) Developing Climate Resilient Grain and Forage Legumes. Springer, Singapore. Doi: https://doi.org/ 10.1007/978-981-16-9848-4_5.

Parmar, S., Raidas, D.K., Sahu R., Jaiswal R.K., 2021.Study of morphological and seed yield architecture in genotypes of fenugreek (*Trigonella foenum-graecum* L.). *Biological Forum – An International Journal,* 13(3), pp. 289-294.

Qiao, S., Ma, C., Li, H., Zhang, Y., Zhang, M., Zhao, W., and Liu, B. 2024. Responses of growth and photosynthesis to alkaline stress in three willow species. *Scientific Reports,* 14(1), pp. 14672. Doi: https://doi.org/10.1038/s41598-024-65004-5.

Roba, R., and Mohammed, W. 2024. Genetic variability of fenugreek (*Trigonella foenum-graecum* L.) accessions from agro-ecological and morphoagronomic traits, Ethiopia. *Beverage Plant Research*, 4(1), pp. e014 doi: 10.48130/bpr-0024-0003.

Rostami, M., Shokouhian, A., and Mohebodini, M. 2022. Effect of humic acid, nitrogen concentrations and application method on the morphological, yield and biochemical characteristics of strawberry 'Paros'. *International Journal of Fruit Science,* 22(1), pp. 203-214. Doi: https://doi.org/ 10.1080/15538362.2021.2022566.

Sabaghnia, N., Mohebodini, M., Ebadi, A., and Janmohammadi, M. 2025. Correlation and path analysis of morphologic characters associated with yield performance in black cumin. *Journal of Plant Biological Sciences,* 17, pp. 1-13. 10.22108/ijpb.2025.144116.1394.

Seal, D., Layek, A., and Pramanik, K. (2025). Origin and Geographical Distribution of Fenugreek. In Fenugreek (pp. 1-16). Apple Academic Press.

Sengul, S. 2006. Using path analysis to determine lucerne (*Medicago sativa* L.) seed yield and its components. *New Zealand Journal of Agricultural Research,* 49(1), pp. 107-115. Doi: https://doi.org/10.1080/00288233.2006.9513700.

Shahrajabian, M.H., Sun, W., Magadlela, A., Hong, S., and Cheng, Q. 2021. Fenugreek cultivation in the middle east and other parts of the world with emphasis on historical aspects and its uses in traditional medicine and modern pharmaceutical science. In Fenugreek: Biology and Applications (pp. 13-30). Singapore: Springer Singapore. Doi: https://doi.org/10.1016/B978-0-12-813148-0.00028-1.

Shakthi, P.N., Meena, K.C., Naruka, I.S., Haldar, A., and Soni, N. 2020. Performance of fenugreek (*Trigonella foenum-graecum* L.) genotypes for yield and yield contributing traits. *International Journal of Seed Spices,* 10(1), pp. 11-15.

Shamuyarira, K.W., Shimelis, H., Figlan, S., and Chaplot, V. 2023. Combining ability analysis of yield and biomass allocation related traits in newly developed wheat populations. *Scientific Reports,* 13(1), pp. 11832. Doi: https://doi.org/10.1038/s41598-023-38961-6.

Sharma, K.C., and Sastry, E.V. D. 2008. Path analysis for seed yield and its component characters in fenugreek (*Trigonella foenum-graecum* L.). *Journal of Spices and Aromatic Crops*, 17(2), pp. 69-74.

Sharma, K., Chaturvedi, U., Sharma, S.,

Vaishnav, A., and Singh, S.V. 2021. Fenugreek-rhizobium symbiosis and flavonoids under stress condition. In Antioxidants in Plant-Microbe Interaction (pp. 449-459). Singapore: Springer Singapore. Doi: https://doi.org/10.1007/978-981-16-1350-0_21.

Shekari, F., Sabaghnia, N., Abbasi, A., and Baljani, R. 2025. Evaluation of important traits affecting yield in safflower (*Carthamus tinctorius* L.). *Genetika,* 57(1), pp. 23-35. Doi: https://doi.org/10.2298/GENSR2501023S.

Singh R., Meena R.S., Choudhary S, Meena N.K., Meena R.D., Verma A.K., Ravi Y., and S Lal., 2025. Comparative evaluation of seed chlorophyll content, colour, and yield traits in Fenugreek (*Trigonella foenum-graecum* L.). *Journal of Agriculture and Ecology,* 20, pp. 18-26. 2025. Doi: https://doi.org/10.58628/JAE-2520-103.

Singh, A.K., Singh, D.R., Singh, A., Maurya, J.K., Pandey, V.P., and Sriom, D.R. 2019. Studies on character association and path analysis of yield with important yield contributing traits in fenugreek (*Trigonella foenum-graecum* L.). *Journal of Pharmacognosy and Phytochemistry,* 8(3), pp. 4616-4619.

Syed, Q.A., Rashid, Z., Ahmad, M.H., Shukat, R., Ishaq, A., Muhammad, N., and Rahman, H.U. U. 2020. Nutritional and therapeutic properties of fenugreek (*Trigonella foenum-graecum*): a review. *International Journal of Food Properties*, 23(1), pp. 1777-1791. Doi: https://doi.org/10.1080/10942912.2020.1825482.

Tewari, A., Brar, J.K., Singh, R., and Singh, A. 2024. Agronomic biofortification of fenugreek (*Trigonella foenum-graecum*) seeds with chromium: Implication on nutritional, anti-nutritional, mineral and in-vitro protein digestibility. *Food Bioscience,* 60, pp. 104481. Doi: https://doi.org/10.1016/j.fbio.2024.104481.

Tilahun, G.W., Zeleke, A.A., and Limeneh, D.F. 2025. Agronomic evaluation and genetic variability studies among fenugreek (*Trigonella foenum-graecum* L.) genotypes at Kulumsa, southeastern Ethiopia. *Ecological Genetics and Genomics,* 35, pp. 100343. Doi: https://doi.org/10.1016/j.egg.2025.100343.

Yaldiz, G., and Camlica, M. 2022. Performance of fenugreek (*Trigonella foenum-graecum* L.) genotypes towards growth, yield and UPOV properties. *Legume Research-An International Journal*, 45(1), pp. 10-17. Doi: https://doi.org/10.18805/LR-639.

Zhang, H., and Flottmann, S. 2016. Seed yield of canola (*Brassica napus* L.) is determined primarily by biomass in a high-yielding environment. *Crop and Pasture Science,* 67(4), pp. 369-380. Doi: https://doi.org/10.1071/CP15236.

Bayesian Model Averaging for Estimating Evapotranspiration and Water Footprint in Wheat Cultivation

Arezoo Kazemi[1], Zahra Aghashariatmadari[1*]

Received: 2025-08-29 Accepted: 2025-10-25

Abstract

Water resource management is of utmost importance in arid and semi-arid regions. The incorporation of the water footprint (WF) concept, which connects various water-consuming sectors in crop production, serves as a practical tool for water sector policies. The accuracy of three crop models (CropSyst, DSSAT, and SSM-Wheat) in estimating evapotranspiration (ET) was compared with the FAO Penman-Monteith (FAO56) reference model. Subsequently, the Bayesian model averaging (BMA) approach was employed to integrate the models. The application of the BMA approach resulted in a reduction of the Normalized Root Mean Square Error (NRMSE) in comparison to the individual models. Moreover, the coefficient of determination (R2), Nash-Sutcliffe efficiency (EF), and Kling-Gupta efficiency (KGE) achieved values of 99%, 0.99, and 0.96, respectively. In the subsequent step, the WF was calculated based on the yield and evapotranspiration values. The findings revealed that the green WF exceeded the blue WF in most fields, primarily due to sufficient rainfall in the area during the growth period, which allowed the plants to utilize soil moisture. Consequently, the pressure on soil moisture (effective rainfall) surpassed that on blue water. The objective of this study was to calculate the WF of wheat in Gorgan, Iran and the results highlight the requirement of effective crop management strategies to achieve a balance in water consumption, thereby minimizing the blue WF and maximizing yield. For instance, modifying the planting date to align with rainfall during the growth period can significantly reduce the blue WF.

Keywords: Crop modelling, Virtual water, Water policy, Water demand

Introduction

Access to water is a fundamental consideration in the establishment of advanced civilizations and plays a critical role in global development. The increasing depletion of freshwater resources, driven by population growth, economic advancement, and climate change, necessitates a heightened focus on water harvesting in the upcoming decade.

1-Irrigation and Reclamation Engineering Department, University College of Agriculture and Natural Resources, University of Tehran, Karaj, Iran
*Corresponding author email address: zagha@ut.ac.ir
Doi: 10.48308/PAE.2026.242112.1126

To ensure effective water resource management, thorough studies of water resources are essential. Notably, the agricultural sector consumes over 85% of global freshwater resources (D'Odorico et al. 2020), underscoring the need for a comprehensive evaluation of water availability. While access to water is recognized as a fundamental human right, the rising demand for this vital resource calls for the application of concepts such as the water footprint (WF), introduced by Hoekstra (2002), to assess freshwater utilization in terms of quantity, timing, and location.

The WF of a crop represents the volume of freshwater used in its production, encompassing the entire supply chain (Hoekstra et al. 2009). Virtual water trade and footprint studies have been conducted across different geographical scales, ranging from local to global. The WF serves as an appropriate method for estimating the international flow of water through the trade of goods. Water trade plays a vital role in national policy and food security matters. Importing crops that have high water requirements instead of relying solely on domestic production helps conserve water resources within a region.

Arunrat et al. (2022) assessed the implications of climate change on the yield and water footprint (WF) of key crops in Thailand's drought- and flood-prone areas, utilizing climate projections from the Coupled Model Intercomparison Project Phase 6 (CMIP6). Their study revealed an expected increase in precipitation, as well as maximum and minimum temperatures, highlighting that substituting rice with crops like corn, soybeans, or mung beans could mitigate climate-related impacts. Moreover, implementing twice-yearly corn cultivation and cassava planting could enhance agricultural viability in rainfed areas. Notably, the WFs of these alternatives were approximately half that of rice, designating them as viable options in the region.

The research conducted by Wang et al. (2022) revealed significant findings regarding the impact of plastic mulch on the agricultural water footprint within various crop systems. By analyzing data from 394 published studies on corn, wheat, and potatoes, the study determined that the implementation of plastic mulch resulted in notable reductions in volume of available water (VWA), global water footprint weighted by stress per unit of energy output (WFo), and water footprint per unit of net economic efficiency in crop production (WFe). Specifically, VWA decreased by 15.3% for corn, 14.1% for wheat, and 16.3% for potatoes, with corresponding reductions in WFo and WFe. Similarly, Deihimfard et al. (2022) assessed future climate implications on water footprint metrics for rainfed and irrigated wheat in Iran, predicting a decrease in total water footprint alongside an increase in the gray water footprint under future scenarios. Both studies underscore the potential for enhanced water resource management through strategic agricultural practices.

Iran, characterized by mean annual rainfall of approximately 250 mm—less than one-third of the global average—faces significant water resource challenges due to its classification as a dry and semi-arid region (Dehaghani et al., 2023). The distribution of rainfall varies significantly across the country, exacerbated by a rising population and

increasing demand for water across multiple sectors. Consequently, effective management of water resources is imperative, tailored to the existing water potential. The Water Footprint (WF) index provides insight into actual water consumption relative to regional climatic conditions, enabling a nuanced study of virtual water trade within the agricultural sector. By analyzing the interplay between climate, crop production, water consumption, and WF, stakeholders can enhance their understanding of policies and foster more efficient planning for sustainable water resource management in Iran. In the current study, an investigation was conducted to assess the individual capabilities of the DSSAT, CropSyst, and SSM-Wheat models in calculating evapotranspiration. Subsequently, the collective abilities of the models obtained through the BMA method in estimating evapotranspiration (ET) were analyzed. Furthermore, the blue and green water footprints (WFs) were calculated for the studied fields based on the output of both the individual crop models and the BMA models.

Material and methods

This study was conducted in Golestan province, which is located in the northeast of Iran. The geographical location of Golestan province, including the meteorological station and the selected farms is illustrated in Figure 1.

Data source

Wheat yield simulation using the CropSyst, DSSAT, and SSM-wheat models requires accurate data. Given the limited availability of field study data, we have utilized data from field experiments carried out at Gorgan University of Agricultural Sciences and Natural Resources for the Koohdasht, Tajan, and Zagros wheat varieties during the years 2007-08 and 2008-09 (Table 1).

The daily meteorological data for the Hashem Abad synoptic station was obtained from Iran's National Meteorological Organization. This data includes information on maximum and minimum air temperature, relative humidity, rainfall, wind speed, and sunshine hours. The station experiences an annual minimum temperature of -10°C and a maximum temperature of 45°C. Based on a 30-year average, the station receives an average annual precipitation of 527.4 mm. According to the Köppen climate classification, the station has a moderate and humid climate (Salarieh et al., 2021). The fields

Fig. 1. Location of study farms and research stations

under study have a soil texture of silty clay loam, and the experiments were conducted under normal water and nitrogen conditions. Additionally, effective management of pests, diseases, and weeds was carried out during the experiments.

WF (Water Footprint)

The WF_{total} in the crop growing process (WF_{proc}) includes the sum of blue, green, and gray components (Hoekstra et al. 2009).

$$WF = WF_{green} + WF_{blue} + WF_{gray} \quad [1]$$

Where WF_{Blue} is blue water footprint, WF_{green} is green water footprint and WF_{gray} is gray water footprint which determines the volume of water employed to eliminate pollution created by plant cultivation and crop production in the environment. The WF during the growth process is expressed in terms of production units, i.e. water volume per mass (m^3/ton, which equals Lit/kg).

In this study, by entering the required data in selected crop models (DSSAT, SSM-wheat and CropSyst), wheat evapotranspiration and yield during the growing season were calculated. A summary of the research process is shown in Figure 2**.** Finally, The WF is calculated in the form of Equations (2-4) (Ventrella et al. 2015).

$$WF_{green} = \frac{GW}{Y_{irr}} \quad [2]$$

$$WF_{blue} = \frac{BW}{Y_{irr}} \quad [3]$$

$$WF_{total} = WF_{irr} = WF_{green} + WF_{blue} = \frac{GW+BW}{Y_{irr}} \quad [4]$$

Where GW includes the volume of effective rainfall stored as moisture in the soil to be used by plants for crop production (m^3/ha), BW is considered as the water applied from surface and underground sources (m^3/ha) and Y_{irr} (ton/ha) represents the overall yield of the plant in irrigated condition (irrigation is applied in addition to rainfall).

BMA (Bayesian model averaging)

The BMA method combines the probability density function (pdf) of the predictions of different models and creates a weighted prediction distribution from them. Neuman (2003) proposed a maximum likelihood version (MLBMA) of BMA to render it computationally feasible and to allow dealing with cases where reliable prior information is lacking. Here, BMA method was applied

Table 1. Properties of the surveyed farms

Field ID	Cultivar	planting density (grains per square meter)	Planting date	References
1	Koohdasht	350	2008/1/30	(Dastmalchi et al. 2012)
2	Koohdasht	350	2007/12/29	
3	Koohdasht	350	2008/2/27	
4	Koohdasht	300	2008/12/20	(Ghadiryan 2011)
5	Tajan	300	2008/12/20	
6	Tajan	350	2008/1/30	(Dastmalchi et al. 2012)
7	Zagros	350	2008/2/27	

to combine crop models to increase accuracy in estimating wheat yield and WF. BMA is considered as an approach to combine the densities predicted by different models and generate a new prediction of their PDF. BMA method works on a dependent variable y, the training data y_t, and the sum of all predictions for members $X\{x_1,x_2,x_3,...,x_k\}$, where y is related to crop models and K represents the number of models. Based on the probability rule of sum, the PDF can display as equation [5] (Chen et al. 2015; kazemi et al. 2021).

$$p(y|x_1,x_2,\ldots,x_k)=\sum_{k=1}^{k} g(y|\theta_k).w_k \qquad [5]$$

Where g refers to the Gaussian distribution, $\Theta_k=\{\mu_k,\sigma_k, k=1,\ldots,k\}$ is the parameter vector, and W_K is statistical weight. W_K Shows the amount of correspondence between X_K and Y_T and the sum of weights of all models is 1 ($\sum_{k=1}^{k} w_k=1$).

In equation (6) the Bayesian model to calculate yield from selected crop models in Golestan province is represented (Kazemi and Aghashriatmadari 2022).

$$BMA_{Best} = 0.627\, Y_{DSSAT} + 0.373\, Y_{SSM} \qquad [6]$$

Where Y_{DSSAT} and Y_{SSM} are wheat yields calculated from DSSAT and SSM-Wheat crop models.

Evaluation: verification and validation

To evaluate the accuracy of the models in estimating the evapotranspiration, R^2, RMSE, NRMSE, EF, and KGE indicates were employed.

$$R^2=\left(\frac{n(\sum O_iS_i)-(\sum O_i)(\sum S_i)}{\sqrt{[n\sum O_i^2-(\sum O_i)^2][n\sum S_i^2-(\sum S_i)^2]}}\right)^2 *100 \qquad [7]$$

$$RMSE=\sqrt{\frac{1}{n}\sum_{i=1}^{n}(S_i-O_i)^2} \qquad [8]$$

$$NRMSE=\frac{RMSE}{\overline{O_i}} * 100 \qquad [9]$$

$$EF=1-\frac{\sum_{i=1}^{n}(S_i-O_i)^2}{\sum_{i=1}^{n}(O_i-\overline{O_i})^2} \qquad [10]$$

Where O_i,$\bar{O}_i$, n, and S_i indicate the observed values, average of the observed values,

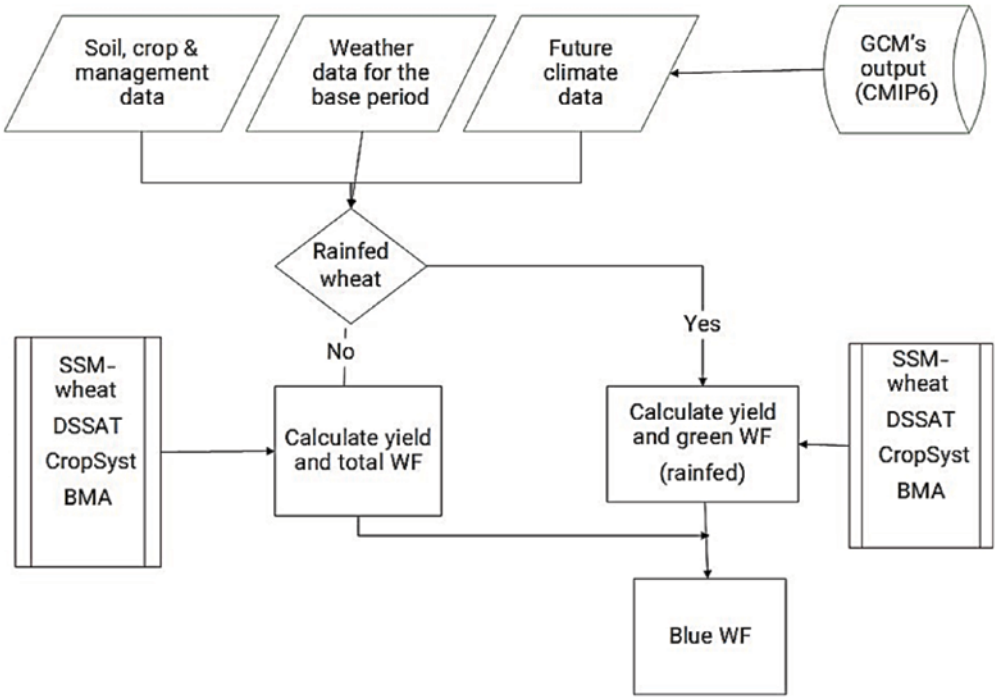

Fig. 2. Water footprint calculation flowchart (Kazemi., 2022)

number of observations, and simulated values, respectively.

The Kling–Gupta efficiency (KGE) is a goodness-of-fit indicator that was used to comprehensively evaluate the efficiency of the models, which is calculated based on Equations (11-14) (Knoben et al. 2019).

$$KGE=1-ED \quad [11]$$

$$ED=\sqrt{(r-1)^2+(\alpha-1)^2+(\beta-1)^2} \quad [12]$$

$$\alpha=\frac{\sigma_s}{\sigma_o} \quad [13]$$

$$\beta=\frac{\mu_s}{\mu_o} \quad [14]$$

Where ED is Euclidean distance from the ideal point, and r is correlation coefficient between simulations and observations. In addition, μ_o and σ_o represent the mean and standard deviation (SD) of the observations, while μ_s and σ_s indicate the mean and SD of the simulations. The KGE ranges between -infinity and 1, where a value of 1 indicates perfect agreement between the model predictions and the observed data. The KGE measures not only the accuracy of the model predictions but also its ability to reproduce the variability and timing of the observed data.

Results

ET calculating

The evapotranspiration (ET) calculated by the crop models and BMA-Best for rainfed conditions in the studied fields (Table 2). Previous studies have shown that the FAO-Penman-Monteith (FAO56) method is more accurate in estimating ET and its results are closer to lysimeter values. The International Commission on Irrigation and Drainage (ICID) and the Food and Agriculture Organization of the United Nations (FAO) have also recommended the FAO56 as the standard for comparing other models (Allen et al., 1998; Hargreaves, 1994). Therefore, the ET was calculated using the FAO56 model and used as a benchmark to compare the results of other models. The SSM-wheat and DSSAT models utilize the Priestley-Taylor (PT) method, while the CropSyst model uses the Penman-Monteith

Table 2. ET values calculated by crop models for rainfed wheat (mm in the entire growth period)

ID	CropSyst	DSSAT	SSM	BMA-Best	FAO56
1	216	185	198	190	190
2	243	212	224	216	212
3	182	168	177	171	170
4	303	307	267	292	288
5	301	304	270	291	285
6	218	182	204	190	186
7	182	175	183	178	178

(PM) method to calculate ET. The Table 2 presents the evapotranspiration values calculated by the crop models for rainfed wheat (mm) throughout the entire growth period. Furthermore, in Figure 3, the evapotranspiration estimated by the studied models is illustrated.

As indicated in Table 3, the SSM-Wheat model yields more accurate estimates of ET among the crop models, as evidenced by the NRMSE (6.18) and EF (0.92) indices. The DSSAT model achieves a higher R^2 value of 99.8 compared to the other models. However, its corresponding EF and NRMSE values are not considered satisfactory. The CropSyst model achieves a maximum KGE value of 0.91. Taking into account all evaluation indices, these models estimate ET with comparable accuracy, without a clear advantage over one another. Nevertheless, the BMA model outperforms the others, as indicated by all evaluation indices. In the BMA-Best model, the maximum R^2 value is 99.9, with an RMSE value of 3.5 mm throughout the entire growth period of wheat. This indicates a mere 3.5 mm error in ET calculation. The optimal EF value is 1, while the BMA-Best model achieves an EF value of 0.99, highlighting its high efficiency. Overall, the BMA-Best model provides the most accurate ET simulation based on all evaluation indices. In a study conducted by Attarod et al. (2015) comparing radiation and temperature-based methods of ET estimation to the FAO56 method in Gorgan, the turk method was suggested as the best model with an R^2 value of 98%. However, by employing the BMA approach, the R2 value increased to 99.9%.

Water fooprint (WF)

The values of WF_{blue} and WF_{green} derived from crop models and BMA (Table 4). As mentioned previously, the BMA-Best method demonstrates the highest level of accuracy in estimating ET. Kazemi and Shariatmadari (2022), state that the BMA model outperforms individual models in accurately estimating wheat yield. Consequently, utilizing the BMA approach to calculate the water footprint, taking into account the precise amount of wheat yield and evapotranspiration, yields more accurate results.

Total water footprint (WF_{total}) calculated by crop models and the BMA model, which is

Table 3. Comparison of statistical indices for the evaluation of crop models and BMA model performance in estimating evapotranspiration

statistical index	CropSyst	DSSAT	SSM-Wheat	BMA-Best
R^2	95.79	99.83	97.02	99.91
RMSE (mm/plant season)	21.64	50.60	13.32	3.56
EF	0.78	-0.19	0.92	0.99
NRMSE	10.04	23.47	6.18	1.65
KGE	0.91	0.79	0.76	0.96

the sum of the blue water footprint and the green water footprint, is shown in Figure 4 (in this study the grey water footprint is neglected).

The WF_{blue} values for the studied models are presented side by side in Figure 5. According to the BMA-Best model, the WF_{blue} in the fields ranges from 96 to 561 millimeters. The Koohdasht variety was planted in fields 2 and 3. However, in field 2, which was planted on 29/12/2007 during a period of heavy rainfall and the potential for more rainfall usage, the WF_{blue} is approximately 100 millimeters lower compared to field 3, which was planted on 27/2/2008. Fields 1 and 6 were both planted on 30/01/2008 and managed similarly in terms of agronomics. Nevertheless, field 1 was planted with the Koohdasht variety, while field 6 was planted with the Tajan variety. This difference in varieties has resulted in variations in the water footprint for these fields. It can be concluded that the water footprint of the Tajan variety is higher compared to that of the Koohdasht variety. The calculated water footprint for fields 4 and 5 also supports this finding.

The quantity of WF_{green} for each assessed model is presented in Figure 6. According to the BMA-Best model, the amount of WF_{green} on farms ranges from 455 to 553 m^3 per ton. The highest value of WF_{green}, 553 m3 per ton, is associated with farm 6, which was

Table 4. Blue and green WF values for irrigated conditions (m^3/ ton)

Field	CropSyst		DSSAT		SSM-wheat		BMA-Best	
ID	WF_{green}	WF_{blue}	WF_{green}	WF_{blue}	WF_{green}	WF_{blue}	WF_{green}	WF_{blue}
1	506	286	457	427	451	455	455	437
2	558	285	441	371	492	163	460	296
3	470	284	495	482	422	289	464	400
4	468	170	472	115	497	58	480	96
5	519	169	524	122	579	249	541	163
6	553	289	557	498	548	521	553	507
7	446	331	456	559	480	564	465	561

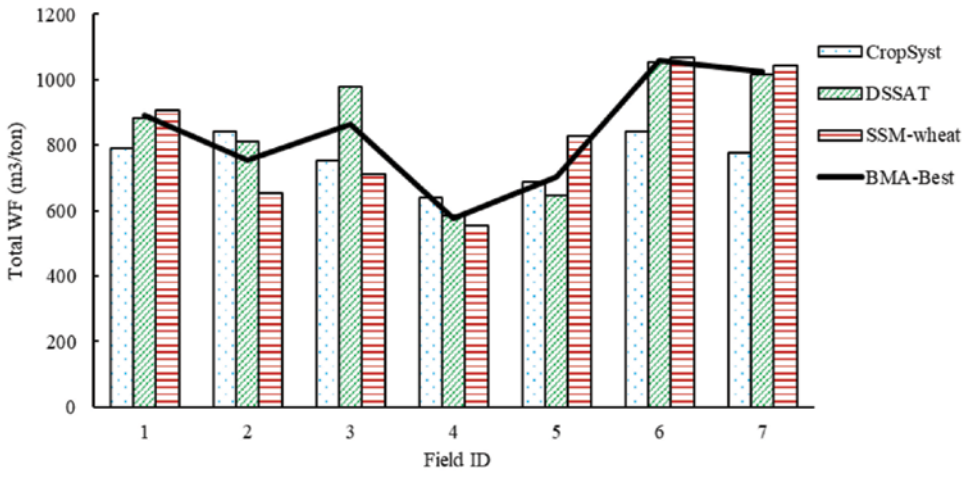

Fig. 4. Comparison of total WF calculated by individual crop models and BMA

cultivated on January 30, 2008, using the Tajan variety. Conversely, the lowest value is observed in farm 1, also cultivated on the same date but with the Koohdasht variety. Farms 4 and 5 have identical planting dates. However, farm 5, where the Tajan variety is planted, exhibits a higher amount of WF_{green}. Both farms 2 and 3 are cultivated using the Koohdasht variety. Nevertheless, farm 2, which was cultivated earlier on December 29, 2007, has a lower WF_{green} value.

A comparison of the amounts of WF_{blue}, WF_{green}, and WF_{total} in the farms analyzed using the BMA-Best model is illustrated in Figure 7. The highest WF_{total}, which accounts for the sum of WF_{blue} and WF_{green}, is observed in farm 6. This is attributed to the relatively later cultivation date (January 30, 2008) and the usage of the Tajan variety. On the other hand, farm 4 exhibits the lowest WF, primarily due to the cultivation of the Koohdasht variety and an earlier planting date (December 20, 2008) compared to the other farms. These findings indicate that the differences in WF among the farms can be related to variations in planting dates and wheat varieties.

Based on the results, the WF_{green} is higher

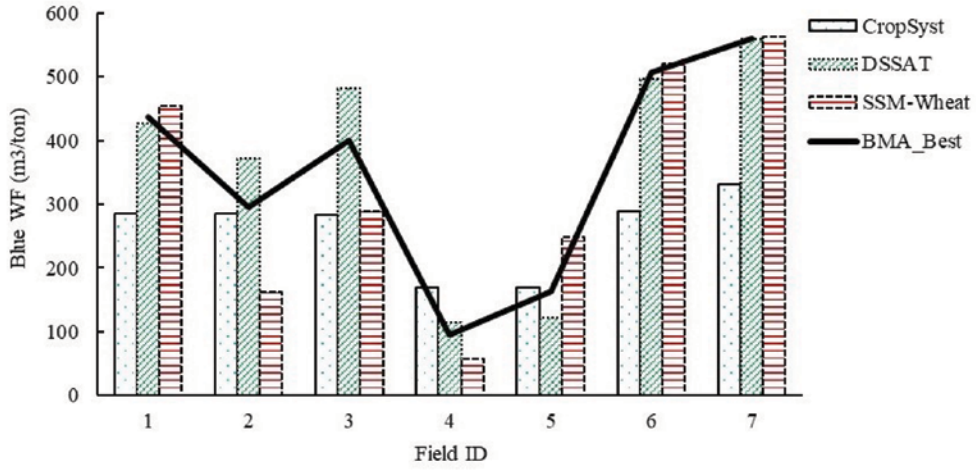

Fig. 5. Comparison of blue WF calculated by individual crop models and BMA

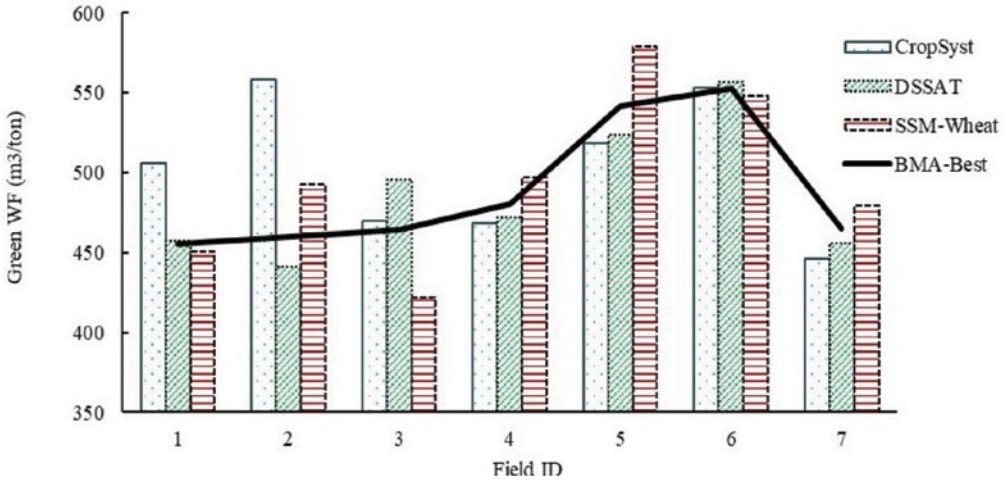

Fig 6. Comparison of green WF calculated by individual crop models and BMA

than the WF_{blue} in all farms except Farm 7, indicating that the pressure on soil moisture (effective rainfall) is greater than irrigation water for wheat production. In Farm 7, the late cultivation prevents the use of effective rainfall during the growth period, resulting in the need to compensate for the water requirement using blue water. These findings are consistent with previous studies in this field, highlighting the significant role of green water in wheat production. According to Anafajeh et al. (2020), the WF_{green} for wheat production is higher than the WF_{blue} in Khuzestan province. Additionally, Aligholinia et al. (2020) suggest that the highest WF_{green} for wheat can be found in the northern and western parts of the country due to abundant rainfall in these areas.

As mentioned before, the main water requirement for wheat production in the farms is met through green water. However, the lack of blue water utilization leads to a decrease in yield. Therefore, careful planning is necessary to balance the use of blue water through supplementary irrigation in order to minimize the WF_{blue} and maximize yield.

The WF_{total} for wheat cultivation under WF_{irr} and $WF_{rainfed}$ conditions is presented in Figure 8. It can be observed that the WF for wheat cultivation under rainfed condition is higher than that under irrigated condition in all farms except Farms 4 and 5. The pres-

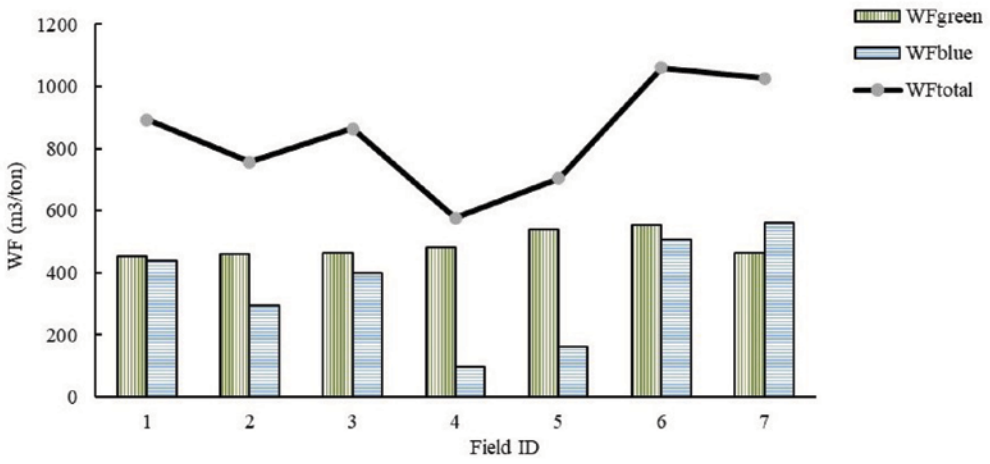

Fig. 7. Comparison of blue, green and total WF calculated by BMA-Best

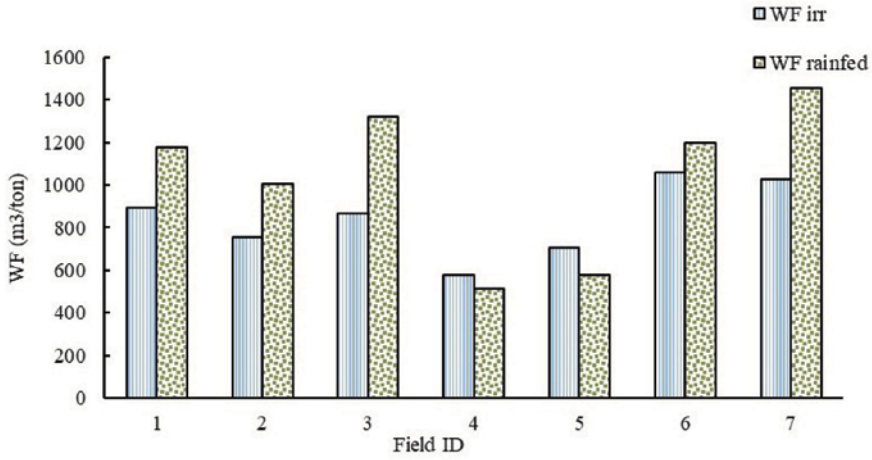

Fig. 8. Comparison of irrigated and rainfed wheat WF calculated by BMA-Best

ence of irrigation increases yield compared to the rainfed condition in all mentioned farms, resulting in a decrease in the WF for wheat cultivation under irrigated condition compared to that under rainfed condition. Furthermore, Ababaei and Ramezani (2016) have argued that the WF_{total} of rainfed wheat is higher than that of irrigated wheat in Golestan province. Farms 4 and 5 have earlier planting dates, allowing for the use of rainfall. Irrigating these farms increases water consumption and the WF for irrigated wheat without increasing yield compared to the rainfed condition. In other word, their early planting, which allows for synchronization of the rainy season with the growing season, resulting in the plants' water needs being met through precipitation. In essence, irrigation does not contribute to an increase in wheat yield compared to rainfed conditions. Therefore, determining the appropriate planting date can be instrumental in conserving surface and underground water consumption.

Discussion

The present study assessed the accuracy of the crop models DSSAT, CropSyst, and SSM-Wheat, along with the BMA approach, in estimating ET (evapotranspiration). The evaluation was based on the NRMSE, R^2, KGE, and EF indices, and the results were compared with those of FAO56, a standard method proposed by FAO (Allen et al. 1998; Hargreaves 1994). The findings indicate that all three investigated crop models estimate ET with similar accuracy, without any clear advantage of one model over the others. However, the application of the BMA approach significantly enhances the accuracy of ET estimation. In the BMA-Best model, the values of NRMSE, R2, KGE, and EF were found to be 1.65, 99.9, 0.96, and 0.99%, respectively.

Moreover, the amount of WF (water footprint), including WF_{blue} and WF_{green}, for the studied farms was determined by utilizing the values of ET and yield calculated by the individual models under study and the BMA-Best. According to the outputs of the BMA-Best model, the farm cultivating the Tajan variety and planting it later than other farms had the highest WF. On the other hand, the farm cultivating the Koohdasht variety and planting it earlier than other farms had the lowest WF. Furthermore, WF_{green} was found to be higher than WF_{blue} in most farms. The cultivation date was identified as a crucial factor influencing the WF of the crop. For future studies, it is recommended to focus on comparing the ET estimated by the models to the lysimeter-based measurements.

Acknowledgments

The research was supported by the University of Tehran. The authors would like to express their special thanks to the vice chancellor for research affairs. This research did not receive any specific grant from funding agencies in the public, commercial, or not-for-profit sectors.

References

Ababaei, B. and Ramezani Etedali, H., 2016. Estimation of water footprint compartments in national Wheat Production. *Water and Soil, 29 (6)*, 1458-1468. https://

doi.org/10.22067/jsw.v29i6.36927. (In Persian)

Aligholinia, T., Ghorbani, K., Rezaie, H., Gorbani nasr abad, G., 2020. Evaluation and simulation of water footprints of agricultural crops in different climates of Iran considering of climate change scenarios. *Iran-Water Resources Research, 16(3)*, 80-97. https://doi.org/20.1001.1.17352347.1399.16.3.6.4. (In Persian)

Allen, R. G., Pereira, L. S., Raes, D., Smith, M., 1998. Crop evapotranspiration-guidelines for computing crop water requirements-FAO irrigation and drainage paper 56. FAO, Rome, 300(9), D05109.

Anafajeh, Z., Banayan aval, M., Rezvani Moghaddam, P., Andarzian, B., 2020. Estimation and zoning of water footprints in wheat production (Case study: Khuzestan Province). *Iranian Journal of Irrigation & Drainage, 14(3),* 993-1003. https://doi.org/20.1001.1.20087942.1399.14.3.22.9. (In Persian)

Arunrat, N., Sereenonchai, S., Chaowiwat, W., Wang, C., 2022. Climate change impact on major crop yield and water footprint under CMIP6 climate projections in repeated drought and flood areas in Thailand. *Science of the Total Environment, 807*, 150741. https://doi.org/10.1016/j.scitotenv.2021.150741.

Attarod, P., Sadeghi, S. M. M., Fathizadeh, O., Motahari, M., Rahbari Sisakht, S., Ahmadi, M. T., Bayramzade, V., 2015. Temperature- and radiation based methods against the standard FAO Penman-Monteith for estimating the reference evapotranspiration (ET0) in Gorgan. *Forest and Wood Products, 68(2)*, 359-369. https://doi.org/10.22059/jfwp.2015.54837. (In Persian)

Chen, Y., Yuan, W., Xia, J., Fisher, J. B., Dong, W., Zhang, X., Feng, J., 2015. Using Bayesian model averaging to estimate terrestrial evapotranspiration in China. *Journal of Hydrology, 528,* 537-549. https://doi.org/10.1016/j.jhydrol.2015.06.059.

D'Odorico, P., Chiarelli, D. D., Rosa, L., Bini, A., Zilberman, D., Rulli, M. C., 2020. The global value of water in agriculture. *Proceedings of the national academy of sciences, 117(36),* 21985-21993. https://doi.org/10.1073/pnas.2005835117.

Dastmalchi, A., Soltani, A., Latifi, N., Zeinali, E., 2012. Evaluation of cropsyst-wheat for simulating of development, growth and yield in response to planting date. *Iranian Journal of Field Crops Research, 10(3),* 511-521. https://doi.org/10.22067/gsc.v10i3.17798. (In Persian)

Dehaghani, A. M., Gohari, A., Zareian, M. J., Haghighi, A. T., 2023. A comprehensive evaluation of the satellite precipitation products across Iran. *Journal of Hydrology: Regional Studies, 46,* 101360. https://doi.org/10.1016/j.ejrh.2023.101360.

Deihimfard, R., Rahimi-Moghaddam, S., Collins, B., Azizi, K., 2022. Future climate change could reduce irrigated and rainfed wheat water footprint in arid environments. *Science of the Total Environment, 807,* 150991. https://doi.org/10.1016/j.scitotenv.2021.150991.

Ghadiryan, R., Soltani, A., Zeinali, E., KALATEH, A. M., Bakhshandeh, S., 2011.

Evaluating non-linear regression models for use in growth analysis of wheat. *Journal of Crop Production, 4(3),* 55-77. https://doi.org/20.1001.1.2008739.1390.4.3.4.0. (In Persian)

Hargreaves, G. H., 1994. Defining and using reference evapotranspiration. *Journal of irrigation and drainage engineering, 120(6),* 1132-1139.

Hoekstra, A. Y. and Chung, P. Q., 2002. Virtual water trade: a quantification of virtual water flows between nations in relation to international crop trade. *Value of water research report series (11).* https://doi.org/10.4236/eng.2023.157032.

Hoekstra, A. Y., Chapagain, A. K., Aldaya, M. M., Mekonnen, M. M., 2009. Water footprint manual: State of the art 2009. *Water footprint network*, Enschede, the Netherlands, 255.

Kazemi, A. and Aghashariatmadari, Z., 2022. Application of Bayesian model averaging (BMA) approach to estimating wheat yield in Golestan province. *Iranian Journal of Soil and Water Research, 53(9),* 2045-2059. https://doi.org/10.22059/ijswr.2022.343977.669286. (In Persian)

Kazemi, A., Ghahreman, N., Ghamghami, M., Ghameshloo, A., 2021. Application of Bayesian model averaging (BMA) approach for estimating evapotranspiration in Gorganrood-Gharesoo Basin, Iran. *Journal of Agricultural Science and Technology, 23(6),* 1395-1409.

Knoben, W. J., Freer, J. E., Woods, R. A., 2019. Inherent benchmark or not? Comparing Nash–Sutcliffe and Kling–Gupta efficiency scores. *Hydrology and Earth System Sciences, 23(10),* 4323-4331. https://doi.org/10.5194/hess-23-4323-2019.

Neuman, S. P., 2003. Maximum likelihood Bayesian averaging of uncertain model predictions. *Stochastic Environmental Research and Risk Assessment, 17(5),* 291-305. https://doi.org/10.1007/s00477-003-0151-7.

Salarieh, P., Khoshravesh, M., Norooz Valashedi, R., Kiani, A., 2021. Investigation the effect of climate change and planting Date on Maize Yield using WOFOST Model. *Iranian Journal of Soil and Water Research, 52(10),* 2515-2527. https://doi.org/10.22059/ijswr.2021.327604.669034. (In Persian)

Ventrella, D., Giglio, L., Charfeddine, M., Dalla Marta, A., 2015. Consumptive use of green and blue water for winter durum wheat cultivated in Southern Italy. *Italian Journal of Agrometeorology, 1,* 33-44.

Wang, L., Li, L., Xie, J., Luo, Z., Sumera, A., Zechariah, E., Chen, Y., 2022. Does plastic mulching reduce water footprint in field crops in China? A meta-analysis. *Agricultural Water Management, 260,* 107293. https://doi.org/10.1016/j.agwat.2021.107293.

Vegetation Survey of the Forest Floor in the Sarabtaveh Region of Boyer-Ahmad County (Kohgiluyeh and Boyerahmad, Iran)

Yousef Askari[1*], Hooman Ravanbakhsh[2]

Received: 2025-09-10 Accepted: 2025-12-22

Abstract

This study was conducted in the Sarabtaveh forest stand in Boyer-Ahmad County, Kohgiluyeh and Boyer-Ahmad Province. One-hectare vegetation was selected and sampled using a nested design comprising four 100 m² macro-plots for general survey, with detailed cover assessment in twenty 1 m² micro-plots distributed. The density of species in the sample plots, as well as species frequency, were then determined and reported. In the next stage, biodiversity indices were calculated based on the density of plant species in the sample plots. The results show, the ground vegetation cover at the time of sampling in the Sarabtaveh site was 45.50%. In the region 24 plant species were identified. The Poaceae family with 7 species, and the Fabaceae and Ranunculaceae families, each with 2 species, were the largest plant families in the studied area, respectively. More than half (54%) of the species in this habitat were annual plants (Therophytes), while 21% were Hemicryptophytes, 4.2% were Chamaephytes and Phanerophytes, 8.3% were Geophytes (Cryptophytes), and 12.5% were Phanerophytes. The total number of plants counted in the 20 micro-plots was approximately 1,864 individuals, with an average of about 93 plant individuals per square meter. The highest number of counted individuals belonged to the species *Bromus tectorum* (1,084 individuals), followed by the species *Bromus sterilis* (163 individuals). In other words, over 60% of the plant density in the studied sample plots was attributed to these two short-lived annual species. The abundance of plants from families such as Poaceae, Fabaceae, and Ranunculaceae in the region can be related to vegetation degradation caused by human activities and excessive livestock grazing, a pattern that has also been observed in other vegetation studies conducted in areas with intense human impact. This quantitative baseline is essential for evaluating the long-term effects of coppice management and grazing in the Zagros forests and can inform regional conservation strategies.

Keywords: Poaceae, Species frequency, Therophytes, Vegetation, Yasouj

Introduction

Identifying vegetation cover and floristic composition constitutes the basis of ecological research. It also provides strategies for

1- Forest, Rangeland and Watershed, Kohgiluyeh and Boyerahmad Research Division, Agriculture and Natural Resources Research and Education Center, AREEO, Yasouj, Iran
2- Research Institute of Forests and Rangelands, Agricultural Research Education and Extension Organization (AREEO), Tehran, Iran
*Corresponding author email address: Yousef.askari@gmail.com
Doi: 10.48308/PAE.2026.242839.1133

assessing ecosystem capabilities from multiple perspectives. Furthermore, it serves as an effective factor in assessing and evaluating the current status and predicting the future condition, playing a significant role in implementing management practices in the region (Qahremaninejad and Nafisi, 2011). Studies on the vegetation of Iran, given vegetation capabilities rich plant biodiversity, have a long history. Examining the history of floristic studies indicates that the cornerstone of modern floristic studies in Iran dates back to the research of the German explorer Kaempfer in 1684 AD, who collected plants from areas of Isfahan, Shiraz, and other parts of Iran (Jafari and Zarifian, 2015).

Vegetation cover plays a role in soil formation and water and soil conservation through its above-ground and below-ground parts, controls gaseous exchanges and the water and nutrient cycles (Ferretti and Fischer, 2013). The structure it creates affects wildlife habitat and fertility (Schulz et al., 2009). In recent decades, human and natural disturbances have impacted the functioning of natural ecosystems, highlighting the necessity of assessing the current status, understanding the trends of changes, and the future outlook. The most common concerns that have been considered as international criteria for assessing the sustainability of forestry activities are the changes in species composition and diversity, structural diversity, and the abundance of non-native species (Willis and Whittaker 2002; Schulz et al., 2009). Biodiversity plays a significant role in the function of forests, and assessing it based on various indices is essential for understanding forest ecology and constitutes the foundation of forest conservation (Ravanbakhsh et al., 2024). In forestry studies, species diversity is usually examined, and indices such as diversity, species richness, and evenness are extracted (Lessa derci et al., 2020). Species richness refers to the number of species, and evenness is related to how individuals are distributed among species (Ejtehadi et al., 2004). In a study of plant species biodiversity in natural stands and western Hyrcanian forests, it was found that the Simpson and Shannon-Wiener diversity and the Margalef richness indeces were not statistically significant, while the Menhinik richnessand the Camargo and Smith-Wilson evenness indices showed significant differences (Bazyari et al., 2021).

In a comprehensive flora collection project, Jafari Kukhdan (2013) reported as part of a research project to collect, identify, and establish the herbarium of the provincial flora under the former Jahade Sazandegi, collected about 10,0000 plant samples and reported 95 families, 350 genera, and 900 plant species from all over Kohgiluyeh and Boyer-Ahmad Province. Furthermore, in a report on the status of native plants in the Central Zagros as part of the international project for biodiversity conservation in the Central Zagros landscape, covering an area of 2.5 million hectares in the provinces of Chaharmahal Bakhtiari, Isfahan, Kohgiluyeh and Boyer-Ahmad, and Fars, 2560 species were introduced (Jafari Kukhdan, 2013). Hamze et al. (2008) in a floristic and phytosociological study of the Chaharzabar forests in Kermanshah, identified 161 species and infraspecific units belonging to 124 genera and 40 families, and described the plant

community *Astragalus tortousi – Quercetum persicae* with two sub-communities. In this area, therophytes were the dominant life form, and from a chorological perspective, most species belonged to the "Irano-Turanian" region. Dehshiri et al. (2019) in a floristic study of the Eslamabad-e Gharb area in the Central Zagros, stated that about 65% of the flora belongs to the Irano-Turanian region. Additionally, in an ecophytosociological study of the western Dena protected area, while introducing the plant communities of the region, 65 families, 400 genera, and 750 species were identified (Jafari Kukhdan, 2003). In similar studies in the eastern Dena protected area, 67 families, 256 genera, and 410 species were reported, and from the Del protected area, 67 families, 174 genera, and 224 plant species were collected (Hosseini, 2014). According to studies by Jafari and Zarifian on Mount Savior, 295 species from 202 genera belonging to 62 plant families were reported, of which 47 were endemic to Iran, 47 were rare, 60 were medicinal, and 52 were toxic (Jafari and Zarifian, 2015). Studies by Karimian et al. (2012) on identifying the medicinal and industrial properties of forest species in Kohgiluyeh and Boyer-Ahmad Province showed that 41 species from 23 families have medicinal applications. Besides, 16 species having a tree growth form and 25 being shrubs which form these, 10 identified species fell within the Rosaceae family (Karimian et al., 2017). From the protected areas of Kuh-e Khayiz and Kuh-e Sorkh, with an area of approximately 32,232 hectares, 71 families, 208 genera, and 278 species, and 43 families, 90 genera, and 116 species were reported, respectively. From the protected area of Sulk, covering about 2,322 hectares, 40 families, 92 genera, and 184 species were reported (Jafari Kukhdan, 2011).

Despite these numerous regional studies, long-term monitoring using permanent plots in the specific forest under study is still lacking. Therefore, this study aims to establish permanent sample plots for periodic monitoring of forest floor vegetation, as no permanent sample plots had been previously established for long-term and periodic studies in these forests. Furthermore, this research investigates the floristic composition, cover, and species diversity of plants within the monitoring sample plots in the studied forest.

Material and methods

Initially, through a forest reconnaissance walk and utilizing the expertise of specialists, a one-hectare sample plot was selected in the Sarabtaveh forest habitat in Boyer-Ahmad County. Within this sample plot, 20 of 1 m^2micro-plots were established and surveyed using a specific pattern to study the forest floor cover (Figure 1).

According to the European ICP Forests program (2016), a 400 m^2 sampling area for vegetation cover is recommended, described as a feasible and realistic compromise among various methods. This area can be achieved from several smaller sampling units without restrictions on their shape or number (Figure 1). This size 400 m^2, composed of four 100 m^2 sub-plots was adopted for the sample plots in the vegetation cover study of this project.

In each sample plot, the percentage of forest

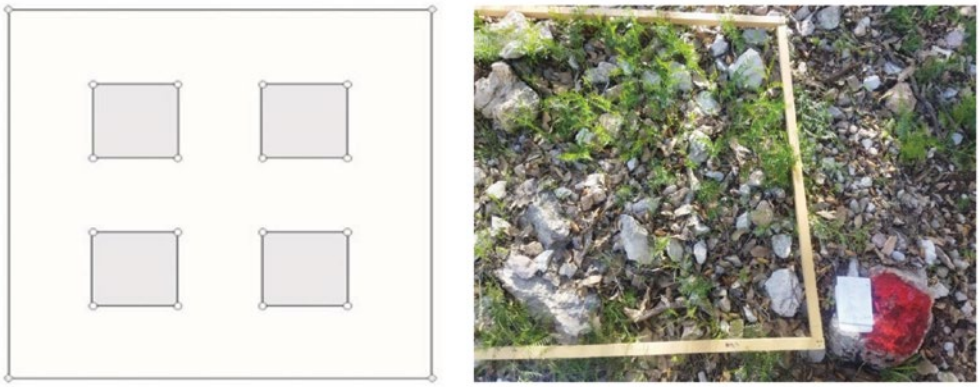

Fig. 1. Sampling design consisting of four 100 m² sample plots with the implementation of 20 micro-plots

floor cover was first recorded. Subsequently, environmental data for the plots were meticulously documented, including topographic status (slope, aspect, and elevation), soil erosion status (surface/low erosion, rill erosion/moderate, rill-gully erosion/significant), spatial location, percentage of litter, and percentage of bare soil (ICP Forests, 2016). All existing plant species were separately measured and recorded based on the characteristics of density (count within the sample plot) and life form. Table 1 was used to record species density when counting certain species was impossible due to their high abundance and density.

In addition to the micro-plot studies, a comprehensive floristic survey was conducted across the entire one-hectare plot to record all plant species present. For this general survey, only species presence was noted, documented either on a separate form or on the form of the nearest micro-plot. Following field collection, plant species were identified using the authoritative references *Flora of Iran* (Assadi et al., 1988–2019) and *Flora Iranica* (Rechinger, 1963-2005). A descriptive floristic list was compiled, including plant family distribution, biological life forms (following Raunkiaer's classification), and observed phenology at the time of sampling. Species density (within micro-plots and for the total area) and frequency were calculated. To quantify biodiversity, standard indices were computed based on species density data. These included: richness (Menhinick and Margalef), evenness (Pielou and Shel-

Table 1. Summary of the Braun-Blanquet (1964) abundance-dominance scale

Scale (Class)	Frequency range	N individual/ m²
1	Rare	1- 4
2	Low frequency	5-14
3	Moderate frequency	15-29
4	Many individuals	30-99
5	Very numerous individuals	>100

don), and diversity (Shannon-Wiener and Simpson) indices. This suite of indices was chosen to provide a multifaceted assessment of the vegetation's taxonomic structure, as is standard practice in comparative forest ecology (Magurran, 2004). Recent observations (Duelli and obrist, 2003) have shown that when undergraduate biodiversity students in entomology lectures have to choose one of the two communities shown in Figure 2 (without seeing the text below them) they consider to be more diverse, more than half of them decide for the left population, because they consider evenness to be of greater importance than species numbers. When individuals from other disciplines were asked during lectures and seminars, particularly conservationists and extension workers in agriculture and forestry, species numbers are decisive. In recent years, indices involving evenness have essentially fallen out of favour, mostly because they are difficult to interpret (Gaston, 1996). Particularly in agriculture and forestry, standardized methods frequently result in the collection of large numbers of numerous single species. This causes a sharp decline in evenness, thereby yielding low diversity values notwithstanding relatively high species richness.

The software packages Excel 2007 and SPSS 22 were used for the analysis of quantitative and qualitative variables, while PAST version 3 was employed for calculating the biodiversity indices. To assess data normality, the Kolmogorov-Smirnov test was employed, and the homogeneity of variances was checked using Levene's test.

Results

A total of 24 plant species were identified, belonging to 16 genera and 14 plant families. The Poaceae family with 7 species, followed by the Fabaceae and Ranunculaceae families, each with 2 species, were the highest plant families in the studied area, respectively (Figure 3).

According to the obtained results, more than half (54%) of the species present in the Sarabtaveh site were therophytes (annual plants), 21% were hemicryptophytes, 4% were chamaephytes, 12.5% were phanerophytes, and 8% were geophytes (cryptophytes) (Figure 4).

The phenological stage of the species in the

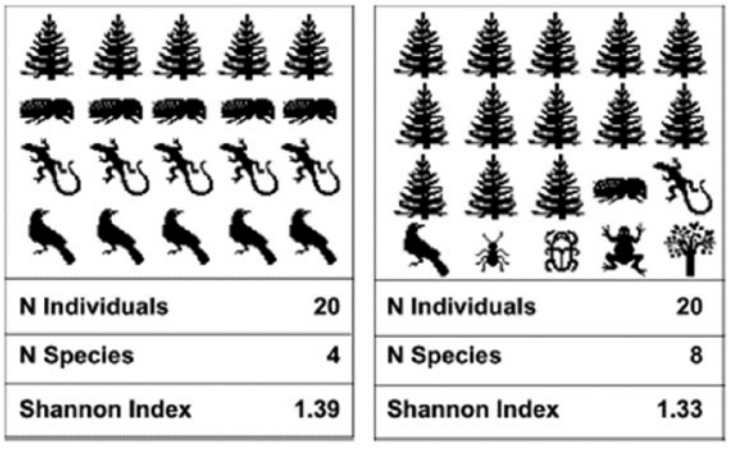

Fig. 2. Comparing differences among populations for biodiversity evaluation (Duelli and Obrist, 2003).

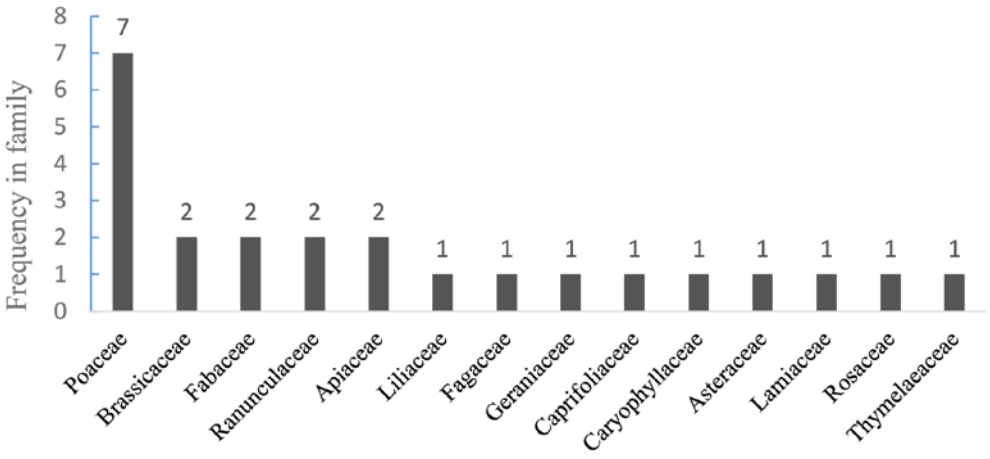

Fig. 3. Species frequency distribution in plant families

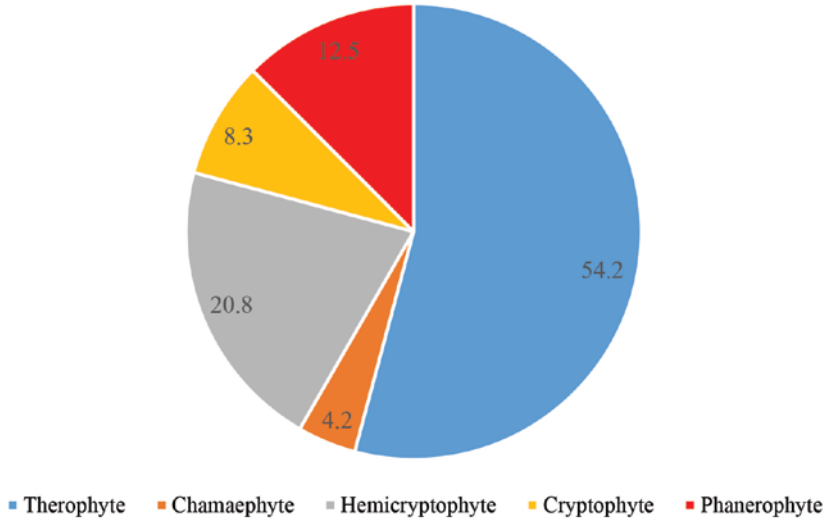

Fig. 4. The life form of plant species in the region based on Raunkiaer's classification (Raunkiaer, 1934).

studied area at the time of data collection the first week of Khordad 1400, late May 2021, has been determined. In total, 4.8% of the present species were in the seed dispersal stage, 20% were at the stage of flower formation where the plant was dry but still green, 33.3% had completed their vegetative and reproductive stages and were fully dried, and 43% were in the vegetative stage with only visible leaves (Figure 5).

Plant species density in the forest floor sample plots

The total number of plants counted in the 20 micro-plots was approximately 1, 864 individuals, resulting in an average density of about 93 plant individuals/ m^2. Among the species, *Bromus tectorum* (1,084 individuals) and *Bromus sterilis* (163 individuals) exhibited the highest counts (Figure 6).

In other words, over 74% of the plant density in the studied sample plots was attributed to these three short-lived annual species (Table 2).

Out of the total 1,864 individuals counted in the micro-plots of the Sarabtaveh site, 95.8% belonged to species with the therophyte life

form, 3.3% to hemicryptophytes, and less than 1% to chamaephyte and cryptophyte life forms (Figure 7).

Plant species diversity in the habitat

The species richness, evenness, and diversity indices for the forest floor micro-plots in the Sarabtaveh region are presented in Table 3. According to the results, the number of species per micro-plot, as a simple index of species richness, averaged 5.1 species/ micro-plot/per square meter. The maximum species richnesswas 11 species/micro-plot, while the minimum was one species/ micro-plot.

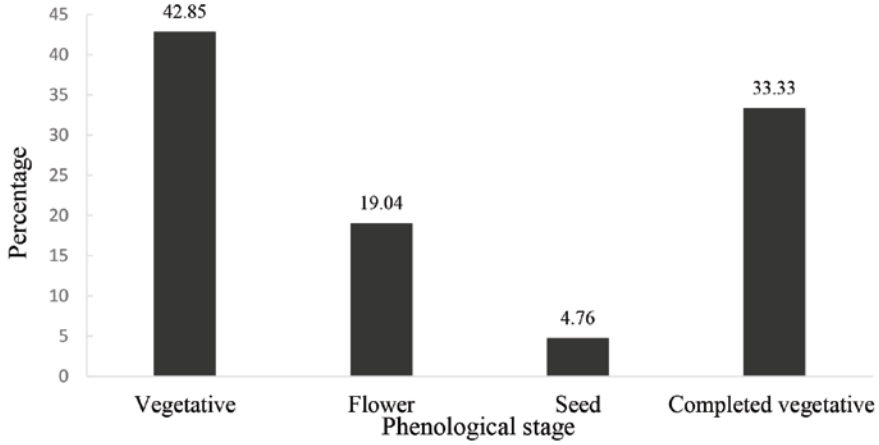

Fig. 5. The overall phenological status of different species in the region

Fig. 6. The species *Bromus tectorum* (left side) and *Bromus sterilis* (Schematic image)

Table 2. Number of species related to different density classes (average of all sample plots)

Density class (Individual/ m^2)	species Number/class	Ratio (%)
1-4	5	23.8
5-14	4	19.04
15-29	5	23.8
30-99	1	4.76
> 99	6	28.57

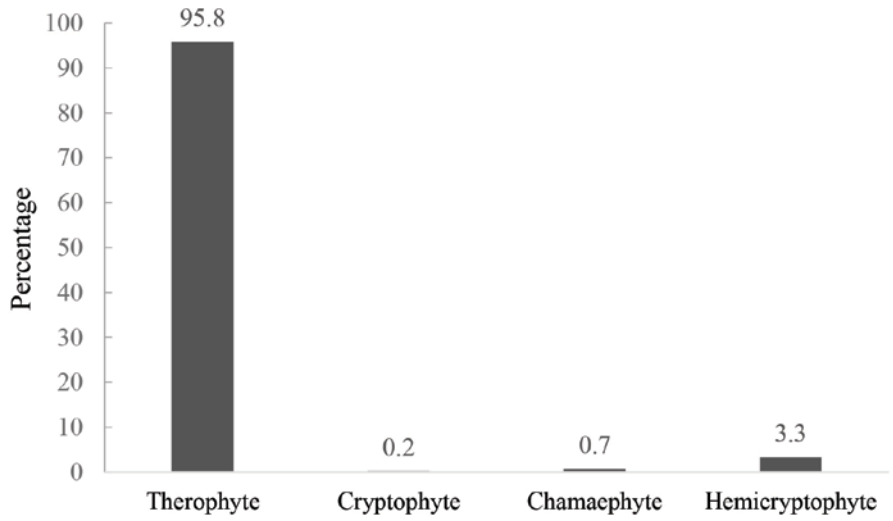

Fig. 7. Biodiversity form of plant species in the region

Table 3. Biodiversity indices of forest floor cover in the sub-sample plots of the region

Plot	Micro Plot	Pilou uniformity	Sheldon uniformity	Margalef richness	Menhinik richnesss	Shannon	Simpson	Dominance index	N individual	N spieses
1	1	0.79	0.62	1.62	0.63	1.82	0.79	0.21	255.00	10.00
	2	0.66	0.52	1.27	0.66	1.29	0.64	0.36	111.00	7.00
	3	0.58	0.36	2.16	1.09	1.38	0.57	0.43	102.00	11.00
	4	0.72	0.58	1.43	0.86	1.40	0.66	0.34	67.00	7.00
	5	0.59	0.45	1.18	0.55	1.16	0.61	0.39	164.00	7.00
2	1	0.63	0.41	2.09	1.00	1.50	0.63	0.37	121.00	11.00
	2	0.62	0.54	0.85	0.48	0.99	0.57	0.43	109.00	5.00
	3	0.68	0.60	0.88	0.52	1.09	0.61	0.39	92.00	5.00
	4	0.74	0.63	1.06	0.57	1.33	0.65	0.35	110.00	6.00
	5	0.78	0.67	1.11	0.63	1.39	0.71	0.29	90.00	6.00
3	1	0.41	0.52	0.41	0.26	0.45	0.23	0.77	138.00	3.00
	2	059	1.00	0.00	0.20	0.00	0.00	1.00	25.00	1.00
	3	0.68	0.80	0.32	0.43	0.47	0.30	0.70	22.00	2.00
	4	0.30	0.38	0.70	0.47	0.42	0.18	0.82	72.00	4.00
	5	0.63	1.00	0.00	0.13	0.00	0.00	1.00	60.00	1.00
4	1	0.53	0.52	0.64	0.39	0.74	0.39	0.61	105.00	4.00
	2	0.54	0.53	0.74	0.53	0.75	0.38	0.62	58.00	4.00
	3	0.44	0.68	0.26	0.30	0.30	0.17	0.83	44.00	2.00
	4	0.77	0.78	0.44	0.31	0.85	0.50	0.50	93.00	3.00
	5	0.56	0.62	0.61	0.59	0.62	0.33	0.67	26.00	3.00
Mean		0.61	0.61	0.89	0.53	0.90	0.45	0.55	93.20	5.10

Discussion

The establishment of permanent plots in the Sarabtaveh coppice forests has provided a foundational dataset, recording a total vegetation cover of 45.5%. This value falls within the reported range for similar Zagros oak forests under coppice management (Mirzaei et al., 2008 reported ~40-50%). Shokrollahi et al. (2012) in the highland pastures of Polur region, and Askari and Mirdavoudi (2023) studied the effect of slope aspect on vegetation of Astragalus cover density in the Central Zagros. The predominance of the coppice growth form across the stand strongly indicates a history of recurrent cutting or browsing; a common anthropogenic influence in the Zagros region.

In this research, 24 plant species were identified in the Sarabtaveh site. In this region, the Poaceae family with 7 species, followed by the Fabaceae and Ranunculaceae families, each with 2 species, were the dominant plant families in the studied area. In studies on the diversity of herbaceous plant species in the Mid-Zagros (part of the forests north of Ilam), Poaceae reported as the largest family in the studied area (Mirzaei et al., 2008). In a study by Hamze et al. (2008) in Chaharzabar, Kermanshah, the largest families were Poaceae, Fabaceae, and Asteraceae, respectively. Besides, in the Educational-Research Forest of Razi University, Kermanshah, the Asteraceae, Poaceae, Rosaceae, and Fabaceae families were reported as the dominant families (Heidari et al., 2019). In the Zagros forests in Baneh county, the highest number of species belonged to the genus Astragalus, and the largest families were Asteraceae, Fabaceae, Apiaceae, and Poaceae (Shakeri et al., 2021). The low number of plant species in the enclosed area compared to the typical habitat is probably related to the shrub understory cover; in this regard, over 70% of the forest floor in the enclosed area is covered by various Astragalus species.

Overall, annual herbaceous species played a significant role in the forest vegetation of the region. Based on the obtained results, more than half (54%) of the species in this habitat were therophytes (annual plants), 21% hemicryptophytes, 4.2% chamaephytes, 12.5% phanerophytes, and 8.3% geophytes (cryptophytes). In studies by Mirzaei et al. (2007) and Dehshiri (2020) on the forest vegetation of Mid-Zagros forests, therophytes were also reported as dominant. In the coppiced stands of the northern Zagros, most species belonged to the therophyte life form, while in the forest relics, they belonged to phanerophytes (Shakeri et al., 2021).

At the time of sampling during Khordad 1401/late May-early June 2022), in the Sarabtaveh site, 43% of the species were in the vegetative stage, and 57% were in reproductive and fruiting stages or had dried.

In the studied area, the average number of species per sample plot was 8.7, and the average number of individuals per sample plot was 126.5. Our recorded Shannon index of 1.56, which is lower than values from less-disturbed stands (e.g., Mirzaei et al., 2008) and comparable to managed stands (Heidari et al., 2019), supports this intermediate disturbance hypothesis. The dominance of therophytes (54%) and the significant shrub understory cover further suggest our site is in a secondary successional stage

following moderate historical disturbance (coppicing), consistent with the 'minor intervention' phase of the model we propose.

In the forests of Piranshahr, enclosure did not have a significant effect on the richness of woody species, but the Shannon diversity index increased significantly (Rashe Shaeri et al., 2014). In studies of Dinar-Kuh in Ilam, the Menhinick and Margalef richness indices and the Simpson diversity index did not alter significantly under enclosure and management practices, while significant changes in the Shannon diversity index was observed (Azizi et al., 2022). Furthermore, studies in the forests of Eyvan Gharb county, Ilam, showed that species richness was higher in the control area than in the degraded area, and evenness was higher in the degraded area (Azami et al., 2018). Results from studies in the semi-steppe rangelands of the Central Zagros indicated that with increasing grazing intensity, the Shannon-Wiener diversity and Margalef richness indices decreased, but the Menhinick index and evenness were higher in the heavily grazed area (Gholami et al., 2020). In a study in the Sar-Khalaj forests of the Mid-Zagros, vegetation diversity indices were significantly lower in the heavily grazed area compared to the enclosed area, while the indices in the moderately grazed area had higher values than in the heavily grazed area.

Briefly, it can be stated that with minor intervention in the climax ecosystem (limited tree removal or limited grazing), reduced competition, canopy opening, and decreased litter depth and coverage create conditions for the establishment of new species and increased species richness. However, through continious degradation and the extensive tree cutting, overgrazing and soil degradation, removal of the litter layer, soil erosion, and increased evaporation and severe soil dryness, species richness and diversity decrease significantly. It seems that various results of studies are attributed to differences in the level of degradation and the specific stage of succession. In the present study, the non-enclosed areas were not under severe degradation. On the other hand, the difference in conditions between the enclosed and non-enclosed sample plots was not very pronounced overall are due to the incomplete and non-strict implementation of enclosure.

References

Askari, Y., and Mirdavoudi, H., 2023. Astragalus ovinus Boiss. Responses Along the Gradient of Environmental Factors in Oak Forests of Yasouj, Iran. *Iranian Journal of Forest*, 15(1En (English issue)), pp. 11-24. https://doi.org/10.22034/ijf.2022.317383.1826.

Assadi, M., Maassoumi, A.A., Khatamsaz, M., and Mozaffarian, V., (Eds.) 1988-2011. Flora of Iran. *Research Institute of Forests and Rangelands Publications*, Tehran, pp. 1-74.

Aazami, F., and Heydari, M., 2018. Response of vegetation composition and diversity to degradation to soil physical, chemical and biological properties, Zagros forest ecosystem. *Journal of Plant Research (Iranian Journal of Biology)*, 31(2), pp. 221-234. https://doi.org/10.7717/peerj.12222.

Bazyari, M., Etemad, V., Kooch, Y., and Shirvany, A., 2021. Analysis of composi-

tion and biodiversity of understory plants in natural and afforestation stands of western Hyrcanian (Case study: Ramsar Sang Poshteh). *Iranian Journal of Forest and Range Protection Research*, 18(2), pp. 103-116. https://doi.org/10.22092/ijfrpr.2020.128266.1401.

Braun-Blanquet, J., 1964. Pflanzensoziologie, grundzüge der vegetationskunde (3rd ed.). New York: Springer., 607p.

Dehshiri, M.M., Nooraei, F.,and Maassoumi, S.M., 2019. Floristic study of Islamabad Gharb area in the central Zagros. PEC; 7 (14), pp. 21-44. http://pec.gonbad.ac.ir/article-1-399-fa.html.

Duelli, P., and Obrist, M.K., 2003. Biodiversity indicators: the choice of values and measures. *Agriculture, Ecosystems and Environment*. 98, pp. 87–98. https://doi.org/10.1016/S0167-8809(03)00072-0.

Ejtehadi, H., and Zare, H., 2015. Plant Species Diversity in Relation to topography in the East of Dodangeh Forests, Mazandaran Province, Iran. *Journal of Plant Research (Iranian Journal of Biology)*, 28(1), pp. 1-11.

Lessa Derci, A., Gutsch, M., Basile, M., and Suckow, F., 2020. Socially optimal forest management and biodiversity conservation in temperate forests under climate change. *Journal of Ecological Economics*, 169, pp. 1-16. https://doi.org/10.1016/j.ecolecon.2019.106504.

Ferretti, M.. and Fischer, R., 2013. Forest Monitoring; methods for terrestrial investigations in Europe with an overview of North America and Asia. Elsevier, Netherland, 507p.

Gaston, K.J., (Ed.) 1996. What is Biodiversity? Biodiversity: A Biology of Numbers and Difference. *Blackwell Scientific Publications*, London.

Ghahermaninejad, F., and Nafisi, H., 2011. Floristic study of Munjughlu sanctuary zone in Marakan protected area (East Azarbaijan province, NW Iran). Rostaniha, 12(1), 73-82. https://doi.org/10.22092/botany.2011.101433.

Gholami, P., Shirmardi, H., and Lashkari Sanami, N., 2019. Changes in species diversity and vegetation groups in relation to different intensities of grazing in the semi-steppe pastures of Central Zagros. *Journal of Rangeland*, 14 (4), pp. 621-609.

Haidari, R.H., Sohrabi Zadeh, A., and Haidari, M., 2019. Effect of physiographic factors on plant biodiversity in the Central Zagros Forests (Case study: Educational Forest of Razi University of Kermanshah). *Ecology of Iranian Forest*, 7(13), pp. 66-75. http://dx.doi.org/10.29252/ifej.7.13.66.

Hamzeh'ee, B., Khanhasani, M., Khodakarami, Y., and Nemati Peykani, M., 2008. Floristic and phytosociological study of Chaharzebar forests in Kermanshah. *Iranian Journal of Forest and Poplar Research*, 16(2), pp. 229-211.

Hosseini, Z., 2014. Floristic Studies of Northeast Mountains Yasouj (Kachian and Ab-nahr Mountains). MSc Thesis, Yasouj University, Yasouj, Iran (in Persian), 85p.

ICP Forests. 2016. Manual on methods and criteria for harmonized sampling, assessment, monitoring, and analysis of the effects of air pollution on forests. Part

VII.1. Assessment of Ground Vegetation. http://www.icp-forests.org/Manual.htm.

Jafari Kukhdan, A., 2003. A Survey of Eco-Phytosociology in Dena vegetation. PhD Thesis, The University of Tehran, Tehran, Iran (in Persian), 125p.

Jafari Kukhdan, A., 2011. Plant Biodiversity in Protection Central Zagros. The First National Seminar on Threats to Biological Diversity Resources and Root Causes of Biodiversity Lose in the Central Zagros. Feb 16-17, 2011. Isfahan University of Technology.

Jafari Kukhdan, A., 2013. Collection and Identification of the Flora of Province Kohgiloyeh and Boyerahmad and the Establishment of Province Herbarium. Yasouj: Yasouj University (in Persian).

Jafari Kukhdan, A., and Zarifian, A., 2015. Floristic Study of Mount Saverz in Kohgiluyeh and BoyerAhmad Province. Journal of Plant Research (*Iranian Journal of Biology*), 5(28), pp. 951-929.

Karimian, V., Vahabi, M.R., Roustakhiz, J., and Nodehi, N., 2017. Identification of Some Ecological Factors Affecting on Essential Oil of Verbascum songaricum Schrenk Shoots (Case Study: Rangelands of Isfahan and Kohgiluyeh and Buyerahmad Provinces, Iran). *Journal of Rangeland Science*. 7, pp. 183-194.

Magurran, A.E., 1988. Ecological Diversity and its Measurement. Croom Helm Limited, London.

Mirzaei, J., Akbarinia, M., Hosseini, S.M., Sohrabi, H., and Hosseinzadeh, J., 2008. Species diversity of herbaceous plants in relation to physiographic factors in Middle Zagros forest ecosystems. *Biology of Iran*, 20(4), pp. 375-382. http://dx.doi.org/10.29252/ifej.5.9.24.

Rashe Shaeri, S., Salehi, A., Pourbabaei, H., Eshaghi Rad, J., and Moradi, S., 2014. Effect of short term exclosure on physical and chemical properties soil and woody species diversity in Piranshahr forests, northern Zagros. *Forest Sustainable Development*, 1(1), pp. 87-101.

Raunkiaer, C., 1934. The life forms of plants and statistical plant geography; being the collected papers of C. Raunkiaer. *Clarendon press, Oxford*, 632 p.

Rechinger, K.H., 1963–2005. Flora Iranica, no. pp. 1–176. Akademische Druck, Graze.

Ravanbakhsh, H., Pourhashemi, M., Hamzeh'ee, B., Rashidi, F., Iranmanesh, Y., Bordbar, S.K., Jahanbazi, H., Ramak, P., Rastgar, A., Alimahmoudi-Sarab, S., Askari, Y., Khanhasani, M., Mohammadian, A., Mohammadpour, M., Negahdar Saber, M., Henareh Khalyani, J., Najafifar, A., and Rahimi, H., 2024. Analysis of ground vegetation of Zagros forests using monitoring plots. *Forest and Wood Products*, 77(2), pp. 153-171. https://doi.org/10.22059/jfwp.2024.376418.1293.

Schulz, B.K., Bechtold, W.A., and Zarnoch, S.J., 2009. Sampling and estimation procedures for the vegetation diversity and structure indicator. Gen. Tech. Rep. PNW-GTR-781. Portland, OR: US Department of Agriculture, Forest Service, Pacific Northwest Research Station. 53 p, 781.

Shakeri, Z., Mohammadi-Samani, K., Maarofi, H., Khoonsiavashan, S., and Sharifi, K., 2021. Species diversity, life form,

and chorotypes of plant species in sacred groves and surrounding silvopastoral woodlands of Northern Zagros, Iran. *Iranian Journal of Forest and Poplar Research*, 29(2), pp. 113-101. https://doi.org/10.22092/ijfpr.2021.354366.1998.

Shokrollahi, S., Moradi, H., and Dianati Tilaki, G.A., 2013. Effects of soil properties and physiographic factors on vegetation cover (Case study: Polur Summer Rangelands). *Iranian Journal of Range and Desert Research*, 19(4), pp. 655-668. https://doi.org/10.22092/ijrdr.2013.3043.

Simpon, E., 1949. Measurement of diversity. Nature, 688, 163.

Willis, K.J., and Whittaker, R.J., 2002. Species diversity--scale matters. Science. 295, pp. 1245-1248. https://doi.org/10.1126/science.1067335.

Antioxidant Properties of the Red Seaweed *Gelidium pusillum* Extracts from the Oman Sea: an *in vitro* Study

Morteza Ebrahimi[1], Ali Taheri[1*]

Received: 2025-10-25 Accepted: 2025-12-06

Abstract

Oxidation is a key factor in reducing the quality of aquatic feed and lead to undesirable changes in the nutritional composition of the diet. The usageof antioxidants in aquatic diets can reduce the damage caused by oxidative stress. Although synthetic antioxidants are used in livestock and aquatic feed, there are growing concerns about their toxicity and long-term effects on consumer health. Due to possessing a wide range of secondary metabolites, seaweeds have been considered as a natural source for producing natural antioxidants. Therefore, this research investigated the *in vitro* antioxidant properties of the red seaweed *Gelidium pusillum* from the Oman Sea. The seaweed was collected during low tide from the Oman Sea, dried, and powdered. Extraction was performed using methanol, chloroform, dichloromethane, and hexane solvents over 24 hours. After calculating the total phenolic content in the extracts, the antioxidant properties of the extracts were evaluated using three methods: free radical scavenging (DPPH), ferrous ion chelating activity, and reducing power. The IC50 value was calculated by plotting a graph. For statistical analysis, one-way ANOVA was used, and the Tukey post-hoc test was used for mean comparison. Experiments were performed in triplicate. Investigation of extraction yield revealed that the methanolic extract (1.5%) had the highest extraction yield compared to dichloromethane, chloroform, and hexane extracts. Examination of total phenolic compounds in *Gelidium pusillum* showed that the methanolic extract (23.14 mg GA/100g) had the highest total phenolic content, and the hexane extract (22.9 mg GA/100g) ranked second. The highest free radical scavenging activity was observed in the methanolic extract (90%), followed by the hexane extract (80%). The highest chelating activity (31.3%) was observed at a concentration of 1 mg/mL of the methanolic extract. The methanolic extract showed the highest reducing power (λ=0.56) among the extracts at different concentrations and had a significant difference with the other three extracts ($p< 0.05$). The antioxidant effect was dose-dependent and all extracts showed a significant difference in all three tests compared to the positive control ($p< 0.05$). Total phenolic content had a positive effect on the antioxidant activity of the seaweed extract, and solvents with higher total phenolic content exhibited higher antioxidant activity compared to other extracts. The high free radical scavenging activity of the methanolic extract confirmed its potential for further studies. Accordingly, investigating the *in vivo* activity

1- Faculty of Marine Sciences, Chabahar Maritime University, Iran
*Corresponding author email address: taheri@cmu.ac.ir
Doi: 10.48308/pae.2026.243889.1138

of the methanolic seaweed extract in aquatic diets is recommended.

Keywords: Chelation, Free radical, Oman Sea, *Gelidium pusillum*, Reducing power

Introduction

Algae are increasingly being considered as potential sources of bioactive compounds with pharmaceutical, biological, medical, and nutritional significance. Various macroalgal species have been traditionally used as ingredients in pharmaceutical and food products across the world. Furthermore, some of them are common sources of phycocolloids, gel-forming agents, of commercial value. In fact, there are 250 species of macroalgae that are commercially utilized worldwide, of which 150 species are consumed as human food. They are also regarded as low-calorie foods with high contents of minerals, vitamins, proteins, and carbohydrates (Kumar et al., 2011). In addition to primary metabolites, seaweeds can accumulate microelements, macroelements, and trace elements that are essential for their survival (Makkar et al., 2016; Salehi et al., 2019; Matos et al., 2021). They can also synthesize a wide array of secondary metabolites, which largely determine their bioactive potential (Øverland et al., 2019; Salehi et al., 2019).

An important group of secondary metabolites in seaweeds is phenolic compounds, which include simple phenols such as phenolic acids and polyphenols, including flavonoids and non-flavonoids such as tannins (Salehi et al., 2019). Most of these compounds exhibit antioxidant activity. Seaweed antioxidants act as free radical scavengers and prevent or repair damage induced by oxidative stress which possess high potential for treating various diseases (Liu and Sun, 2020). Seaweed-based antioxidants are primarily discussed in the context of cosmetic, pharmaceutical, and biomedical, food applications as stabilizers and preservatives, agriculture as plant growth biostimulants, as well as in livestock, poultry, and aquaculture nutrition (Cotas et al., 2020).

Reactive oxygen species (ROS), consisting of free radicals such as the hydroxyl radical (HO•) and superoxide anion (O_2^-), as well as non-radical species such as singlet oxygen ($^1O_2$) and H_2O_2, are various forms of activated oxygen. These ROS cause irreversible oxidative damage to biomolecules, leading to a range of pathophysiological disorders (Senevirathne et al., 2006). Increased ROS disrupts redox homeostasis and leads to either enhanced ROS production or reduced ROS scavenging capacity, a condition termed oxidative stress. ROS can interfere with the expression of numerous transcription factors and signaling proteins primarily involved in stress responses and cell survival mechanisms (Trachootham et al., 2008). Oxidation in aquafeed compositions leads to damage to the aquatic consumer, negatively impacts growth and physiology, and ultimately results in economic losses (Peixoto et al., 2016). To prevent this, cells have developed various protective mechanisms to prevent ROS formation or to detoxify ROS with the aid of antioxidants. These antiox-

idants are either cellular enzymes, such as glutathione peroxidase, or antioxidant compounds that are ingested through food. Antioxidants neutralize the excess production of oxidants and convert them into less harmful or harmless species (Moylan and Reid, 2007).

The main groups of antioxidants in seaweeds include phenolic compounds, polysaccharides, and pigments. Phenolic compounds found in seaweeds consist of (a) simple phenols such as phenolic acids (de Quiros et al., 2010): hydroxycinnamic acids – caffeic, p-coumaric, ferulic, sinapic acid; and hydroxybenzoic acids – gallic, vanillic, 4-hydroxybenzoic, protocatechuic, syringic, gentisic acid (Farvin and Jacobsen, 2013); and (b) polyphenols encompassing flavonoids and non-flavonoids. Other polyphenols that can be identified in seaweeds include phenolic terpenes such as rosmanol, carnosol, carnosic acid(Zhong et al., 2020) and terpenoids including chromene, chromanol, plastoquinone(Cotas et al., 2020). Phenolic terpenoids have been determined and characterized in red and brown seaweeds (Stengel et al., 2011).

Several seaweed-based products are available on the market, such as OceanFeed® (Milltown, Ireland), which is designed for swine, equine, and cattle nutrition. A commercial seaweed product with antioxidant properties is Tasco®, produced by Acadian AgriTech™ (Dartmouth, Nova Scotia, Canada). This product is available in two forms: Tasco-Forage and Tasco-EX. The former is used as an extract applied to plant foliage and grazed by livestock, while the latter is used for direct supplementation of livestock, poultry, and aquatic animals. Both forms are responsible for enhanced antioxidant responses measured in livestock, poultry, and aquatic animals (Allen et al., 2001; Saker et al., 2001; Saker et al., 2004; Ruiz et al., 2018; Del Tuffo et al., 2019). Therefore, the commercial products derived from seaweeds indicates the high potential of these valuable aquatic organisms for the development of biotechnological products using for aquafeed.

The southern coasts of Iran, particularly the Sea of Oman in the Chabahar region, possess a remarkable biodiversity of seaweeds, which represent a genetic reservoir and a valuable source of bioactive compounds and have not yet been fully studied or scientifically exploited. To date, the antioxidant and anticancer properties of more than 30 species from this region have been investigated by the author; however, given the identification of over 157 species, a systematic study of the antioxidant activity of the remaining species is necessary. One of the red algal species found in this area is *Gelidium pusillum* from the family Gelidiaceae. This alga, purplish to dark brown in color, is observed in intertidal zones on rocky substrates. Its distribution in the coastal areas of Ramin, Chabahar, and Tang has been reported mainly during winter and spring (Gharanjik and Rohani-ghadikalaee, 2010). Considering the reported potential of related algal species and the necessity of identifying native natural antioxidant resources, the present study was designed and conducted to investigate the antioxidant activity of various organic extracts including methanolic, chloroformic, dichloromethanic, and hexanic obtained

from the red alga *Gelidium pusillum* collected from the coasts of Chabahar. In this study, the antioxidant potential of the extracts was evaluated using various assays, including DPPH free radical scavenging, ferrous ion chelating ability, reducing power, as well as measurement of total phenolic compound content, and the results were compared with standard antioxidants.

Material and methods

Algae collection

In this study, sampling of the seaweed species *G. pusillum* was conducted during autumn and early winter of 2024 (1403 Persian calendar) at maximum low tide. Samples were collected from the coastal station of Pelag-e-Tiss (coordinates 25°17′71″ N and 60°37′17″ E) and Daryaye Bozorg station (coordinates 25°16′37″ N and 60°39′59″ E). To determine the appropriate sampling time (maximum low tide), weekly data from the EasyTide online database were used. Following transfer to the laboratory, the samples were first washed with seawater and then placed in labeled plastic bags containing some seawater. Subsequently, they were rinsed again with freshwater to remove impurities such as mineral particles, epiphytes, and other associated organisms. Species identification was performed using valid taxonomic keys, specialized image resources (Gharanjik and Rohani-ghadikalaee, 2010), as well as searches in international scientific databases such as Algaebase (www.algaebase.org). The samples were then air-dried for several days in a shaded area away from direct sunlight until a constant weight was achieved. Subsequently, they were ground into a powder using an electric grinder and stored at -20°C until further experiments were conducted (Mosaddegh et al., 2014).

Extraction and Preparation

To isolate the active compounds, 25 g of dried algal powder was mixed with 80–100 mL of four different organic solvents (methanol, chloroform, dichloromethane, and hexane). The containers holding these mixtures were placed in an incubator shaker for 24 hours at room temperature with shaking at 100 rpm. The mixtures were then filtered using Whatman No. 1 filter paper. To ensure complete extraction, this process (addition of fresh solvent, shaking, and filtration) was repeated twice more on the solid residue. After three successive extraction steps, the filtered solutions obtained from each solvent were collected in separate, labeled glass Petri dishes according to the algal species and the solvent used. Excess solvent was removed by placing the Petri dishes under a chemical fume hood and allowing evaporation at room temperature. The final concentrated extracts were stored at -20°C until subsequent experiments. The extraction yield for each extract was calculated using Formula 1. This method was performed according to the protocol described in the study by Lim et al. (2002).

Extraction yield (%) = (Dried extract weight / Initial dried algal weight) × 100 (Formula 1)

Evaluation of antioxidant activity of extracts

DPPH free radical scavenging activity

The antioxidant activity of the obtained extracts was assessed using the DPPH free radical scavenging assay. Initially, different

concentrations of each extract (starting from a stock solution of 1000 µg/mL) were prepared in 50% methanol and homogenized using a vortex mixer. Concurrently, a working solution of DPPH radical was freshly prepared daily by dissolving 2 mg of the solid compound in 50 mL of 95% methanol. According to the standard method (Blois, 1958), 1.5 mL of the DPPH solution was added to an equal volume of each extract concentration, and the mixture was vortexed for one minute. The samples were then kept in the dark at room temperature for 30 minutes. After this period, the optical absorbance of each mixture was measured at 517 nm using a spectrophotometer. A decrease in the absorbance of the DPPH solution indicates the antioxidant capacity of the extract and its ability to neutralize free radicals (Ganesan et al., 2011).

The percentage of free radical inhibition for each extract was calculated using Formula 2.

$$\% \text{ Free radical inhibition} = [(A_{Control} - A_{Sample}) / A_{Control}] \times 100 \quad \text{(Formula 2)}$$

In the above equation, A_{Sample} represents the absorbance of the mixture containing different concentrations of the extract and the DPPH solution, and $A_{Contrxol}$ is the absorbance of the control sample (containing DPPH solution and 50% methanol, without the extract). To correct for the possible effect of the intrinsic color of the extracts on the assay results, a blank sample (containing the same amount of extract and 95% methanol, but without DPPH) was prepared for each extract concentration, and its absorbance was measured. To investigate the relationship between extract concentration and antioxidant activity, the experiment was performed at various concentration levels. Additionally, an ascorbic acid solution at a concentration of 0.02 mg/mL was used as a positive control and a strong antioxidant to compare the performance of the samples.

Ferrous ion chelating activity

To evaluate the ferrous ion chelating capacity of the extracts, the standard method described by Dinis et al. (1994) was used. First, extract solutions of different concentrations were prepared from the stock solution (1000 µg/mL) in distilled water. To 3.7 mL of each extract concentration, 0.1 mL of ferrous chloride ($FeCl_2$) solution was added, and the mixture was kept for 3 minutes. Subsequently, 0.2 mL of ferrozine reagent was added, and after thorough mixing, the samples were incubated for 10 minutes at room temperature. Finally, the optical absorbance of each sample was measured at 562 nm using a spectrophotometer. The percentage inhibition of iron-ferrozine complex formation, which indicates the chelating activity of the extract, was calculated according to Formula 3.

$$\% \text{ Inhibition} = [(A_0 - A_1) / A_0] \times 100 \quad \text{(Formula 3)}$$

In this equation, A_0 is the absorbance of the control group, and A_1 is the absorbance of the sample containing the extract or positive control. An EDTA solution at a concentration of 0.1 mg/mL was used as a positive control.

Determination of IC_{50}

The effective concentration of the extract required to inhibit 50% of ferrous ions (IC_{50}) was calculated using linear regression analysis between the extract concentration and

the percentage of inhibition (chelating activity).

Reducing Power Assay

To assess the reducing power of the extracts, the protocol described by Oyaizu (1986) was employed. Extract solutions at various concentrations were prepared from the stock solution (1000 µg/mL) using distilled water. A mixture was prepared containing 1 mL of the extract, 1 mL of 0.2 M phosphate buffer (pH 6.6), and 1 mL of 1% potassium ferricyanide solution. The mixture was then incubated for 20 minutes at 50°C. Subsequently, 1 mL of 10% trichloroacetic acid (TCA) was added to the mixture. Then, 2 mL of the supernatant was separated and mixed with 2 mL of distilled water. Finally, 0.4 mL of 0.1% ferric chloride ($FeCl_3$) solution was added, and the mixture was kept at room temperature for 10 minutes. The optical absorbance of the samples was measured at 700 nm using a spectrophotometer. An ascorbic acid solution at a concentration of 0.02 mg/mL was used as a positive control. In this method, an increase in absorbance at the specified wavelength indicates a higher reducing power of the sample.

Total phenolic content (TPC)

The total phenolic content of the extracts was measured using the Folin-Ciocalteu spectrophotometric method according to the protocol of Taga et al. (1984). In this method, 200 µL of the extract sample was mixed with 4 mL of 2% sodium carbonate solution and kept at room temperature for 2 minutes. Then, 200 µL of 50% Folin-Ciocalteu reagent was added to the mixture, and after stirring, it was incubated for 30 minutes at room temperature (26–28°C) in the dark. After this period, the absorbance of the samples was read at 720 nm using a spectrophotometer. A standard gallic acid solution at concentrations of 0.002, 0.01, and 0.05 mg/mL was used to prepare a calibration curve. The final results were reported as milligrams of gallic acid equivalent (GAE) per gram of dried algal powder. The linear equation derived from the standard curve was as follows:

$Y = 0.0141x \ (R^2 = 0.98)$

In this equation, Y represents the absorbance, and x represents the gallic acid concentration in µg/mL.

Statistical analysis

After confirming normality using the Shapiro-Wilk test, one-way analysis of variance (One-way ANOVA) was used for statistical evaluation. Tukey's test was employed for multiple mean comparisons using GraphPad Prism 9 software.

Results and Discussion

Extraction yield

The extraction yields are presented in figure 1. The methanolic extract exhibited the highest extraction yield. The hexanic extract showed the lowest extraction yield ($p < 0.05$). The dichloromethanic and chloroformic extracts did not show a significant difference from each other, but they differed significantly from the hexanic and methanolic extracts ($p < 0.05$).

The extraction yield in this study was consistent with reported values for other types of seaweeds, ranging from 2.9% to 12.7% (Ganesan et al., 2008). In a study by Sharifian et al. (2019) on the extraction of phenolic compounds and antioxidant properties

of the seaweeds *Padina australis* (2.62%) and *Nizimuddinia zanardinii* (6.71%), the highest extraction yield was reported for the methanolic solvent. In another study on the antioxidant properties of the red alga *Laurencia snyderiae*, the methanolic extract (6.12%) also showed the highest yield compared to chloroform and ethyl acetate (Karimzadeh and Zahmatkesh, 2021).

DPPH free radical scavenging activity

The results of the free radical scavenging activity are presented in Table 1. The highest free radical scavenging activity was observed in the methanolic extract, followed by the hexanic, dichloromethanic, and chloroformic extracts ($p < 0.05$). The lowest activity was measured at a concentration of 0.1 mg/mL for the chloroformic extract. Free radical scavenging activity was dose-dependent for each extract, and the activity decreased significantly with decreasing extract concentration ($p < 0.05$). All extracts differed significantly from the positive control (97.77 ± 0.5%) and exhibited lower

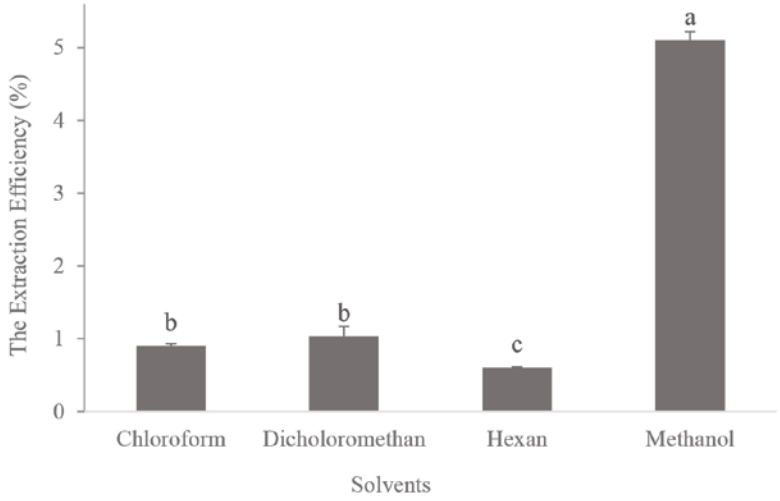

Fig. 1. The extraction efficiency of *Gelidium pusillum* (%) with 4 differenct organic solvents (Chloroform, Dichloromethan, Hexan, and Methanol).The results are Mean value from three replicates ± standard error. The letters a, b, c represent statistical significant differences betwheen means, as determines whit Tukey's post hoc test ($p< 0.05$).

Table 1. Effect of different solvents and different concentrations of organic extracts of algae *Gelidium pusillum* at DPPH free radical scavenging assay (%)

	Concentration of organic extracts (mg/mL)			
Solvent	0.1	0.3	0.5	1
Methanol	10.22 ± 0.9^{dA}	22.33 ± 1.55^{cA}	59.1 ± 3.22^{bA}	90 ± 1.76^{aA}
Hexan	6.6 ± 0.77^{dAB}	15.88 ± 4.30^{cB}	50.1 ± 2.67^{bB}	80.1 ± 1.49^{aB}
Dicholoromethan	4.2 ± 0.19^{dB}	12.18 ± 1.10^{cB}	32.91 ± 1.19^{bC}	55.16 ± 1.44^{aC}
Chloroform	1.4 ± 0.27^{cB}	6.1 ± 1.44^{cC}	12.2 ± 0.33^{bB}	22.1 ± 3.40^{aD}

The results are as Mean±SD from 3 repetition. The letters a, b, c in each row and A, B, C in each columns represent statistical differences ($p<0.05$).

free radical scavenging activity. Free radical scavenging activity was significantly dose-dependent for each extract.

The DPPH free radical, due to its unpaired electron, exhibits a characteristic purple color with maximum absorbance at 517 nm. In the presence of an antioxidant compound capable of acting as a hydrogen donor, this unpaired electron is neutralized, and the radical is converted to its reduced, stable form. The single electrons on the nitrogen atoms of DPPH are reduced to hydrazine (DPPH-H) by abstracting hydrogen atoms from antioxidants (Febrina et al., 2025). Previous research on the DPPH free radical scavenging activity of methanolic extracts of red algae revealed that Gracilaria corticata (44.32%), Gracilaria dura (33.03%), Gracilaria debilis (53.34%), and Gracilaria salicornia (53.43%) exhibited good free radical scavenging activity (Kumar et al., 2011; Karimzadeh and Zahmatkesh, 2021). Similar to the present study, in the research by Samir et al. (2019), *Bifurcaria bifurcata* with a methanolic extract, which was the richest in phenolic compounds and showed the highest inhibition percentage (81%), was the best, followed by *Cystoseira tamariscifolia* (50%) and *Fucus spiralis* (37.74%). Furthermore, in the study by Abdul Hamid et al. (2024), DPPH scavenging values ranged from 15.25% to 64.83%, where the methanolic extract of brown algae recorded the highest inhibition percentage, followed by red algae. Most extracts exhibited higher inhibitory activity when extracted with polar solvents. In this study, the concentration-dependent free radical scavenging activity was confirmed for the different algal species studied, but they showed weaker scavenging performance compared to the positive control.

Chelating activity of Organic algal extracts

The results of the chelating activity percentage of the organic extracts of *Gelidium pusillum* at different concentrations are presented in Table 2. Based on the results, all extracts at all concentrations differed significantly from the EDTA positive control and showed lower chelating activity ($p< 0.05$). Chelating

Table 2. The percentage of chelating activity of algae *Gelidium pusillum* organic extracts at different concentrations compared with the positive control of EDTA

	Concentration of organic extracts (mg/mL)			
Solvent	0.1	0.3	0.5	1
Methanol	4.14 ± 1.12^{dB}	11.5 ± 2^{cB}	18 ± 4^{bB}	31.3 ± 2^{aB}
Hexan	1.4 ± 0.35^{bB}	2.7 ± 0.98^{bC}	9 ± 2^{aC}	13 ± 6.8^{aC}
Dicholoromethan	1.8 ± 1.0^{bB}	3.3 ± 0.7^{bC}	6.3 ± 2.3^{abC}	10 ± 1.1^{aC}
Chloroform	0.98 ± 0.8^{dB}	2.5 ± 0.66^{cC}	7 ± 1^{bC}	12 ± 0.22^{aC}
EDTA	83 ± 3.1^{A}	83 ± 3.1^{A}	83 ± 3.1^{A}	83 ± 3.1^{A}

The results are as Mean±SD from 3 repetition. The letters a, b, c in each row and A, B, C in each columns represent statistical differences ($p< 0.05$).

activity did not exceed 34% even under optimal conditions. The highest value (31.3%) was observed at a concentration of 1 mg/mL for the methanolic extract. The chelating activity of the methanolic extract at concentrations of 1, 0.5, and 0.1 mg/mL showed significant differences compared to hexane, dichloromethane, and chloroform ($p< 0.05$), but no significant difference was observed among these three extracts ($p > 0.05$). The chelating activity of each extract was also dose-dependent.

The extracts of *G. pusillum* exhibited moderate to weak chelating properties, with the highest ferrous ion chelating activity belonging to the methanolic extract (31.3%). Chelating activity was directly correlated with total phenolic content in the extract. The ability of seaweeds to adsorb and chelate ferrous ions may be attributed to the presence of endogenous chelating agents, mainly phenolic compounds; because some phenolic compounds possess functional groups with appropriate orientations that can chelate metal ions (Wang, 2009). Similarly, in the study by de Alencar et al. (2016), it was found that the methanolic (54.7%) and hexanic (52.27%) extracts of the red alga *Pterocladiella capillacea* and the hexanic (33%) and methanolic (27.7%) extracts of the red alga *Osmundaria obtusiloba* exhibited the best ferrous ion chelating activity. In the study by Krishnan et al. (2019), the metal chelating activity of the alga *Actinotrichia fragilis* was 77.09 µg/mL.

According to studies by Lindsay (1996), chemical compounds containing functional groups such as hydroxyl (–OH), carboxyl (–COOH), thiol (–SH), ether (–O–), amino ($–NR_2$), phosphonate (PO_3H_2), and sulfide (–S–) have the ability to adsorb metal ions under favorable environmental conditions and can act as effective secondary antioxidants. Therefore, the presence of different functional groups in different solvents may account for the differential chelating performance of the extracts. Nevertheless, the algal extracts in the present study exhibited moderate to weak chelating activity and showed less type II antioxidant properties compared to free radical scavenging activity.

Reducing power of organic algal extracts

Table 3. Organic extracts reduction power of alga *Gelidium pusillum* at different concentrations (λ) compared with the control of ascorbic acid

	Concentration of organic extracts (mg/mL)			
Solvent	0.1	0.3	0.5	1
Methanol	0.1 ± 0.03^{dB}	0.21 ± 0.03^{cB}	0.4 ± 0.05^{bB}	0.56 ± 0.12^{aB}
Hexan	0.01 ± 0.0^{cB}	0.05 ± 0.02^{bcC}	0.12 ± 0.03^{abC}	0.17 ± 0.02^{aC}
Dicholoromethan	0.04 ± 0.01^{cB}	0.09 ± 0.01^{bcC}	0.16 ± 0.03^{abC}	0.22 ± 0.13^{aC}
Chloroform	0.0 ± 0.0^{cB}	0.05 ± 0.01^{bC}	0.09 ± 0.01^{aC}	0.12 ± 0.02^{aC}
ascorbic acid	0.9 ± 0.006^{A}	0.9 ± 0.006^{A}	0.9 ± 0.006^{A}	0.9 ± 0.006^{A}

The results are as Mean±SD from 3 repetition. The letters a, b, c in each row and A, B, C in each columns represent statistical differences ($p< 0.05$).

Based on the reducing power results presented in Table 3, the methanolic extract, except at the concentration of 0.01 mg/mL, exhibited the highest reducing power among the extracts at different concentrations and showed a significant difference from the other three extracts ($p < 0.05$). However, the hexanic, dichloromethanic, and chloroformic extracts did not show significant differences from each other. A dose-dependent effect was observed for all four extracts to varying degrees, with the most significant difference between concentrations observed for the methanolic extract. All extracts differed significantly from the positive control and showed lower reducing activity than ascorbic acid ($p < 0.05$).

The methanolic extract (0.56) exhibited the highest reducing power, while the other three extracts showed no significant differences among themselves. Reducing power, like the other two assays, was dose-dependent. In the study by de Alencar et al. (2016), the methanolic (0.136) and hexanic (0.167) extracts of the red alga *Pterocladiella capillacea* and the hexanic (0.101) and methanolic (0.180) extracts of the red alga *Osmundaria obtusiloba* exhibited reducing power that was weaker than the positive control. Reducing power has been reported for the species *Hypnea musciformis* (absorbance 1.46), *Hypnea valentiae* (0.48), and *Jania rubens* (0.45) (Chakraborty et al., 2015). In the species *Turbinaria ornata*, reducing power increases with increasing extract concentration, with values measured in the range of 0.2 ± 0.04 to 0.72 ± 0.07 (Vijayabaskar and Shiyamala, 2012). Other studies have shown that polyphenols extracted from *Gracilaria edulis* and *Hypnea valentiae* have reducing power of 80.56% and 75.09%, respectively (Mahendran et al., 2021).

Compounds with reducing power are electron donors and can reduce oxidized intermediates in lipid peroxidation processes. Therefore, these compounds are capable of acting as both primary and secondary antioxidants. Reducing agents present in a solution facilitate the reduction of the Fe^{3+}/ferricyanide complex to the ferrous (Fe^{2+}) form, which can be measured by absorbance at 700 nm (Ganesan et al., 2011). Red algae contain antioxidant compounds such as phenolic compounds (phenolic acids, bromophenols, flavonoids, phlorotannins), pigments (beta-carotene, bromophenol, phycobiliproteins, chlorophyll), sulfated galactans (carrageenan, agar), vitamins (B1, B3, C, and E), terpenoids, tannins, and peptides (Kumar et al., 2021; Wells et al., 2017). According to studies, the antioxidant activity of red algae is not limited to phenolic compounds, and other bioactive compounds also contribute to their antioxidant properties (Yabuta et al., 2010; Ngo et al., 2011).

Total phenolic content (TPC)

The total phenolic content is presented in figure 2. The phenolic content of the methanolic extract was significantly higher than that of the other three extracts ($p < 0.05$). Furthermore, the hexanic extract showed higher phenolic content than the dichloromethanic and chloroformic extracts ($p < 0.05$), but there was no significant difference in phenolic content between the dichloromethanic and chloroformic extracts ($p > 0.05$). The lowest total phenolic content was observed in the chloroformic extract.

In a study by Ismail et al., the seaweeds *Turbinaria decurrens*, *Ulva lactuca*, *Padina pavonica*, *Pterocladia capillacea*, *Sargassum muticum*, and *Sargassum acinarium* were investigated (Ismail et al., 2020). Total phenolic content was measured in methanolic, acetone, and aqueous extracts, and the results showed that the methanolic extract contained a higher amount of total phenols compared to the acetone and aqueous extracts. The polarity of the solvent and the solubility of the target compounds play a crucial role in determining the yield of polyphenols (Wakeel et al., 2019). In the study by Abdul Hamid et al. (2024), the TPC of methanolic algal extracts showed the highest values, ranging from 30.54 to 50.67 mg phloroglucinol equivalent (PGE)/g sample. The methanolic extract of *Caulerpa lentillifera* (35.77 mg PGE/g sample) exhibited a relatively high value. In the study by Bouzenad et al. (2024), the highest total phenolic content was also reported in the polar ethyl acetate extract of the seaweeds *Sargassum muticum*, *Cladophora laetevirens*, *Corallina officinalis*, *Dictyota dichotoma*, and *Ulva lactuca* (TPC ranging from 158.89 to 235.67 µg gallic acid/mg).

Higher phenolic content in algae indicates higher antioxidant activity, which is attributed to their ability to act as reducing agents. Many studies have reported a significant correlation between antioxidant activity and phenolic compound content (Honey et al., 2024; Li et al., 2007). However, in contrast to these findings, some other studies, such as that by Lim et al. (2002) on the alga *S. siliquastrum*, did not observe a direct relationship between the antioxidant effect of the extract and its total phenol content. It should be considered that in addition to phenolic compounds, other compounds such as

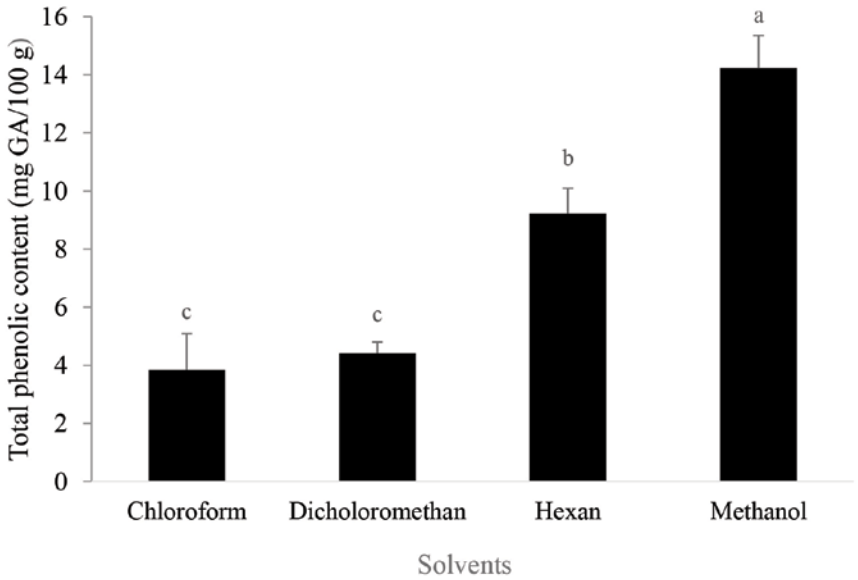

Fig. 2. Total phenolic content of *Gelidium pusillum* algae organic extracts with 4 differenct organic solvents (Chloroform, Dichloromethan, Hexan, and Methanol) represented as mg GA/100g. The results are Mean value from three replicates ± standard error. The letters a, b, c represent statistical significant differences betwheen means, as determines whit Tukey's post hoc test ($p < 0.05$).

carotenoids, unsaturated fatty acids, as well as low-molecular-weight compounds like polysaccharides, peptides, and some chromophytes, may also play a role in free radical scavenging activity.

IC_{50} values of organic algal extracts

Based on the results presented in Table 4, the methanolic extract, with an IC_{50} value of 0.54, exhibited the best DPPH free radical scavenging performance, followed by the hexanic, dichloromethanic, and chloroformic extracts, which required higher concentrations of active compounds to achieve the same effect. Regarding metal ion chelating activity, methanol again showed the best performance with 1.63 mg/g, followed by hexanic > chloroformic > dichloromethanic extracts.

Conclusion

The highest free radical scavenging activity of *Gelidium pusillum* algal extract was observed in the methanolic extract (90%), followed by the hexanic extract (80%). The highest chelating activity (31.3%) was observed in the methanolic extract. The methanolic extract exhibited the highest reducing power ($\lambda = 0.56$) among the extracts at different concentrations. Antioxidant activity was dose-dependent for each extract, and the activity decreased significantly with decreasing extract concentration. All extracts showed significant differences from the positive control in all three assays. The red alga *G. pusillum* demonstrated acceptable in vitro antioxidant properties, which were similar to or better than those reported for other red algae. Higher antioxidant activity might be achieved from this alga through purification or extraction with other solvents such as ethyl acetate and acetone, or through solvent-solvent fractionation.

Author contributions

M.E. was responsible for conceptualizing the study, planning the experiments, conducting the experimental procedures, interpreting the results, and writing the initial draft of the manuscript; A.T. supervised the research, assisted in the experimental design, offered critical feedback, and gave final approval for the manuscript. Both authors reviewed and endorsed the final version of the manuscript.

Acknowledgements

The authors would like to thank Chabahar Maritime University for technical and financial support required for the successful completion of this research as a thesis.

Table 4. The IC_{50} values of the organic extracts of alga *Gelidium pusillum in vitro* antioxidant assays

Test	Chloroform	Dicholoromethan	Hexan	Methanol
DPPH Free Radical Scavenging (mg/mL)	2.19	0.88	0.61	0.54
Metal Chelating (%)	3.98	5.28	3.69	1.63

References

Abdul Hamid, M., Yeap, C.H., Wan Mustapha, W.A., Martony, O. and Fatmawati, F. 2024. Effects of Different Solvents on the Antioxidant Activity of Several Seaweed Species from Semporna, Sabah, Malaysia. *Indonesian Journal of Marine Sciences*, 29(1), 29-36. https://doi.org/10.14710/ik.ijms.29.1.29-36.

Allen, V.G., Pond, K.R., Saker, K.E., Fontenot, J.P., Bagley, C.P., Ivy, R.L., Evans, R.R., Schmidt, R.E., Fike, J.H., Zhang, X. and Ayad, J.Y., 2001. Tasco: Influence of a brown seaweed on antioxidants in forages and livestock—A review. *Journal of Animal Science*, *79*(suppl_E), 21-31. https://doi.org/10.2527/jas2001.79E-SupplE21x.

Blois, M. S. 1958. Antioxidant determinations by the use of a stable free radical. *Nature, 181*(4617), 1199–1200. https://doi.org/10.1038/1811199a0.

Bouzenad, N., Ammouchi, N., Chaib, N., Messaoudi, M., Bousabaa, W., Bensouici, C., Sawicka, B., Atanassova, M., Ahmad, S.F. and Zahnit, W. 2024. Exploring bioactive components and assessing antioxidant and antibacterial activities in five seaweed extracts from the northeastern coast of Algeria. *Marine Drugs, 22*(6), 273. https://doi.org/10.3390/md22060273.

Chakraborty, K., Joseph, D. and Praveen, N. K. 2015. Antioxidant activities and phenolic contents of three red seaweeds (Division: Rhodophyta) harvested from the Gulf of Mannar of Peninsular India. *Journal of Food Science and Technology, 52*(4), 1924–1935. https://doi.org/10.1007/s13197-013-1181-x.

Cotas, J., Leandro, A., Monteiro, P., Pacheco, D., Figueirinha, A., Gonçalves, A. M. M., da Silva, G. J. and Pereira, L. 2020. Seaweed phenolics: From extraction to applications. *Marine Drugs,18*(8), 384. https://doi.org/10.3390/md18080384

de Alencar, D.B., de Carvalho, F.C.T., Rebouças, R.H., Dos Santos, D.R., dos Santos Pires-Cavalcante, K.M., de Lima, R.L., Baracho, B.M., Bezerra, R.M., Viana, F.A., dos Fernandes Vieira, R.H.S. and Sampaio, A.H., 2016. Bioactive extracts of red seaweeds *Pterocladiella capillacea* and *Osmundaria obtusiloba* (Floridophyceae: Rhodophyta) with antioxidant and bacterial agglutination potential. *Asian Pacific Journal of Tropical Medicine*, *9*(4), pp.372-379. https://doi.org/10.1016/j. apjtm.2016.03.015.

de Quirós, A.R.B., Frecha-Ferreiro, S., Vidal-Pérez, A.M., and López-Hernández, J. 2010. Antioxidant compounds in edible brown seaweeds. *European Food Research and Technology, 231*(3), 495–498. https://doi.org/10.1007/s00217-010-1305-8.

Del Tuffo, L., Laskoski, F., Vier, C.M., Tokach, M.D., Dritz, S.S., Woodworth, J.C., DeRouchey, J.M., Goodband, R.D., Constance, L.A., Niederwerder, M. and Arkfeldt, E., 2019. Effects of Oceanfeed Swine feed additive on performance of sows and their offspring. *Kansas Agricultural Experiment Station Research Reports*, *5*(8), p.4. https://doi.org/10.4148/2378-5977.7850.

Dinis, T.C.P., Madeira, V.M.C., and Almeida, L.M. 1994. Action of phenolic deriv-

atives (acetaminophen, salicylate, and 5-aminosalicylate) as inhibitors of membrane lipid peroxidation and as peroxyl radical scavengers. *Archives of Biochemistry and Biophysics, 315*(1), 161–169. https://doi.org/10.1006/abbi.1994. 1485.

Farvin, K.H.S., and Jacobsen, C. 2013. Phenolic compounds and antioxidant activities of selected species of seaweeds from Danish coast. *Food Chemistry, 138*(2–3), 1670–1681. https://doi.org/10.1016/j.foodchem. 2012. 10. 078.

Febrina, A., Falah, S., Suryanegara, L., and Safithri, M. 2025. Antioxidant activity and tyrosinase inhibition of red seaweed (*Kappaphycus alvarezii*) extracted using different solvents. *BIO Web of Conferences, 184*, 01006. https://doi.org/10.1051/bioconf/202518401006.

Ganesan, K., Kumar, C.S., and Rao, P.V.S. 2011. Comparative assessment of antioxidant activity in three edible species of green seaweed, *Enteromorpha* from Okha, Northwest coast of India. *Innovative Food Science and Emerging Technologies, 12*(1), 73–78. https://doi.org/10.1016/j.ifset.2010.11.005.

Ganesan, P., Chandini, S.K., and Bhaskar, N. 2008. Antioxidant properties of methanol extract and its solvent fractions obtained from selected Indian red seaweeds. *Bioresource Technology, 99*(8), 2717–2723. https://doi.org/10.1016/j.biortech.2007.07.005.

Qaranjik, B.M., and Rohani Ghadi Kailayi, K., 2010. Atlas of Marine Seaweeds from the Coasts of the Persian Gulf and the Oman Sea. 170 pages. [In Persian]

Honey, O., Islam Nihad, S.A., Rahman, Md.A., Rahman, Md.M.I., Chowdhury, M.Z.R. (2024). Exploring the antioxidant and antimicrobial potential of three common seaweeds of Saint Martin's Island of Bangladesh. *Heliyon*, 10, e26096. https://doi.org/10.1016/j.heliyon.2024.e26096.

Ismail, G.A., Gheda, S.F., Abo-Shady, A.M. and Abdel-Karim, O.H. 2020. In vitro potential activity of some seaweeds as antioxidants and inhibitors of diabetic enzymes. *Food Science and Technology, 40*(3), 681–691. https://doi.org/10.1590/fst.15619.

Karimzadeh, K. and Zahmatkesh, A. 2021. Phytochemical screening, antioxidant potential and cytotoxic effects of different extracts of red algae (*Laurencia snyderiae*) on HT29 cells. *Research in Pharmaceutical Sciences, 16*(4), 400–413. https://doi.org/10.4103/1735-5362.319578.

Manoj Kumar, M.K., Puja Kumari, P.K., Nitin Trivedi, N.T., Shukla, M.K., Vishal Gupta, V.G., Reddy, C.R.K. and Bhavanath Jha, B.J., 2011. Minerals, PUFAs and antioxidant properties of some tropical seaweeds from Saurashtra coast of India. *Journal of Applied Phycology, 23*, 797–810. https://doi.org/10.1007/s10811-010-9578-7.

Kumar, Y., Tarafdar, A. and Badgujar, P.C. 2021. Seaweed as a source of natural antioxidants: Therapeutic activity and food applications. *Journal of Food Quality,* 5753391. https://doi.org/10.1155/2021/5753391.

Li, K., Li, X.M., Ji, N.Y. and Wang, B.G. 2007. Natural bromophenols from the marine red alga *Polysiphonia ur-*

ceolata (Rhodomelaceae): Structural elucidation and DPPH radical-scavenging activity. *Bioorganic and Medicinal Chemistry, 15*(21), 6627–6631. https://doi.org/10.1016/j.bmc.2007.08.023.

Lim, S.N., Cheung, P.C.K., Ooi, V.E.C. and Ang, P.O. 2002. Evaluation of antioxidative activity of extracts from a brown seaweed, *Sargassum siliquastrum*. *Journal of Agricultural and Food Chemistry, 50*(13), 3862–3866. https://doi.org/10.1021/jf020096b.

Lim, S.N., Cheung, P.C.K., Ooi, V.E.C. and Ang, P.O. 2002. Evaluation of antioxidative activity of extracts from a brown seaweed, *Sargassum siliquastrum*. *Journal of Agricultural and Food Chemistry, 50*(13), 3862–3866. https://doi.org/10.1021/jf020096b.

Lindsay, R.C. 1996. Food additives. In O. R. Fennema (Ed.), *Food chemistry* (3rd ed., pp. 767–823). Marcel Dekker.

Liu, Z.W. and Sun, X. 2020. A critical review of the abilities, determinants, and possible molecular mechanisms of seaweed polysaccharides antioxidants. *International Journal of Molecular Sciences, 21*(20), 7774. https://doi.org/10.3390/ijms21207774.

Makkar, H.P.S., Tran, G., Heuzé, V., Giger-Reverdin, S., Lessire, M., Lebas, F. and Ankers, P. 2016. Seaweeds for livestock diets: A review. *Animal Feed Science and Technology, 212*, 1–17. https://doi.org/10.1016/j. anifeedsci.2015.09.018.

Matos, G.S., Pereira, S.G., Genisheva, Z., Gomes, A.M., Teixeira, J.A. and Rocha, C.M.R. 2021. Advances in extraction methods to recover added-value compounds from seaweeds: Sustainability and functionality. *Foods, 10*(3), 516. https://doi.org/10.3390/foods10030516.

Mosaddegh, M., Gharanjik, B.M., Naghibi, F., Esmaeili, S., Pirani, A., Eslami Tehrani, B., Keramatian, B. and Hassanpour, A. 2014. A survey of cytotoxic effects of some marine algae in the Chabahar coast of Oman Sea. *Research Journal of Pharmacognosy, 1*(4), 27–31.

Moylan, J.S. and Reid, M.B. 2007. Oxidative stress, chronic disease, and muscle wasting. *Muscle and Nerve, 35*(4), 411–429. https://doi.org/10.1002/mus.20743.

Ngo, D.H., Wijesekara, I., Vo, T.S., Van Ta, Q. and Kim, S.K. 2011. Marine food-derived functional ingredients as potential antioxidants in the food industry: An overview. *Food Research International, 44*(2), 523–529. https://doi.org/10.1016/j.foodres.2010.12.030.

Øverland, M., Mydland, L.T. and Skrede, A. 2019. Marine macroalgae as sources of protein and bioactive compounds in feed for monogastric animals. *Journal of the Science of Food and Agriculture, 99*(1), 13–24. https://doi.org/10.1002/jsfa.9143.

Oyaizu, M. 1986. Studies on products of browning reaction: Antioxidative activities of products of browning reaction prepared from glucosamine. *Japanese Journal of Nutrition and Dietetics, 44*(6), 307–315. https://doi.org/10.5264/eiyogakuzashi.44.307.

Peixoto, M.J., Svendsen, J.C., Malte, H., Pereira, L.F., Carvalho, P., Pereira, R., Gonçalves, J.F.M. and Ozório, R.O.A. 2016. Diets supplemented with seaweed

affect metabolic rate, innate immune, and antioxidant responses, but not individual growth rate in European seabass (*Dicentrarchus labrax*). *Journal of Applied Phycology*, 28, 2061–2071. https://doi.org/10.1007/s10811-015-0735-x.

Ruiz, A.R., Gadicke, P., Andrades, S.M. and Cubillos, R. 2018. Supplementing nursery pig feed with seaweed extracts increases final body weight of pigs. *Austral Journal of Veterinary Sciences, 50*(2), 83–87. https://doi.org/10.4067/S0719-81322018000200083.

Saker, K.E., Allen, V.G., Fontenot, J.P., Bagley, C.P., Ivy, R.L., Evans, R.R. and Wester, D.B. 2001. Tasco-Forage: II. Monocyte immune cell response and performance of beef steers grazing tall fescue treated with a seaweed extract. *Journal of Animal Science, 79*(4), 1022–1031. https://doi.org/10.2527/2001.7941022x.

Saker, K.E., Fike, J.H., Veit, H. and Ward, D.L. 2004. Brown seaweed- (Tasco™) treated conserved forage enhances antioxidant status and immune function in heat-stressed wether lambs. *Journal of Animal Physiology and Animal Nutrition, 88*(3-4), 122–130. https://doi.org/10.1111/j.1439-0396.2003.00468. x.

Salehi, B., Sharifi-Rad, J., Seca, A.M.L., Pinto, D.C.G.A., Michalak, I., Trincone, A., Mishra, A.P., Nigam, M., Zam, W. and Martins, N. 2019. Current trends on seaweeds: Looking at chemical composition, phytopharmacology, and cosmetic applications. *Molecules, 24*(22), 4182. https://doi.org/10. 3390/molecules24224182.

Samir, N., Hsaine, L., El Kafhi, S., Khlifi, S. and Etahiri, S. 2019. Radical scavenging activity and phenolic contents of brown seaweeds harvested from the coast of Sidi Bouzid (El Jadida, Morocco). *International Journal of Pharmaceutical Sciences Review and Research, 54*(21), 116–122.

Senevirathne, M., Kim, S.H., Siriwardhana, N., Ha, J.H., Lee, K.W. and Jeon, Y.J. 2006. Antioxidant potential of *Ecklonia cava* on reactive oxygen species scavenging, metal chelating, reducing power, and lipid peroxidation inhibition. *Food Science and Technology International, 12*(1), 27–38. https://doi.org/10.1177/1082013206062422.

Sharifian, S., Shahbanpour, B., Taheri, A. and Kordjazi, M. 2019. Effects of different solvents on the phenolic compounds and antioxidant properties of brown seaweeds, *Nizimuddinia zanardinii* (Schiffner) P.C. Silva and *Padina australis* Hauck. *Journal of Aquatic Ecology*, *8*(4), 76-86. [In Persian]

Stengel, D.B., Connan, S. and Popper, Z.A. 2011. Algal chemodiversity and bioactivity: Sources of natural variability and implications for commercial application. *Biotechnology Advances, 29*(5), 483–501. https://doi.org/10.1016/j.biotechadv.2011.05.016.

Taga, M.S., Miller, E.E. and Pratt, D.E. 1984. Chia seeds as a source of natural lipid antioxidants. *Journal of the American Oil Chemists' Society, 61*(5), 928–931. https://doi.org/10.1007/BF02542169.

Trachootham, D., Lu, W., Ogasawara, M.A., Nilsa, R. D. V. and Huang, P. 2008. Redox regulation of cell survival. *Antioxidants*

and Redox Signaling, 10(8), 1343–1374. https://doi.org/10.1089/ars.2007.1957.

Vijayabaskar, P. and Shiyamala, V. 2012. Antioxidant properties of seaweed polyphenol from *Turbinaria ornata* (Turner) J. Agardh, 1848. *Asian Pacific Journal of Tropical Biomedicine, 2*(1), S90–S98. https://doi.org/10.1016/S2221-1691(12)60136-6.

Mahendran, S., Maheswari, P., Sasikala, V., Rubika, J.J. and Pandiarajan, J. 2021. In vitro antioxidant study of polyphenol from red seaweeds dichotomously branched *Gracilaria edulis* and robust sea moss *Hypnea valentiae*. *Toxicology Reports, 8*, 1404–1411. https://doi.org/10.1016/j.toxrep.2021.07.006.

Wakeel, A., Jan, S.A., Ullah, I., Shinwari, Z.K. and Xu, M. 2019. Solvent polarity mediates phytochemical yield and antioxidant capacity of *Isatis tinctoria*. *PeerJ, 7*, e7857. https://doi.org/10.7717/peerj.7857.

Wang, B.G. 2009. In vitro antioxidative activities of extract and semi-purified fractions of the marine red alga, *Rhodomela confervoides* (Rhodomelaceae). *Food Chemistry, 113*(4), 1101–1105. https://doi.org/10.1016/j. foodchem.2008.08.078.

Wells, M.L., Potin, P., Craigie, J.S., Raven, J.A., Merchant, S.S., Helliwell, K.E., Smith, A.G., Camire, M.E. and Brawley, S.H. 2017. Algae as nutritional and functional food sources: Revisiting our understanding. *Journal of Applied Phycology, 29*, 949–982. https://doi.org/10.1007/s10811-016-0974-5.

Yabuta, Y., Fujimura, H., Kwak, C.S., Enomoto, T. and Watanabe, F. 2010. Antioxidant activity of the phycoerythrobilin compound formed from a dried Korean purple laver (*Porphyra* sp.) during in vitro digestion. *Food Science and Technology Research, 16*(4), 347–352. https://doi.org/10.3136/fstr.16.347.

Zhong, B., Robinson, N.A., Warner, R.D., Barrow, C.J., Dunshea, F.R. and Suleria, H.A.R. 2020. LC-ESI-QTOF-MS/MS characterization of seaweed phenolics and their antioxidant potential., *Marine Drugs, 18*(6), 331. https://doi.org/10.3390/md18060331.

Potential Antibacterial Activity of Plant Compounds against Carbapenem-Resistant Bacteria

Maryam Behboudipour[1], Neda Soleimani[1*], Negar Azarpira[2]

Received: 2025-11-08 Accepted: 2026-01-10

Abstract

Antimicrobial resistance, especially in carbapenem-resistant Gram-negative bacteria, is a global and urgent threat to public health. Carbapenems, the last line of defense, are now being challenged by the spread of resistance mechanisms among bacteria, especially the production of carbapenemases. Infections caused by carbapenem-resistant Gram-negative bacilli are associated with higher mortality rates and much more severe outcomes than drug-susceptible infections due to the failure of conventional therapies. This growing crisis has led researchers to urgently search for alternative therapeutic strategies. In the meantime, plant compounds have shown significant potential in combating these bacteria due to their unique chemical diversity and multiple mechanisms of action. These compounds exert their antibacterial effects through mechanisms such as the induction of oxidative stress and cell membrane damage, direct inhibition of carbapenemase enzymes, inhibition of efflux pumps, and inhibition of biofilm formation. In addition, many of these plant metabolites have shown a synergistic effect in combination with carbapenem antibiotics, leading to a significant reduction in the minimum inhibitory concentration (MIC) of these antibiotics. Plant compounds are promising candidates for the development of new antimicrobial agents or therapeutic adjuvants against carbapenem-resistant bacteria because of their multi-target arsenal, favorable safety profile, and ability to create synergy with conventional antibiotics. However, a large proportion of the world's plant species remain unknown. Extensive research and the use of *in silico* techniques can be effective in the discovery and development of plant compounds with antimicrobial activity. Although there are challenges in the path to the clinical development of these compounds, research in this area opens a promising path to overcoming antimicrobial resistance.

Keywords: Antimicrobial resistance, Carbapenem, Carbapenemase, Herbal compounds, Synergy

Introduction

Antimicrobial resistance (AMR), often described as a "silent pandemic," is widely recognized as one of the most serious chal-

1-Department of Microbiology and Microbial Biotechnology, Faculty of Life Sciences and Biotechnology, Shahid Beheshti University, Tehran, Iran
2-Transplant Research Center, Shiraz University of Medical Sciences, Shiraz, Iran
*Corresponding Author email address: N_soleimani@sbu.ac.ir
Doi: 10.48308/pae.2026.242712.1132

lenges to global health. This crisis has extensive consequences, reaching beyond clinical medicine to affect other critical sectors such as agriculture, economics, and food security (Read and Woods, 2014, Tang et al., 2023, Rafeeq et al., 2025). The proliferation of multidrug-resistant (MDR) bacteria represents a central aspect of this global challenge. Leading health authorities, including the Centers for Disease Control and Prevention (CDC) and the World Health Organization (WHO), have classified AMR among the most critical threats to human health (Salam et al., 2023, Rafeeq et al., 2025). According to estimates in 2021, AMR directly caused 1.5 million deaths and was associated with 4.71 million other deaths (Collaborators, 2024). Projections show that this figure will increase by 2050, with direct deaths reaching 1.91 million and related deaths reaching 8.22 million (Collaborators, 2024, Cesaro et al., 2025). The main drivers of this multifaceted crisis include the overuse and misuse of antibiotics in human medicine and agriculture, their environmental release, inadequate infection control, and a weak pipeline for new antibiotics. These elements have collectively accelerated the spread of MDR bacteria, posing a serious global challenge (Mancuso et al., 2023, Rafeeq et al., 2025).

Among these, carbapenem-resistant bacteria, particularly Gram-negative ones, represent the most challenging cases to treat. This is very important because carbapenems have long been considered the "last line of defense" and the most reliable weapon against the most dangerous pathogens (Aurilio et al., 2022). Infections caused by carbapenemase-producing Gram-negative bacilli, due to the failure of conventional treatments, are associated with an alarming mortality rate and have far more severe outcomes than drug-sensitive infections (Hu et al., 2020, Shariati et al., 2024). Given the critical importance of this type of resistance, the WHO has placed carbapenem-resistant Gram-negative bacteria, including *Acinetobacter baumannii*, (Enterobacteriales) and *Pseudomonas aeruginosa* on its priority list of pathogens requiring urgent research and development of new antimicrobial treatments (Sati et al., 2025). This growing crisis has led researchers to urgently search for alternative therapeutic strategies. In this regard, approaches such as the use of natural compounds, bacteriophages, probiotics, monoclonal antibodies, and antimicrobial peptides have received attention (Dhanarani et al., 2017, Shariati et al., 2024). Among these options, plant compounds have emerged as very promising candidates. These compounds show tremendous potential due to their unique chemical diversity, multi-target mechanisms, and historical safety record in human consumption (Abdallah et al., 2023). The exploitation of plants is not only a leading scientific opportunity but also a socio-economic necessity in the global fight against antimicrobial resistance (Rafeeq et al., 2025). Accordingly, this review aimed to investigate the potential of plant-derived compounds as alternative solutions for the control of carbapenem-resistant bacteria.

Carbapenems and their importance in clinical settings

Carbapenems, along with *penicillins, cephalosporins* and monobactams, belong to the diverse and widely used family of β-Lactam

antibiotics (Figure 1). However, what distinguishes carbapenems is their unique chemical structure, which includes an unsaturated, sulfur-free beta-lactam ring. This structural feature gives them two major advantages: higher stability against β-lactamase enzymes and a much broader spectrum of activity (Tooke et al., 2019).

Well-known examples of this group include imipenem, meropenem, and ertapenem, and newer generations such as doripenem, biapenem, panipenem, razupenem, and tomopenem have also been developed (El-Gamal et al., 2017).

The mechanism of action of these drugs, similar to other beta-lactams, is through the inhibition of penicillin-binding proteins (PBPs) and the disruption of bacterial cell wall synthesis. Among these molecular targets, PBPs 1a, 1b, 2, and 3 serve as the primary sites of inhibition, with PBPs 2 and 3 being particularly specific to Gram-negative bacteria (Aurilio et al., 2022). Over the past decade, the use of carbapenems in clinical settings has increased dramatically, by 45%. This trend has been a response to the spread of strains producing extended-spectrum β-lactamases (ESBLs), as carbapenems serve as the last line of defense in the treatment of serious infections caused by resistant pathogens(Blair et al., 2015, Patrier and Timsit, 2020).

These drugs are used to treat several infections, including those of the lower respiratory tract, skin and soft tissue, urinary tract, central nervous system, abdomen, and pelvis. They are also used in managing complex conditions such as febrile neutropenia and complications arising from cystic fibrosis (Lo et al., 2008, Nguyen and Joshi, 2021).

Carbapenems possess a broad antibacterial spectrum and are primarily employed to treat infections caused by highly resistant Gram-negative bacteria, including members of the *Enterobacteriaceae* family and non-fermentative bacteria. They also demonstrated efficacy against certain drug-resistant Gram-positive bacteria (Au-

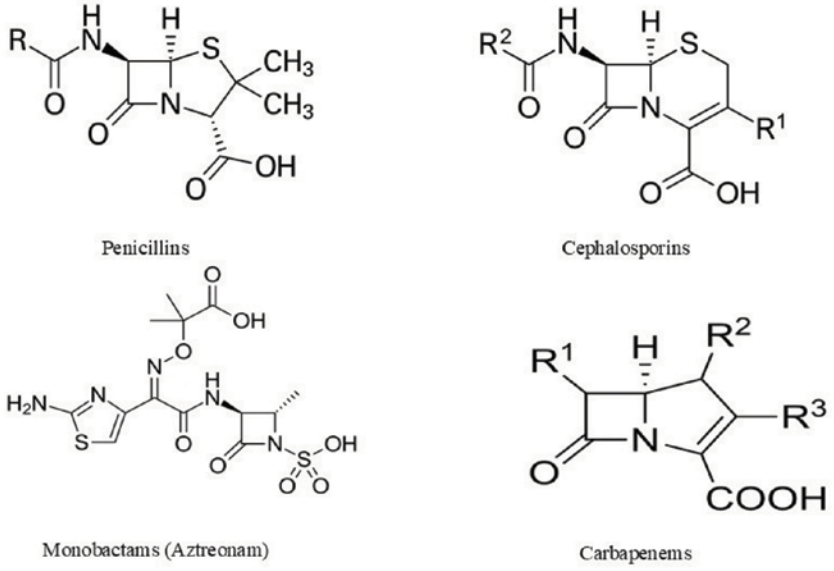

Fig. 1. Chemical structure of the main classes of β-lactam antibiotics (Terico and Gallagher, 2014, Lee et al., 2016)

rilio et al., 2022).

Furthermore, due to their more favorable safety profile and fewer side effects compared with other last-line agents such as polymyxins, carbapenems are regarded as one of the safest and most reliable classes of antibiotics in modern medicine (Meletis, 2016). However, their excessive and irrational use has led to resistance to carbapenems.

Carbapenem resistance and its underlying mechanisms

Carbapenem resistance has emerged as a critical and growing threat to global public health. Over the past decade, the global dissemination of carbapenem-resistant pathogens has reached alarming levels, particularly in certain European and Asian nations where the resistance rates have surpassed 50% (Hansen, 2021).

The magnitude of this threat is clearly illustrated by data from the United States, where an estimated 13.100 infections and 1.100 deaths were attributed to carbapenem-resistant pathogens in 2017 alone (Livorsi et al., 2018, Dong et al., 2020).

Patients with compromised immune systems, complex underlying diseases, or those using invasive medical devices such as indwelling catheters are among the groups at the highest risk for these infections (Martin et al., 2018).

This resistance is mediated through diverse molecular mechanisms, broadly categorized into enzymatic and non-enzymatic pathways. Non-enzymatic mechanisms include reduced permeability of the bacterial outer membrane (primarily through the loss or decreased expression of porins) and the activation of efflux pumps that expel the antibiotic from the cell (Tompkins and van Duin, 2021).

In contrast, the primary enzymatic mechanism involves the production of hydrolyzing enzymes called carbapenemases. These enzymes, which belong to a diverse family of β-lactamases, are capable of inactivating a wide range of antibiotics, including carbapenems, cephalosporins, penicillins, and monobactams, and are recognized as the key factor in the global spread of this resistance in Gram-negative bacteria (Suay-García and Pérez-Gracia, 2019, Tompkins and van Duin, 2021).

Currently, the link between specific resistance mechanisms and particular geographic regions is constantly evolving with extensive international travel and widespread exposure to healthcare systems (Bonomo et al., 2018).

Molecular classification of carbapenemases

Based on the Ambler classification system (Table 1), which relies on conserved and variable amino acid motifs in the protein structure, carbapenemases are categorized into three main classes: A, B, and D (Hammoudi Halat and Ayoub Moubareck, 2020, Sawa et al., 2020).

Class A carbapenemases are characterized by a serine residue at their active catalytic site. The genes encoding these enzymes can be chromosomal, plasmid-borne, or both (Aurilio et al., 2022). These carbapenemases hydrolyze a broad spectrum of β-lactam antibiotics, including carbapenems. The most clinically significant member, *Klebsiella pneumoniae* carbapenemase (KPC), has been identified worldwide, while Imipenem-hydrolyzing β-lactamase (IMI) and Guy-

ana extended-spectrum β-lactamase (GES) represent less common variants (Hammoudi Halat and Ayoub Moubareck, 2020, Mancuso et al., 2023). A key therapeutic feature is their susceptibility to conventional β-lactamase inhibitors such as clavulanate, sulbactam, tazobactam, and avibactam (Tehrani and Martin, 2018).

Class B carbapenemases, known as metallo-β-lactamases (MBLs), require a metal ion (Zn^{2+}) as a cofactor for nucleophilic attack on the β-lactam ring and demonstrate the highest carbapenem-hydrolyzing activity. A critical distinction from Class A enzymes (serine β-lactamases) is their resistance to conventional β-lactamase inhibitors. MBLs confer resistance to almost all β-lactam drugs, with the major exception being aztreonam (Hammoudi Halat and Ayoub Moubareck, 2020, Sawa et al., 2020, Ortega-Balleza et al., 2024). The most clinically prevalent MBLs include the Verona integron-encoded MBL (VIM), Imipenemase (IMP), and New Delhi MBL (NDM) (Hammoudi Halat and Ayoub Moubareck, 2020). The number of reported alleles for IMP and VIM carbapenemases is increasing at a remarkable rate, with more than 100 variants of IMP-like enzymes now identified in many parts of the world and in many Gram-negative species (Le Terrier et al., 2025). These figures indicate the continuous and dynamic spread of these resistance mechanisms (Sawa et al., 2020).

MBL genes are frequently located on mobile genetic elements, such as class 1 integrons, which facilitates their rapid dissemination among bacterial species (Aurilio et al., 2022, Behboudipour et al., 2025). While MBL enzymatic activity can be inhibited in laboratory settings by metal chelators (*e.g.*, EDTA) or specific compounds such as sodium mercaptoacetate, the toxicity of these agents prevents their clinical application (Doi and Paterson, 2015). There are current-

Table 1. Ambler classification of carbapenemases.

Class	Active site	Common enzymes	Gene Location	Substrate	Organism	Reference
A	Serine	KPC (*Klebsiella pneumoniae* carbapenemase) GES (Guiana extended spectrum)	Plasmid	Carbapenems Penicillins Cephalosporins Aztreonam		(Lee and Doi, 2014, Rabaan et al., 2022, Mó and da Silva, 2024)
B	Metal ion (zinc)	IMP (Imipenemase) VIM (Verona integron-encoded metallo-β-lactamase) NDM (New Delhi metallo-β-lactamase)	Plasmid	Most β-lactam antibiotics, except aztreonam	*Enterobacteriaceae* *P. aeruginosa* *A. baumannii*	
D	Serine	OXA (Oxacillin-hydrolyzing carbapenemases)	Plasmid	Oxacillin Third-generation cephalosporins Carbapenems		

ly no approved inhibitors for therapeutic use against MBLs. Given their importance, the development of new anti-MBL agents is a high priority (Ortega-Balleza et al., 2024).

Class D carbapenemases, known as oxacillinases, include OXA-type enzymes such as OXA-48, OXA-72, and OXA-244 (Mancuso et al., 2023). It should be noted, however, that oxacillin hydrolysis is not a universal characteristic of all class D enzymes, as the hundreds of known OXA variants exhibit substantial diversity in their substrate profiles (Bahr et al., 2021). OXA-48 and its variants are the most clinically significant Class D carbapenemases. These enzymes demonstrate hydrolytic capacity against various β-lactams, including carbapenems and third-generation cephalosporins (Pitout et al., 2019).They are resistant to classical β-lactamase inhibitors (Kyriakidis et al., 2021). These enzymes present significant diagnostic challenges as they often exhibit only low-level *in vitro* resistance to carbapenems. Nevertheless, their clinical impact remains substantial (Boyd et al., 2022).

Plants natural reservoirs of antimicrobial compounds

Plants have been an indispensable source of medicine for thousands of years. This role is so undeniable that today more than a quarter of modern drugs are either directly extracted from or inspired by natural compounds. This long history of use affirms their effectiveness and safety in human health (Khameneh et al., 2015, Rafeeq et al., 2025). Plants are estimated to account for a large proportion of the total biomass on Earth, accounting for ≈450 gigatonnes of carbon (Bar-On et al., 2018). Estimates indicate that there are between 250.000 and 500.000 species of angiosperms in the world. Interestingly, less than 10% of these plants are consumed as a food source by humans and other animals, and many of them also have medicinal uses (Cowan, 1999, Abdallah et al., 2023). Phytochemicals are a broad range of bioactive molecules of natural origin (Harvey et al., 2015). Some of these compounds are secondary metabolites of small organic compounds that, although not essential for the initial growth of the plant, play a vital role in its survival and reproduction (Muthamilarasan and Prasad, 2013). Because plants are stationary organisms and cannot escape threats, they have evolved a complex defense system based on these metabolites. This powerful chemical arsenal has enabled them to resist a variety of pathogens (such as viruses, bacteria, and fungi), predators, and adverse environmental conditions and to survive in diverse ecosystems (Mawalagedera et al., 2019, Álvarez-Martínez et al., 2020b). These valuable metabolites are scattered throughout the plant structure, from the roots and stems to the leaves, flowers, fruits, and seeds (Li et al., 2024). Secondary metabolites are extremely diverse in terms of their chemical structure, composition, solubility and biosynthetic pathways, and this characteristic has led to the creation of an amazing range of these compounds with specific defensive functions (Tiwari and Rana, 2015, Anjali et al., 2023).

It is estimated that approximately 200.000 plant secondary metabolites (PSM) have been identified and isolated. Any plant species is capable of producing a complex chem-

ical arsenal of 500–800 different secondary metabolites, many of which have antimicrobial properties. These compounds are mainly classified into four main groups: terpenes, phenols, and nitrogen- and sulfur-containing compounds (Figure 2) (Satish et al., 2020, Yadav et al., 2020, Yeshi et al., 2022, Lorca et al., 2024).

Studies have focused primarily on complex plant extracts (which have been studied the most), pure compounds, and essential oils (which rank fifth among the studied agents). Among the pure isolated compounds, terpenes are the most studied antimicrobial compounds, while polyphenols and alkaloids, and other categories, have also accounted for a significant portion of this research (Álvarez-Martínez et al., 2020a, Li et al., 2024). The recent increase in the number of scientific papers on the potentiation of antibiotic effects by plant agents confirms the importance of this area of research in the modern battle against antimicrobial resistance. According to reports, the global herbal medicine market was estimated to be worth $170 billion in 2022 and is expected to grow significantly to $600 billion by 2033 (Sarkar et al., 2024, Zouine et al., 2024). However, most plant species remain unknown, and plants serve as a promising and unexplored frontier for the discovery of new therapeutic agents against drug-resistant bacteria.

Herbal compounds effective against carbapenem-resistant bacteria (CRB)

Terpenes and terpenoids

Terpenes are the key constituents of essential oils. These compounds, which are among the most diverse plant secondary metabolites, are formed by connecting isoprene (C5) units. These compounds include the main classes of monoterpenes, sesquiterpenes, diterpenes, and triterpenes. From a chemical perspective, terpenes have a remarkable structural diversity, with prominent examples including linalool, geraniol, menthol, citral, thymol, carvacrol, carotenoid, cam-

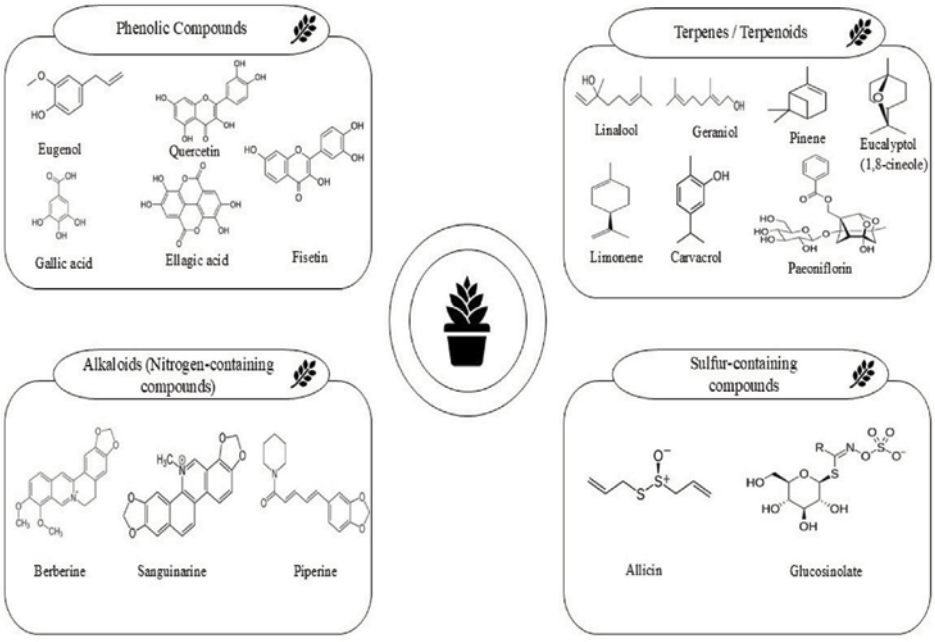

Fig. 2. Structure of plant secondary metabolites (Wang et al., 2019, Al-Khayri et al., 2023, Upadhyay et al., 2024, Sana et al., 2025).

phor, eucalyptol, cymene, pinene, and limonene (Guimarães et al., 2019).

Studies have shown that both the chemical structure and the kinetics of the antibacterial effect of these compounds differ from each other. On the one hand, the presence of polar functional groups such as hydroxyl in phenolic (such as thymol and carvacrol) and alcoholic (such as geraniol and terpineol) compounds is associated with stronger antimicrobial activity (Guimarães et al., 2019). On the other hand, compounds such as terpineol, geraniol, carotenol and citronellol are known as fast-acting agents that are able to inactivate bacteria such as *Escherichia coli* and *Salmonella* Typhimurium in a short time (Friedman et al., 2004, Guimarães et al., 2019).

Accordingly, screening terpenes and terpenoids based on the structure-activity relationship as well as the kinetics of their antibacterial effect can provide a valuable criterion for identifying promising candidates against carbapenem-resistant bacteria. *In vitro* evidence has shown that 1,8-cineole (CN) as a monoterpene exhibits significant bactericidal activity against carbapenemase-producing *Klebsiella pneumoniae* (KPC-KP) (Moo et al., 2021).

Similarly, paeoniflorin ($C_{23}H_{28}O_{11}$), a monoterpene bicyclic glycoside derived primarily from the roots of the peony plant (*Paeonia lactiflora*), has shown promising activity against carbapenem-resistant *K. pneumoniae* (CRKP) with a reported MIC of 1.2 mg/mL (Qian et al., 2020). Although paeoniflorin is traditionally known for its anti-inflammatory and neuroprotective properties in traditional medicine, recent research has revealed significant antimicrobial potential, indicating its effective antibacterial activity (Hou et al., 2025).

Phenolic compounds

Phenolic compounds (PCs) are key secondary metabolites in horticultural plants that contain one or more hydroxyl groups attached to aromatic rings. Structurally, they are classified into major groups such as simple phenols, flavonoids, stilbenes, and tannins. These compounds are not only responsible for the attractive colors and unique flavors of fruits and flowers but also play vital ecological roles (Rafeeq et al., 2025, Xu and Wang, 2025).

Notably, their biological significance also extends to good antimicrobial activity, showing promising potential against carbapenem-resistant bacteria. For example, tannic acid, epigallocatechin gallate, quercetin, and epicatechin have shown significant inhibitory effects on β-lactamases in both *in vitro* and *in silico* analyses (Mandal et al., 2017).

A prominent example is eugenol, a major phenolic compound found in the extracts of cloves (*Syzygium aromaticum*) and cinnamon, which exhibits broad-spectrum efficacy, including against carbapenem-resistant bacteria (Liu et al., 2023a).

According to Liu et al. (2023), eugenol exerted significant and dose-dependent inhibitory effects on planktonic CRKP bacteria. At a concentration of 0.5 mg/mL, the compound killed more than 85% of the bacterial population, and when the concentration was increased to 1.0 mg/mL, almost complete (100%) eradication of bacteria was observed (Liu et al., 2023a).

Quercetin is a common flavonoid of the fla-

vonol type in nature, which is of plant origin and is widely found in fruits (such as berries, apples and grapes), vegetables (especially the cabbage family), seeds, nuts and various flowers (Yang et al., 2020a). This compound has been studied as an effective agent in inhibiting carbapenem-resistant Gram-negative bacteria (Blair et al., 2014, Pal and Tripathi, 2020). Quercetin has also shown significant synergistic interactions with antibiotics such as colistin and amikacin against the resistant bacterium *A. baumannii in vitro* (Pal and Tripathi, 2020, Odabaş Köse et al., 2023).

Fisetin, which belongs to the flavonoid group, is a naturally occurring chemical compound in several fruits and vegetables, including strawberries, apples, and grapes. Its amount in plant foods varies from 2 to 160 μg/g. This compound is known as a health-promoting agent because of its antioxidant, anti-inflammatory, and anticancer properties and is even found in some dietary supplements (Kubina et al., 2021, Cordaro et al., 2022, Dong et al., 2025).

Interestingly, in one study, fisetin, with the lowest MIC (0.0625 mg/mL) among the compounds tested, showed significant antibacterial activity against CRKP (ATCC BAA-1705) (Adeosun et al., 2022).

A study on the bark extract of *Matayba opositifolia* showed specific efficacy against CRKP (MIC = 31.25–500 μg/mL) and *A. baumannii* (MIC = 125–250 μg/mL). GC-MS analysis identified several bioactive compounds in the extract, with palmitic acid, friedelan-3-one and 7-dehydrodiosgenin as the main components (de Jesús Dzul-Beh et al., 2023).

A study by Uc-Cachón et al. showed that *Schoepfia schreberi* extracts containing gallic acid (GA) and ellagic acid (EA) derivatives showed significant growth inhibition against carbapenem-resistant *A. baumannii* (CRAB). Furthermore, *S. schreberi* exhibits broad anti-infective properties against different *A. baumannii* strains by simultaneously targeting multiple pathogenic mechanisms, including biofilm formation, efflux pump activity, motility, and resistance to catalase-mediated oxidative stress(Uc-Cachón et al., 2024).

The pentagalloyl glucose (PGG) compound obtained from the *Schinus terebinthifolia* extract showed broad-spectrum antimicrobial activity against CRAB (MIC 64-256 μg/mL) and *P. aeruginosa* (MIC 16 μg/mL). Mechanistic studies showed that PGG acts through iron chelation and, remarkably, no resistant mutants emerged after 21 days of passage (Dettweiler et al., 2020).

Nowadays, molecular docking studies provide valuable insights into the mechanism of action of phenolic compounds. For example, a study on mangiferin revealed that this compound interacts with the NDM-1 enzyme through the formation of hydrogen bonds and hydrophobic interactions. Interestingly, the Glide docking score of mangiferin (-9.12 kcal/mol) was even negative than that of the antibiotic meropenem (-8.77 kcal/mol), indicating a more stable binding and higher potential for this plant compound to inhibit the NDM-1 enzyme. This finding makes mangiferin a promising candidate for inhibiting carbapenemases (Vasudevan et al., 2022).

Alkaloids compounds

Alkaloids are a large class of natural secondary metabolites characterized by a basic nitrogen atom in their structure. More than 18.000 distinct alkaloids have been identified from diverse sources(Gutiérrez-Grijalva et al., 2020, Heinrich et al., 2021, Thawabteh et al., 2021).

These compounds have attracted much attention due to their broad spectrum of pharmacological activities, including antibacterial, anticancer, antiviral, and central nervous system depressant effects. In particular, the antimicrobial potential of alkaloids has been promising in combating infections caused by multidrug-resistant (MDR) pathogens. Well-known alkaloids such as berberine, sanguinarine, and piperine have shown potent antibacterial activity against several microorganisms (Horani et al., 2015, Thawabteh et al., 2021, Plazas et al., 2022).

Mechanisms of action of plant compounds against CRB

Induction of oxidative stress and cell membrane damage

The induction of oxidative stress is one of the key mechanisms of plant compounds in combating resistant bacteria. A review by Itri et al. (2014) documented the role of this mechanism in the killing of bacteria. According to this study, oxidative stress leads to bacterial cell death by destroying the integrity of the plasma membrane and causing the leakage of intracellular contents (Itri et al., 2014).

Considerable evidence supports the role of this mechanism in the activity of various plant extracts and compounds. Proteomic analyses have shown that cinnamon bark essential oil (*Cinnamomum verum*) disrupts the membrane of KPC-KP by inducing oxidative stress, which is characterized by an increase in oxidative stress-regulating proteins such as glycyl radical cofactor, catalase peroxidase, and DNA mismatch repair protein. This oxidative attack damages the cell membrane, facilitates the penetration of reactive oxygen species (ROS), and disrupts the DNA and membrane repair systems (Yang et al., 2019).

Similarly, lavender essential oil (LVO) exerts its antibacterial effect against KPC-KP by increasing ROS levels, lipid peroxidation, and increasing membrane permeability, which not only causes content leakage but also enhances the uptake of other antimicrobial agents (Yang et al., 2020b).

In addition, certain phytochemicals have been identified as oxidative stress-inducing agents. Notable examples include eugenol, which significantly increases ROS and decreases glutathione (GSH) in CRKP, leading to membrane disruption and leakage of cytoplasmic components such as DNA, proteins, and β-galactosidase (Liu et al., 2023a).

Other compounds such as acetic acid, geranyl acetate, linalool, and various pyrrolidine derivatives are also capable of inducing oxidative stress, highlighting the broad applicability of this mechanism among diverse plant metabolites (Tafazoli and O'Brien P, 2004, Quintans-Júnior et al., 2013, Riera et al., 2015).

Carbapenemase inhibition

The search for antimicrobial compounds that are safe against carbapenemase-producing bacteria, especially NDM-1 strains, remains an ongoing priority. While some compounds from fungi have been investi-

gated for this purpose, the main source of drugs in the plant kingdom remains largely unexplored (King et al., 2014).

A comprehensive study by Chandar et al. (2017) screened ethanolic leaf extracts of 240 diverse medicinal plant species for antibacterial activity against NDM-1-producing *E. coli*. Extracts of six plants, including *Combretum albidum* and *Hibiscus acetosella Welw. ex Hiern*, showed significant antibacterial activity (MICs ranging from 2.56 to 5.12 mg/mL) and effectively inhibited NDM-1 enzyme activity in vitro. IC50 values ranged from 0.50 to 1.2 ng/μL. Phytochemical analysis of these extracts revealed a diverse profile of secondary metabolites with steroids and saponins being the least abundant. Interestingly, flavonoids and phenolic compounds were identified as the dominant metabolites in several extracts. A notable finding was that *Tamarindus indica* L. extract, despite showing a low MIC of 2.56 mg/ml, contained the lowest overall concentration of secondary metabolites. The inhibitory mechanism against NDM-1 is proposed to involve the direct inactivation of the enzyme or chelation of zinc ions essential for catalytic activity (Chandar et al., 2017).

In the direction of discovering natural adjuvants, quercetin acts as a potent dual inhibitor against carbapenem-resistant Gram-negative bacteria. Evidence suggests that quercetin (at a concentration of 64 μg/mL) significantly inhibits carbapenemase enzyme activity in the resistant strains of *E. coli*, *K. pneumoniae*, *P. aeruginosa*, and *A. baumannii*. The stability of quercetin-carbapenemase complexes was confirmed in molecular docking studies, and it was shown that this compound binds directly to the active site of carbapenem enzymes by a competitive mechanism and prevents the hydrolysis of the carbapenem antibiotic (meropenem) in the periplasmic space (Pal and Tripathi, 2020).

A recent study on coumarin showed that this compound significantly inhibited the activity of carbapenemase enzymes in CRKP. In addition, coumarin reduced the expression of the carbapenemase-encoding genes. Molecular docking revealed significant binding free energies ranging from -7.8757 to -6.2064 kcal/mol for coumarin binding to NDM1, VIM-2, OXA-48 and OXA-9 enzymes. These effects resulted in the restoration of the susceptibility of meropenem-resistant bacteria, with the coumarin-meropenem combination exhibiting a strong synergistic effect (fractional inhibitory concentration index (FICI) ≤ 0.5). These findings suggest that coumarin is a promising candidate for overcoming carbapenem resistance (Abdel-Halim et al., 2024).

In the study by Shi et al. (2019) baicalin was identified as a novel NDM-1 inhibitor, which showed effective inhibition of the enzyme with an IC50 of about 3.8 μM. Docking and molecular dynamics studies showed that the carboxyl group of baicalin directly interacts with the zinc ion (Zn^{2+}) in the active site of the enzyme, and hydrogen bonds with key amino acid residues stabilize the complex (Shi et al., 2019).

In the context of the discovery of natural carbapenem inhibitors, embelin has also been identified as a potent and selective inhibitor of the NDM-1 enzyme. A screening study

showed that embelin has a significant ability to inhibit the activity of the NDM-1 enzyme compared to other natural compounds, inhibiting it by more than 50%. Analyses confirmed its outstanding inhibitory potency with an IC50 value of 2.1 ± 0.2 μM and a Ki value of 0.19 ± 0.02 μM (using meropenem as a substrate). Interestingly, embelin had a weak effect on other carbapenemases such as VIM-1 and IMP-1, which makes its selectivity for NDM-1 outstanding. Molecular modeling studies indicate that this stability and selectivity are most likely due to an extensive van der Waals contact between NDM-1 and the embelin (Ning et al., 2018).

Efflux pump inhibition

Given that the active efflux of antibacterial agents plays an important role in the development of drug resistance in carbapenem-resistant bacteria, inhibition of the efflux pump has emerged as a promising strategy to restore antibacterial efficacy (Liu et al., 2023b). Plant-derived compounds can combat carbapenem-resistant bacteria through this mechanism. Studies have shown that some plant compounds such as α-terpinene, α-pinene, catechol and eugenol acetate fight antibiotic resistance by inhibiting the efflux pump (Prasch and Bucar, 2015, Limaverde et al., 2017).

Similarly, quercetin inhibited the activity of the AcrB efflux pump in enterobacterial strains overexpressing this pump (Pal and Tripathi, 2020).

Consistent with these findings, molecular docking studies have identified α-bisabolol as an inhibitor of the MexB efflux pump in *P. aeruginosa*. α-bisabolol showed a higher affinity for MexB than meropenem. The results of the determination of the MIC showed that the simultaneous application of α-bisabolol and meropenem significantly reduced the MIC by 6.24 μg/mL compared with the application of meropenem alone (12.5 μg/mL) in the resistant strains. These observations indicate the high potential of α-bisabolol in restoring the efficacy of antibiotics through efflux inhibition and providing an adjunct strategy for treating multidrug-resistant infections (Nanjan and Bose, 2025).

Furthermore, several studies have confirmed that ellagic acid (EA) functions as an efflux pump inhibitor, enhancing the in vitro efficacy of various antibiotics against resistant pathogens including *A. baumannii* and *E. coli* (Chusri et al., 2009, Jenic et al., 2021, Uc-Cachón et al., 2024).

Alkaloids can increase the effectiveness of common antibiotics through mechanisms such as the inhibition of efflux pumps and can thus be used as valuable supplements in antimicrobial treatment regimens (Sireesha et al., 2019, Faisal et al., 2023). A notable example of this mechanism is the synergistic effect between imipenem (IMP) and the herbal compound berberine against imipenem-resistant *P. aeruginosa*. Although berberine alone had relatively weak anti-pseudomonal activity (MIC = 512 μg/mL), it showed a strong synergistic effect when combined with IMP. Evidence suggests that the restoration of IMP susceptibility by berberine is likely due to the inhibition of the MexXY-OprM efflux pump. The results confirmed that the combination of berberine with IMP resulted in a significant reduction in the expression levels of the genes encoding MexZ, MexX, MexY, and OprM. Impor-

tantly, no significant change was observed in OprD mRNA expression in clinical isolates after treatment with berberine and/or imipenem (Su and Wang, 2018).

Another example involves piperine (PIP), which shows antibacterial activity against CRPA and targets the MexAB-OprM efflux pump. Molecular docking studies revealed a strong affinity of piperine for efflux pump proteins with a binding affinity of -9.1 kcal/mol. A synergistic effect between PIP and imipenem (IPM) against CRPA was observed. Importantly, PIP effectively inhibited IPM efflux by upregulating *mexR* gene expression and downregulating *mexA*, *mexB*, and *oprM*. In conclusion, PIP enhances the antibacterial activity of IPM by inhibiting the MexAB-OprM efflux pump (Liu et al., 2023b).

However, not all bioactive plant compounds act through this mechanism. Lavender essential oil, despite its strong antimicrobial effect, lacks efflux pump inhibitory activity, and analysis of its composition has not confirmed the presence of any known efflux pump inhibitors (Yang et al., 2020b).

Inhibition of biofilm formation

Plant-derived compounds have shown significant efficacy in disrupting biofilm formation and inactivating cells in the biofilms of carbapenem-resistant bacteria.

The importance of these findings is highlighted by the critical role of biofilms in the pathogenesis of CRKP, where biofilms act as a key factor that protects bacteria from antimicrobial agents and promotes microbial persistence and proliferation (Ernst et al., 2020).

Given that achieving effective antibiotic concentrations to eradicate biofilms in vivo is often impossible due to drug toxicity, the search for alternative therapeutic strategies is increasingly urgent. In this regard, the antibiofilm activity of plant compounds is considered a promising therapeutic alternative (Ciofu et al., 2015, Di Domenico et al., 2020).

For example, Adeosan et al. (2022) showed that phytol significantly altered the biofilm structure in CRKP strains and exhibited significant antibiofilm potential. Their findings showed that phytol and glycitein inhibited the pre-formed biofilm by 43.81% and 39.61%, respectively, against *K. pneumoniae* ATCC BAA-1705 (Adeosun et al., 2022). In a similar vein, another study reported that phytol at concentrations ranging from 5 to 640 μg/mL exhibited significant antibiofilm activity with a maximum of 60% biofilm inhibition against another biofilm-forming pathogen, *A. baumannii* (Ramanathan et al., 2018).

Taken together, these findings position phytol as a promising lead compound for managing carbapenem-resistant bacterial infections. Consequently, targeting biofilm formation with such natural compounds is a critical strategy for developing optimal therapeutic interventions in the future (Adeosun et al., 2022).

Similarly, paeoniflorin showed significant inhibitory effects on CRKP biofilm formation and effectively inactivated CRKP cells in the established biofilms (Qian et al., 2020).

Synergistic Strategies: Plant Compounds and Carbapenems

A promising strategy to restore the efficacy

of carbapenem antibiotics is to use them in combination with herbal adjuvants. There is a growing body of scientific evidence that combining herbal extracts with conventional antibiotics not only reduces the effective dose of antibiotics required but also significantly reduces the associated side effects. Such synergistic interactions are now considered a promising strategy to address the growing challenge of antimicrobial resistance (Stefanovic, 2018).

In support of this approach, Chandar et al. (2017) showed that the plant extracts studied by them, when combined with meropenem, reduced the MIC of this antibiotic by 4- to 16-fold against NDM-1-producing *E. coli*, producing a strong synergistic effect (ΣFIC = 0.313-0.09). The restoration of bacterial sensitivity to this antibiotic was attributed to the dual ability of the extracts to inhibit the NDM-1 enzyme and disrupt the bacterial cell membrane. This dramatic reduction in MIC highlights the great potential for reducing antibiotic doses in combination treatment regimens. However, it is worth noting that the antimicrobial activity in the crude extracts is usually the result of the combined effect of several substances, and the potency of individual components after isolation may be less than the overall effect of the extract (Chandar et al., 2017).

In this regard, another study also showed that the combination of LVO with meropenem has a strong synergistic effect, reducing the effective concentration of LVO and meropenem by 15-fold and 4-fold, respectively. This synergistic effect was confirmed by a FICI of 0.3125. Notably, the rapid killing kinetics of this combination resulted in the complete killing of KPC-KP bacteria in only 1.5 h. However, the use of each of these agents separately at similar concentrations did not affect the viability of KPC-KP cells. This strategy is a practical strategy to overcome bacterial resistance and reduce the dosage of last-line antibiotics (Yang et al., 2020b).

Research data also show that quercetin, fisetin, luteolin, and 3′,4′,7-trihydroxyflavone, by exerting a synergistic effect, restore the antibacterial activity of piperacillin and imipenem against OXA-48-producing *E. coli* and cause a 2- to 8-fold reduction in their MIC. Compared with previously reported inhibitors, quercetin and its analogs have significant advantages: they are inexpensive, readily available, and can be extracted and purified in large quantities from plant sources. Furthermore, they do not exhibit any cytotoxicity, increasing their potential as safe therapeutic adjuvants (Hytti et al., 2015, Hatahet et al., 2018, Zhang et al., 2022).

Similarly, the combination of embelin, a plant benzoquinone found in the fruits of *Embelia ribes* Burm (*E. ribes*) (Ali et al., 2024), with carbapenems also showed a potent synergistic effect against NDM-1-producing pathogens. Studies have shown that embelin effectively inhibits the activity of the NDM-1 enzyme, thereby restoring bacterial susceptibility to β-Lactam antibiotics. When embelin (at a concentration of 32 μg/mL) was combined with meropenem, a 512-fold reduction in the MIC of this antibiotic was observed against an NDM-1-producing strain (ATCC BAA-2146). This synergistic effect was confirmed with FIC values between 0.05 and 0.15 on various clinical iso-

lates (including *E. coli*, *K. pneumoniae* and *A. baumannii*), indicating a strong synergy. It is noteworthy that embelin alone lacked significant antibacterial activity, emphasizing its role as an "adjuvant" focused on inhibiting resistance, rather than as a standalone antimicrobial agent. Therefore, embelin can be considered a promising lead compound for the development of safer and more efficient adjuvants alongside carbapenems to combat these superbugs (Ning et al., 2018).

Conclusion

The growing crisis of antimicrobial resistance in the present era, especially with the emergence of carbapenem-resistant bacteria, has assumed alarming dimensions. This situation makes the urgent attention to finding inhibitors of resistance not only a priority but also an inevitable action. However, the pharmaceutical industry has gradually reduced its investment in this field due to economic challenges such as low financial returns, short antibiotic use periods and high R&D costs. This gap has made the focus on cost-effective strategies such as the use of natural plant compounds as pristine reservoirs of bioactive compounds more prominent than ever. With several advantages such as broad chemical diversity, multi-targeting of resistance mechanisms (including inhibition of carbapenemase enzymes), and favorable safety profile, these compounds have become promising candidates for the development of antimicrobial agents or adjuvants. Furthermore, their potential for synergy with antibiotics, including carbapenems, could lead to the restoration of the efficacy of these drugs, which in turn reduces the need for alternative antibiotics with more side effects, such as colistin.

Although there is a wealth of *in vitro* data on the efficacy of plant metabolites, translating these findings into commercial products faces obstacles, including the lack of large-scale clinical studies, bioavailability challenges, and the absence of clear regulatory frameworks. However, continued investigation of these compounds paves a promising path toward the discovery of new therapeutic agents against carbapenem-resistant bacteria

Finally, the present study only examined a small subset of the thousands of plant metabolites identified and their potential to combat carbapenem resistance. The potential effects of these compounds on other mechanisms involved in carbapenem resistance, such as porin proteins (*e.g*., OprD in *P. aeruginosa*) or additional efflux pumps, were not investigated. Future studies should therefore more broadly address these limitations, as well as research into clinical validation and formulation of plant metabolites to bridge the gap between laboratory discovery and therapeutic application.

Acknowledgments

The authors would like to thank the Microbiology Department of Shahid Beheshti University of Tehran and the Organ Transplant Research Center of Shiraz University of Medical Sciences. It should be noted that this research did not receive any specific financial support.

References

Abdallah, E:M., Alhatlani, B.Y., De Paula

Menezes, R. and Martins, C.H.G., 2023. Back to Nature: Medicinal Plants as Promising Sources for Antibacterial Drugs in the Post-Antibiotic Era. *Plants*, 12(17), p.3077. doi: 10.3390/plants12173077.

Abdel-Halim, M.S., El-Ganiny, A.M., Mansour, B., Yahya, G., Latif, H. and Askoura, M., 2024. Phenotypic, molecular, and in silico characterization of coumarin as carbapenemase inhibitor to fight carbapenem-resistant Klebsiella pneumoniae. *BMC Microbiology*, 24(1), p. 67. doi: 10.1186/s12866-024-03214-7.

Adeosun, I.J., Baloyi, I.T. and Cosa, S., 2022. Anti-Biofilm and Associated Anti-Virulence Activities of Selected Phytochemical Compounds against Klebsiella pneumoniae. *Plants*, 11(11), p.1429. doi: 10.3390/plants11111429.

Al-Khayri, J.M., Rashmi, R., Toppo, V., Chole, P.B., Banadka, A., Sudheer, W.N., Nagella, P., Shehata, W.F., Al-Mssallem, M.Q., Alessa, F.M., Almghasla, M.I. and Rezk, A.A., 2023. Plant Secondary Metabolites: The Weapons for Biotic Stress Management. *Metabolites*, 13(6), p.716. doi: 10.3390/metabo13060716.

Ali, A., Emad, N.A., Sultana, N., Ali, H., Jahan, S., Aqil, M., Mujeeb, M. and Sultana, Y., 2024. Medicinal potential of embelin and its nanoformulations: An update on the molecular mechanism and various applications. *Iranian Journal of Basic Medical Sciences*, 27(10), pp. 1228-1242. doi: 10.22038/ijbms.2024.77888.16850.

Álvarez-Martínez, F.J., Barrajón-Catalán, E., Encinar, J.A., Rodríguez-Díaz, J.C. and Micol, V., 2020a. Antimicrobial Capacity of Plant Polyphenols against Gram-positive Bacteria: A Comprehensive Review. Current Medicinal Chemistry, 27(15), pp. 2576-2606. doi: 10.2174/0929867325666181008115650.

Álvarez-Martínez, F.J., Barrajón-Catalán, E. and Micol, V., 2020b. Tackling Antibiotic Resistance with Compounds of Natural Origin: A Comprehensive Review. *Biomedicines*, 8(10), p.405. doi: 10.3390/biomedicines8100405.

Anjali, Kumar, S., Korra, T., Thakur, R., R, A., Kashyap, A., Nehela, Y., Chapligin, V., Minkina, T. and Keswani, C., 2023. Role of Plant Secondary Metabolites in Defence and Transcriptional Regulation in Response to Biotic Stress. *Plant Stress*, p.100154. doi: 10.1016/j.stress.2023.100154

Aurilio, C., Sansone, P., Barbarisi, M., Pota, V., Giaccari, L.G., Coppolino, F., Barbarisi, A., Passavanti, M.B. and Pace, M.C., 2022. Mechanisms of Action of Carbapenem Resistance. *Antibiotics (Basel)*, 11(3), p.421. doi: 10.3390/antibiotics11030421.

Bahr, G., González, L.J. and Vila, A.J., 2021. Metallo-β-lactamases in the Age of Multidrug Resistance: From Structure and Mechanism to Evolution, Dissemination, and Inhibitor Design. *Chemical Reviews*, 121(13), pp.7957-8094. doi: 10.1021/acs.chemrev.1c00138.

Bar-On, Y.M., Phillips, R. and Milo, R., 2018. The biomass distribution on Earth. *Proceedings of the National Academy of Sciences of the United States of America*, 115(25), pp.6506-6511. doi: 10.1073/

pnas.1711842115.

Behboudipour, M., Soleimani, N., Azarpira, N. and Soleimani, N., 2025. Prevalence of Antibiotic Resistance Determinants in Carbapenem-Resistant Pseudomonas aeruginosa: Focus on Class 1 and 2 Integrons and blaIMP Gene. *International journal of molecular and cellular medicine*, 14(3), p.886. doi: 10.22088/ijmcm.Bums.14.3.886.

Blair, J.M., Richmond, G.E. and Piddock, L.J., 2014. Multidrug efflux pumps in Gram-negative bacteria and their role in antibiotic resistance. *Future Microbiology*, 9(10), pp.1165-1177. doi: 10.2217/fmb.14.66.

Blair, J.M., Webber, M.A., Baylay, A.J., Ogbolu, D.O. and Piddock, L.J., 2015. Molecular mechanisms of antibiotic resistance. *Nature Reviews Microbiology*, 13(1), pp.42-51. doi: 10.1038/nrmicro3380.

Bonomo, R.A., Burd, E.M., Conly, J., Limbago, B.M., Poirel, L., Segre, J.A. and Westblade, L.F., 2018. Carbapenemase-Producing Organisms: A Global Scourge. *Clinical Infectious Diseases*, 66 (8), pp.1290-1297. doi: 10.1093/cid/cix893.

Boyd, S.E., Holmes, A., Peck, R., Livermore, D.M. and Hope, W., 2022. OXA-48-Like β-Lactamases: Global Epidemiology, Treatment Options, and Development Pipeline. *Antimicrobial Agents and Chemotherapy*, 66(8), p.e0021622. doi: 10.1128/aac.00216-22.

Cesaro, A., Hoffman, S.C., Das, P. and De La Fuente-Nunez, C., 2025. Challenges and applications of artificial intelligence in infectious diseases and antimicrobial resistance. *NPJ Antimicrobials and Resistance*, 3(1), p.2. doi: 10.1038/s44259-024-00068-x.

Chandar, B., Poovitha, S., Ilango, K., Mohankumar, R. and Parani, M., 2017. Inhibition of New Delhi Metallo-β-Lactamase 1 (NDM-1) Producing Escherichia coli IR-6 by Selected Plant Extracts and Their Synergistic Actions with Antibiotics. *Frontiers in Microbiology*, 8, p.1580. doi: 10.3389/fmicb.2017.01580.

Chusri, S., Villanueva, I., Voravuthikunchai, S.P. and Davies, J., 2009. Enhancing antibiotic activity: a strategy to control Acinetobacter infections. *Journal of Antimicrobial Chemotherapy*, 64(6), pp.1203-1211. doi: 10.1093/jac/dkp381.

Ciofu, O., Tolker-Nielsen, T., Jensen, P., Wang, H. and Høiby, N., 2015. Antimicrobial resistance, respiratory tract infections and role of biofilms in lung infections in cystic fibrosis patients. *Advanced Drug Delivery Reviews*, 85, pp.7-23. doi: 10.1016/j.addr.2014.11.017.

Collaborators, A.R., 2024. Global burden of bacterial antimicrobial resistance 1990-2021: a systematic analysis with forecasts to 2050. *The Lancet*, 404(10459), pp.1199-1226. doi: 10.1016/S0140-6736(24)01867-1.

Cordaro, M., D'Amico, R., Fusco, R., Peritore, A.F., Genovese, T., Interdonato, L., Franco, G., Arangia, A., Gugliandolo, E., Crupi, R., Siracusa, R., Di Paola, R., Cuzzocrea, S. and Impellizzeri, D., 2022. Discovering the Effects of Fisetin on NF-κB/NLRP-3/NRF-2 Molecular Pathways

in a Mouse Model of Vascular Dementia Induced by Repeated Bilateral Carotid Occlusion. *Biomedicines*, 10(6), p.1448. doi: 10.3390/biomedicines10061448.

Cowan, M.M., 1999. Plant products as antimicrobial agents. *Clinical Microbiology Reviews*, 12 (4), p.p564-82. doi: 10.1128/CMR.12.4.564.

De Jesús Dzul-Beh, A., Uc-Cachón, A.H., González-Sánchez, A.A., Dzib-Baak, H.E., Ortiz-Andrade, R., Barrios-García, H.B., Jiménez-Delgadillo, B. and Molina-Salinas, G.M., 2023. Antimicrobial potential of the Mayan medicine plant Matayba oppositifolia (A. Rich.) Britton against antibiotic-resistant priority pathogens. *Journal of Ethnopharmacology*, 300, p.115738. doi: 10.1016/j.jep.2022.115738.

Dettweiler, M., Marquez, L., Lin, M., Sweeney-Jones, A., Chhetri, B., Zurawski, D., Kubanek, J. and Quave, C., 2020. Pentagalloyl glucose from Schinus terebinthifolia inhibits growth of carbapenem-resistant Acinetobacter baumannii. *Scientific Reports*, 10, p.15340. doi:10.1038/s41598-020-72331-w.

Dhanarani, S., Congeevaram, S., Piruthiviraj, P., Park, J.H. and Kaliannan, T., 2017. Inhibitory effects of reserpine against efflux pump activity of antibiotic resistance bacteria. *Chemical Biology Letters*, 4(2), p.69-72.

Di Domenico, E.G., Cavallo, I., Sivori, F., Marchesi, F., Prignano, G., Pimpinelli, F., Sperduti, I., Pelagalli, L., Di Salvo, F., Celesti, I., Paluzzi, S., Pronesti, C., Koudriavtseva, T., Ascenzioni, F., Toma, L., De Luca, A., Mengarelli, A. and Ensoli, F., 2020. Biofilm Production by Carbapenem-Resistant Klebsiella pneumoniae Significantly Increases the Risk of Death in Oncological Patients. *Frontiers in Cellular and Infection Microbiology*, 10, p.561741. doi:10.3389/fcimb.2020.561741.

Doi, Y. and Paterson, D.L., 2015. Carbapenemase-producing Enterobacteriaceae. *Seminars in Respiratory and Critical Care Medicine*, 36(1), pp.74-84. doi: 10.1055/s-0035-1544208.

Dong, J., Ma, X., Li, S., Zhou, S., Yang, Q. and Ai, X., 2025. Transcriptomic Analysis Reveals the Inhibitory Mechanism of Fisetin Against the Pathogenicity of Aeromonas hydrophila. *Animals*, 15, p.2415. doi:10.3390/ani15162415.

Dong, L.T., Espinoza, H.V. and Espinoza, J.L., 2020. Emerging superbugs: The threat of Carbapenem Resistant Enterobacteriaceae. *AIMS Microbiology*, 6(3), pp.176-182. doi: 10.3934/microbiol.2020012.

El-Gamal, M.I., Brahim, I., Hisham, N., Aladdin, R., Mohammed, H. and Bahaaeldin, A., 2017. Recent updates of carbapenem antibiotics. *European Journal of Medicinal Chemistry*, 131, pp.185-195. doi: 10.1016/j.ejmech.2017.03.022.

Ernst, C.M., Braxton, J.R., Rodriguez-Osorio, C.A., Zagieboylo, A.P., Li, L., Pironti, A., Manson, A.L., Nair, A.V., Benson, M., Cummins, K., Clatworthy, A.E., Earl, A.M., Cosimi, L.A. and Hung, D.T., 2020. Adaptive evolution of

virulence and persistence in carbapenem-resistant Klebsiella pneumoniae. *Nature Medicine*, 26(5), pp.705-711. doi: 10.1038/s41591-020-0825-4.

Faisal, S., Badshah, S.L., Kubra, B., Emwas, A.H. and Jaremko, M., 2023. Alkaloids as potential antivirals. A comprehensive review. *Natural Products and Bioprospecting*, 13(1), p.4. doi: 10.1007/s13659-022-00366-9.

Friedman, M., Henika, P.R., Levin, C.E. and Mandrell, R.E., 2004. Antibacterial activities of plant essential oils and their components against Escherichia coli O157:H7 and Salmonella enterica in apple juice. *Journal of Agricultural and Food Chemistry*, 52(19), pp.6042-6048. doi: 10.1021/jf0495340.

Guimarães, A.C., Meireles, L.M., Lemos, M.F., Guimarães, M.C.C., Endringer, D.C., Fronza, M. and Scherer, R., 2019. Antibacterial Activity of Terpenes and Terpenoids Present in Essential Oils. *Molecules*, 24(13), p.2471. doi: 10.3390/molecules24132471.

Gutiérrez-Grijalva, E., Lopez-Martinez, L., Contreras, L., Romero, C.A. and Heredia, J.B., 2020. Plant Alkaloids: Structures and Bioactive Properties. *Plant-derived Bioactives*, pp 85–117. doi: 10.1007/978-981-15-2361-8_5.

Hammoudi Halat, D. and Ayoub Moubareck, C., 2020. The Current Burden of Carbapenemases: Review of Significant Properties and Dissemination among Gram-Negative Bacteria. *Antibiotics*, 9(4), p.186. doi: 10.3390/antibiotics9040186.

Hansen, G.T., 2021. Continuous Evolution: Perspective on the Epidemiology of Carbapenemase Resistance Among Enterobacterales and Other Gram-Negative Bacteria. *Infectious Diseases and Therapy*, 10(1), pp.75-92. doi: 10.1007/s40121-020-00395-2.

Harvey, A.L., Edrada-Ebel, R. and Quinn, R.J., 2015. The re-emergence of natural products for drug discovery in the genomics era. *Nature Reviews Drug Discovery*, 14(2), pp.111-129. doi: 10.1038/nrd4510.

Hatahet, T., Morille, M., Hommoss, A., Devoisselle, J.M., Müller, R.H. and Bégu, S., 2018. Liposomes, lipid nanocapsules and smartCrystals®: A comparative study for an effective quercetin delivery to the skin. *International Journal of Pharmaceutics*, 542 (1-2), pp.176-185. doi: 10.1016/j.ijpharm.2018.03.019.

Heinrich, M., Mah, J. and Amirkia, V., 2021. Alkaloids Used as Medicines: Structural Phytochemistry Meets Biodiversity-An Update and Forward Look. *Molecules*, 26 (7):1836. doi: 10.3390/molecules26071836.

Horani, W., Thawabteh, A., Scrano, L., Bufo, S., Mecca, G. and Karaman, R., 2015. Anticancer prodrugs - three decades of design. *World Journal of Pharmacy and Pharmaceutical Sciences*, 4, pp.1751-1779. doi: 10.20959/wjpps20157-4678.

Hou, Y., Li, H., Zhu, L., Quan, T., Feng, X., Li, Y., Bian, Y. and Wei, Y., 2025. Advances of paeoniflorin in depression: the molecular mechanism and formula application. *Frontiers in Pharmacology*, 16, p.1614429. doi: 10.3389/fphar.2025.1614429.

Hu, W., Li, M., Lu, W., Guo, S. and Li, J., 2020. Evaluation of MASTDISCS combi Carba plus for the identification of metallo-β-lactamases, KPC and OXA-48 carbapenemase genes in Enterobacteriaceae clinical isolates. *Letters in Applied Microbiology*, 70(1), pp.42-47. doi: 10.1111/lam.13240.

Hytti, M., Piippo, N., Korhonen, E., Honkakoski, P., Kaarniranta, K. and Kauppinen, A., 2015. Fisetin and luteolin protect human retinal pigment epithelial cells from oxidative stress-induced cell death and regulate inflammation. *Scientific Reports*, 5, p.17645. doi: 10.1038/srep17645.

Itri, R., Junqueira, H.C., Mertins, O. and Baptista, M.S., 2014. Membrane changes under oxidative stress: the impact of oxidized lipids. *Biophysical Reviews*, 6(1), pp.47-61. doi: 10.1007/s12551-013-0128-9.

Jenic, D., Waller, H., Collins, H. and Erridge, C., 2021. Reversal of Tetracycline Resistance by Cepharanthine, Cinchonidine, Ellagic Acid and Propyl Gallate in a Multi-drug Resistant Escherichia coli. *Natural Products and Bioprospecting*, 11(3), pp.345-355. doi: 10.1007/s13659-020-00280-y.

Khameneh, B., Iranshahy, M., Ghandadi, M., Ghoochi Atashbeyk, D., Fazly Bazzaz, B.S. and Iranshahi, M., 2015. Investigation of the antibacterial activity and efflux pump inhibitory effect of co-loaded piperine and gentamicin nanoliposomes in methicillin-resistant Staphylococcus aureus. *Drug Development and Industrial Pharmacy*, 41(6), pp.989-994. doi: 10.3109/03639045.2014.920025.

King, A.M., Reid-Yu, S.A., Wang, W., King, D.T., De Pascale, G., Strynadka, N.C., Walsh, T.R., Coombes, B.K. and Wright, G.D., 2014. Aspergillomarasmine A overcomes metallo-β-lactamase antibiotic resistance. *Nature*, 510(7506), pp.503-506. doi: 10.1038/nature13445.

Kubina, R., Iriti, M. and Kabała-Dzik, A., 2021. Anticancer Potential of Selected Flavonols: Fisetin, Kaempferol, and Quercetin on Head and Neck Cancers. *Nutrients*, 13(3). doi: 10.3390/nu13030845.

Kyriakidis, I., Vasileiou, E., Pana, Z.D. and Tragiannidis, A., 2021. Acinetobacter baumannii Antibiotic Resistance Mechanisms. *Pathogens*, 10(3): p.373. doi: 10.3390/pathogens10030373.

Le Terrier, C., Drusin, S.I., Nordmann, P., Pitout, J., Peirano, G., Vila, A.J., Moreno, D.M. and Poirel, L., 2025. The emerging concern of IMP variants being resistant to the only IMP-type metallo-β-lactamase inhibitor, xeruborbactam. *Antimicrobial Agents and Chemotherapy*, 69(7), p.e0029725. doi: 10.1128/aac.00297-25.

Lee, C.-S. and Doi, Y., 2014. Therapy of Infections due to Carbapenem-Resistant Gram-Negative Pathogens. *Infection and Chemotherapy*, 46, pp.149-164. doi: 10.3947/ic.2014.46.3.149.

Lee, D., Das, S., Dawson, N., Dobrijev, D., Ward, J. and Orengo, C., 2016. Novel Computational Protocols for Functionally Classifying and Characterising Serine Beta-Lactamases. *PLoS Computational Biology*, 12, p.e1004926. doi: 10.1371/journal.pcbi.1004926.

Li, S., Jiang, S., Jia, W., Guo, T., Wang, F., Li, J. and Yao, Z., 2024. Natural antimicrobials from plants: Recent advances and future prospects. *Food Chemistry*, 432, p.137231. doi: 10.1016/j.foodchem.2023.137231.

Limaverde, P.W., Campina, F.F., Da Cunha, F.A.B., Crispim, F.D., Figueredo, F.G., Lima, L.F., Datiane De, M.O.-T.C., De Matos, Y., Morais-Braga, M.F.B., Menezes, I.R.A., Balbino, V.Q., Coutinho, H.D.M., Siqueira-Júnior, J.P., Almeida, J. and Tintino, S.R., 2017. Inhibition of the TetK efflux-pump by the essential oil of Chenopodium ambrosioides L. and α-terpinene against Staphylococcus aureus IS-58. *Food and Chemical Toxicology*, 109 (Pt 2), pp.957-961. doi: 10.1016/j.fct.2017.02.031.

Liu, W., Chen, G., Dou, K., Yi, B., Wang, D., Zhou, Q. and Sun, Y., 2023a. Eugenol eliminates carbapenem-resistant Klebsiella pneumoniae via reactive oxygen species mechanism. *Frontiers in Microbiology*, 14, p.1090787. doi: 10.3389/fmicb.2023.1090787.

Liu, Y., Zhu, R., Liu, X., Li, D., Guo, M., Fei, B., Ren, Y., You, X. and Li, Y., 2023b. Effect of piperine on the inhibitory potential of MexAB-OprM efflux pump and imipenem resistance in carbapenem-resistant Pseudomonas aeruginosa. *Microbial Pathogenesis*, 185, p.106397. doi: 10.1016/j.micpath.2023.106397.

Livorsi, D.J., Chorazy, M.L., Schweizer, M.L., Balkenende, E.C., Blevins, A.E., Nair, R., Samore, M.H., Nelson, R.E., Khader, K. and Perencevich, E.N., 2018. A systematic review of the epidemiology of carbapenem-resistant Enterobacteriaceae in the United States. *Antimicrobial Resistance and Infection Control*, 7, p. 55. doi: 10.1186/s13756-018-0346-9.

Lo, T.S., Welch, J.M., Alonto, A.M. and Vicaldo-Alonto, E.A., 2008. A review of the carbapenems in clinical use and clinical trials. *Recent Patents on Anti-Infective Drug Discovery*, 3(2), pp. 123-131. doi: 10.2174/157489108784746588.

Lorca, G., Ballestero, D., Langa, E. and Pino-Otín, M.R., 2024. Enhancing Antibiotic Efficacy with Natural Compounds: Synergistic Activity of Tannic Acid and Nerol with Commercial Antibiotics against Pathogenic Bacteria. *Plants*, 13(19), p.2717. doi: 10.3390/plants13192717.

Mancuso, G., De Gaetano, S., Midiri, A., Zummo, S. and Biondo, C., 2023. The Challenge of Overcoming Antibiotic Resistance in Carbapenem-Resistant Gram-Negative Bacteria: "Attack on Titan". *Microorganisms*, 11(8), p.1912. doi: 10.3390/microorganisms11081912.

Mandal, S.M., Dias, R.O. and Franco, O.L., 2017. Phenolic Compounds in Antimicrobial Therapy. *Journal of Medicinal Food*, 20(10), pp.1031-1038. doi: 10.1089/jmf.2017.0017.

Martin, A., Fahrbach, K., Zhao, Q. and Lodise, T., 2018. Association Between Carbapenem Resistance and Mortality Among Adult, Hospitalized Patients With Serious Infections Due to Enterobacteriaceae: Results of a Systematic Literature Review and Meta-analysis. *Open Forum Infectious*

Diseases, 5(7), p.ofy150. doi: 10.1093/ofid/ofy150.

Mawalagedera, S.M.U.P., Callahan, D.L., Gaskett, A.C., Rønsted, N. and Symonds, M.R.E., 2019. Combining Evolutionary Inference and Metabolomics to Identify Plants With Medicinal Potential. *Frontiers in Ecology and Evolution*, 7. doi: 10.3389/fevo.2019.00267.

Meletis, G., 2016. Carbapenem resistance: overview of the problem and future perspectives. *Therapeutic Advances in Infectious Disease*, 3(1), pp.15-21. doi: 10.1177/2049936115621709.

Mó, I. and Da Silva, G.J., 2024. Tackling Carbapenem Resistance and the Imperative for One Health Strategies-Insights from the Portuguese Perspective. *Antibiotics*, 13(6), p. 557. doi: 10.3390/antibiotics13060557.

Moo, C.L., Osman, M.A., Yang, S.K., Yap, W.S., Ismail, S., Lim, S.H., Chong, C.M. and Lai, K.S., 2021. Antimicrobial activity and mode of action of 1,8-cineol against carbapenemase-producing Klebsiella pneumoniae. *Scientific Reports*, 11(1), p.20824. doi: 10.1038/s41598-021-00249-y.

Muthamilarsan, M. and Prasad, M., 2013. Plant innate immunity: an updated insight into defense mechanism. *Journal of Biosciences*, 38(2), pp.433-449. doi: 10.1007/s12038-013-9302-2.

Nanjam, P. and Bose, B., 2025. In silico Screening of Plant Compounds to Inhibit MexB Efflux Protein for the Enhancement of Meropenem Resistance against Pseudomonas aeruginosa MDR Infections. *Recent Advances in Anti-Infective Drug Discovery*, 20. doi: 10.2174/0127724344343717250404114236.

Nguyen, M. and Joshi, S.G., 2021. Carbapenem resistance in Acinetobacter baumannii, and their importance in hospital-acquired infections: a scientific review. *Journal of Applied Microbiology*, 131(6), pp.2715-2738. doi: 10.1111/jam.15130.

Ning, N.Z., Liu, X., Chen, F., Zhou, P., Hu, L., Huang, J., Li, Z., Huang, J., Li, T. and Wang, H., 2018. Embelin Restores Carbapenem Efficacy against NDM-1-Positive Pathogens. *Frontiers in Microbiology*, 9, p.71. doi: 10.3389/fmicb.2018.00071.

Odabaş Köse, E., Koyuncu Özyurt, Ö., Bilmen, S., Er, H., Kilit, C. and Aydemir, E., 2023. Quercetin: Synergistic Interaction with Antibiotics against Colistin-Resistant Acinetobacter baumannii. *Antibiotics*, 12(4). p.739. doi: 10.3390/antibiotics12040739.

Ortega-Balleza, J.L., Vázquez-Jiménez, L.K., Ortiz-Pérez, E., Avalos-Navarro, G., Paz-González, A.D., Lara-Ramírez, E.E. and Rivera, G., 2024. Current Strategy for Targeting Metallo-β-Lactamase with Metal-Ion-Binding Inhibitors. *Molecules*, 29(16), p.3944. doi: 10.3390/molecules29163944.

Pal, A. and Tripathi, A., 2020. Quercetin inhibits carbapenemase and efflux pump activities among carbapenem-resistant Gram-negative bacteria. *APMIS*, 128(3) , pp.251-259. doi: 10.1111/apm.13015.

Patrier, J. and Timsit, J.F., 2020. Carbapenem use in critically ill patients. *Current Opinion in Infectious*

Diseases, 33(1), pp.86-91. doi: 10.1097/QCO.0000000000000622.

Pitout, J.D.D., Peirano, G., Kock, M.M., Strydom, K.A. and Matsumura, Y., 2019. The Global Ascendency of OXA-48-Type Carbapenemases. *Clinical Microbiology Reviews*, 33(1), e00102-19. doi: 10.1128/CMR.00102-19.

Plazas, E., Avila, M.M., Muñoz, D.R. and Cuca, S.L., 2022. Natural isoquinoline alkaloids: Pharmacological features and multi-target potential for complex diseases. *Pharmacological Research*, 177, p.106126. doi: 10.1016/j.phrs.2022.106126.

Prasch, S. and Bucar, F., 2015. Plant derived inhibitors of bacterial efflux pumps: an update. *Phytochemistry Reviews*, 14, pp.961-974. doi: 10.1007/s11101-015-9436-y.

Qian, W., Zhang, J., Wang, W., Wang, T., Liu, M., Yang, M., Sun, Z., Li, X. and Li, Y., 2020. Antimicrobial and antibiofilm activities of paeoniflorin against carbapenem-resistant Klebsiella pneumoniae. *Journal of Applied Microbiology*, 128(2), pp.401-413. doi: 10.1111/jam.14480.

Quintans-Júnior, L., Moreira, J.C., Pasquali, M.A., Rabie, S.M., Pires, A.S., Schröder, R., Rabelo, T.K., Santos, J.P., Lima, P.S., Cavalcanti, S.C., Araújo, A.A., Quintans, J.S. and Gelain, D.P., 2013. Antinociceptive Activity and Redox Profile of the Monoterpenes (+)-Camphene, p-Cymene, and Geranyl Acetate in Experimental Models. *ISRN Toxicology*, 2013, p.459530. doi: 10.1155/2013/459530.

Rabaán, A.A., Eljaaly, K., Alhumaid, S., Albayat, H., Al-Adsani, W., Sabour, A.A., Alshiekheid, M.A., Al-Jishi, J.M., Khamis, F., Alwarthan, S., Alhajri, M., Alfaraj, A.H., Tombuloglu, H., Garout, M., Alabdullah, D.M., Mohammed, E.A., Yami, F.S.A., Almuthareb, H.A., Livias, K.A., Mutair, A.A., Almushrif, S.A., Abusalah, M.A.H.A. and Ahmed, N., 2022. An Overview on Phenotypic and Genotypic Characterisation of Carbapenem-Resistant Enterobacterales. *Medicina*, 58(11), p. 1675. doi:10.3390/medicina58111675.

Rafeeq, A., Arshad, S., Sajjad, M., Shahzad, M., Qadir, M., Safdar, Z. and Majid, B., 2025. Potential of Plant-Derived Phytochemicals in Combating Antimicrobial Resistance: A Comprehensive Review. *Journal of Health, Wellness and Community Research,* 3(14), e762. doi: 10.61919/ff2cs629.

Ramanathan, S., Arunachalam, K., Chandran, S., Selvaraj, R., Shunmugiah, K.P. and Arumugam, V.R., 2018. Biofilm inhibitory efficiency of phytol in combination with cefotaxime against nosocomial pathogen Acinetobacter baumannii. *Journal of Applied Microbiology*, 125(1), pp.56-71. doi: 10.1111/jam.13741.

Read, A.F. and Woods, R.J., 2014. Antibiotic resistance management. *Evolution, Medicine, and Public Health*, 2014(1), pp.147-147. doi: 10.1093/emph/eou024.

Riera, H., Afonso, V., Collin, P. and Lomri, A., 2015. A Central Role for JNK/AP-1 Pathway in the Pro-Oxidant

Effect of Pyrrolidine Dithiocarbamate through Superoxide Dismutase 1 Gene Repression and Reactive Oxygen Species Generation in Hematopoietic Human Cancer Cell Line U937. *PLoS One*, 10(5), p.e0127571. doi: 10.1371/journal.pone.0127571.

Salam, M.A., Al-Amin, M.Y., Salam, M.T., Pawar, J.S., Akhter, N., Rabaán, A.A. and Alqumber, M.A.A., 2023. Antimicrobial Resistance: A Growing Serious Threat for Global Public Health. *Healthcare*, 11(13), p.1946. doi: 10.3390/healthcare11131946.

Sana, Aftab, T., Naeem, M., Jha, P.K. and Prasad, P.V.V., 2025. Production of secondary metabolites under challenging environments: understanding functions and mechanisms of signalling molecules. *Frontiers in Plant Science*, 16, p.1569014. doi: 10.3389/fpls.2025.1569014.

Sarkar, P., Ahnaf, T., Rouf, R., Shilpi, J. and Uddin, S., 2024. A Review on Bioactive Phytochemical Constituents and Pharmacological Activities of Aegiceras corniculatum: A Pharmaceutically Important Mangrove Plant. *Journal of Chemistry*, 2024, pp.1-19. doi: 10.1155/2024/9992568.

Sati, H., Carrara, E., Savoldi, A., Hansen, P., Garlasco, J., Campagnaro, E., Boccia, S., Castillo-Polo, J.A., Magrini, E., Garcia-Vello, P., Wool, E., Gigante, V., Duffy, E., Cassini, A., Huttner, B., Pardo, P.R., Naghavi, M., Mirzayev, F., Zignol, M., Cameron, A. and Tacconelli, E., 2025. The WHO Bacterial Priority Pathogens List 2024: a prioritisation study to guide research, development, and public health strategies against antimicrobial resistance. *The Lancet Infectious Diseases*, 25(9), pp.1033-1043. doi: 10.1016/S1473-3099(25)00118-5.

Satish, L., Shamil, S., Yolcu, S., Gunamalai, L., Hemasundar, A. and Swamy, M., 2020. Biosynthesis of Secondary Metabolites in Plants as Influenced by Different Factors. *Plant-derived Bioactives*, pp 61–100. doi:10.1007/978-981-15-1761-7_3

Sawa, T., Kooguchi, K. and Moriyama, K., 2020. Molecular diversity of extended-spectrum β-lactamases and carbapenemases, and antimicrobial resistance. *Journal of Intensive Care*, 8, p.13. doi: 10.1186/s40560-020-0429-6.

Shariati, A., Kashi, M., Chegini, Z. and Hosseini, S.M., 2024. Antibiotics-free compounds for managing carbapenem-resistant bacteria; a narrative review. *Frontiers in Pharmacology*, 15, p.1467086. doi: 10.3389/fphar.2024.1467086.

Shi, C., Bao, J., Sun, Y., Kang, X., Lao, X. and Zheng, H., 2019. Discovery of Baicalin as NDM-1 inhibitor: Virtual screening, biological evaluation and molecular simulation. *Bioorganic Chemistry*, 88, p.102953. doi: 10.1016/j.bioorg.2019.102953.

Sireesha, B., Venkateswara Reddy, B., Basha, S.K., Chandra, K. and Anasuya, D., 2019. A Review on Pharmacological Activities of Alkaloids. *World Journal of Current Medical and Pharmaceutical Research*, 01, pp.230-234. doi:10.37022/WJCMPR.2019.01068.

Stefanovic, O., 2018. Synergistic Activity

of Antibiotics and Bioactive Plant Extracts: A Study Against Gram-Positive and Gram-Negative Bacteria. *Bacterial Pathogenesis and Antibacterial Control.* InTech. Available at: http://dx.doi.org/10.5772/intechopen.72026. doi: 10.5772/intechopen.72026.

Su, F. and Wang, J., 2018. Berberine inhibits the MexXY-OprM efflux pump to reverse imipenem resistance in a clinical carbapenem-resistant Pseudomonas aeruginosa isolate in a planktonic state. *Experimental and Therapeutic Medicine*, 15(1), pp.467-472. doi: 10.3892/etm.2017.5431.

Suay-García, B. and Pérez-Gracia, M.T., 2019. Present and Future of Carbapenem-resistant Enterobacteriaceae (CRE) Infections. *Antibiotics*, 8(3), p.122. doi: 10.3390/antibiotics8030122.

Tafazoli, S. and O'Brien P, J., 2004. Prooxidant activity and cytotoxic effects of indole-3-acetic acid derivative radicals. *Chemical Research in Toxicology*, 17(10), pp.1350-1355. doi: 10.1021/tx034217t.

Tang, K.W.K., Millar, B.C. and Moore, J.E., 2023. Antimicrobial Resistance (AMR). *British Journal of Biomedical Science*, 80, p.11387. doi: 10.3389/bjbs.2023.11387.

Tehrani, K. and Martin, N.I., 2018. β-lactam/β-lactamase inhibitor combinations: an update. *MedChemComm*, 9(9), pp.1439-1456. doi: 10.1039/c8md00342d.

Terico, A. and Gallagher, J., 2014. Beta-Lactam Hypersensitivity and Cross-Reactivity. *Journal of Pharmacy Practice*, 27. doi:10.1177/0897190014546109.

Thawabteh, A.M., Thawabteh, A., Lelario, F., Bufo, S.A. and Scrano, L., 2021. Classification, Toxicity and Bioactivity of Natural Diterpenoid Alkaloids. *Molecules*, 26(13). doi: 10.3390/molecules26134103.

Tiwari, R. and Rana, C., 2015. Plant secondary metabolites: a review. *International Journal of Engineering Research and General Science*, 3, pp.661-670.

Tompkins, K. and Van Duin, D., 2021. Treatment for carbapenem-resistant Enterobacterales infections: recent advances and future directions. *European Journal of Clinical Microbiology & Infectious Diseases*, 40(10), pp.2053-2068. doi: 10.1007/s10096-021-04296-1.

Tooke, C.L., Hinchliffe, P., Bragginton, E.C., Colenso, C.K., Hirvonen, V.H.A., Takebayashi, Y. and Spencer, J., 2019. β-Lactamases and β-Lactamase Inhibitors in the 21st Century. *Journal of Molecular Biology*, 431(18), pp.3472-3500. doi: 10.1016/j.jmb.2019.04.002.

Uc-Cachón, A.H., Dzul-Beh, A., González-Cortázar, M., Zamilpa-Álvarez, A. and Molina-Salinas, G.M., 2024. Investigating the anti-growth, anti-resistance, and anti-virulence activities of Schoepfia schreberi J.F.Gmel. against the superbug Acinetobacter baumannii. *Heliyon*, 10 (10), p.e31420. doi: 10.1016/j.heliyon.2024.e31420.

Upadhyay, R., Saini, R., Shukla, P. and Tiwari, K., 2024. Role of secondary metabolites in plant defense mechanisms: a molecular and biotechnological insights. *Phytochemistry Reviews*, 24, pp.953-983. doi: 10.1007/s11101-024-

09976-2.

Vasudevan, A., Kesavan, D.K., Wu, L., Su, Z., Wang, S., Ramasamy, M.K., Hopper, W. and Xu, H., 2022. In Silico and In Vitro Screening of Natural Compounds as Broad-Spectrum β-Lactamase Inhibitors against Acinetobacter baumannii New Delhi Metallo-β-lactamase-1 (NDM-1). *BioMed Research International*, 2022, p.4230788. doi: 10.1155/2022/4230788.

Wang, S., Alseekh, S., Fernie, A.R. and Luo, J., 2019. The Structure and Function of Major Plant Metabolite Modifications. *Molecular Plant*, 12(7), pp.899-919. doi: 10.1016/j.molp.2019.06.001.

Xu, L. and Wang, X., 2025. A Comprehensive Review of Phenolic Compounds in Horticultural Plants. *International Journal of Molecular Sciences*, 26(12), p. 5767. doi: 10.3390/ijms26125767.

Yadav, V., Wang, Z., Wei, C., Amo, A., Ahmed, B., Yang, X. and Zhang, X., 2020. Phenylpropanoid Pathway Engineering: An Emerging Approach towards Plant Defense. *Pathogens*, 9(4), p. 312. doi: 10.3390/pathogens9040312.

Yang, D., Wang, T., Long, M. and Li, P., 2020a. Quercetin: Its Main Pharmacological Activity and Potential Application in Clinical Medicine. *Oxidative Medicine and Cellular Longevity*, 2020, p.8825387. doi: 10.1155/2020/8825387.

Yang, S.-K., Yusoff, K., Thomas, W., Akseer, R., Alhosani, M.S., Abushelaibi, A., Lim, S.-H.-E. and Lai, K.-S., 2020b. Lavender essential oil induces oxidative stress which modifies the bacterial membrane permeability of carbapenemase producing Klebsiella pneumoniae. *Scientific Reports*, 10(1), p.819. doi:10.1038/s41598-019-55601-0.

Yang, S.K., Yusoff, K., Ajat, M., Thomas, W., Abushelaibi, A., Akseer, R., Lim, E. and Koksong, L., 2019. Disruption of KPC-producing Klebsiella pneumoniae membrane via induction of oxidative stress by cinnamon bark (Cinnamomum verum J. Presl) essential oil. *PLOS ONE*, 14, p.e0214326. doi: 10.1371/journal.pone.0214326.

Yeshi, K., Crayn, D., Ritmejerytė, E. and Wangchuk, P., 2022. Plant Secondary Metabolites Produced in Response to Abiotic Stresses Has Potential Application in Pharmaceutical Product Development. *Molecules*, 27(1), p. 313. doi: 10.3390/molecules27010313.

Zhang, Y., Chen, C., Cheng, B., Gao, L., Qin, C., Zhang, L., Zhang, X., Wang, J. and Wan, Y., 2022. Discovery of Quercetin and Its Analogs as Potent OXA-48 Beta-Lactamase Inhibitors. *Frontiers in Pharmacology*, 13, p.926104. doi: 10.3389/fphar.2022.926104.

Zouine, N., El Ghachtouli, N., El Abed, S. and Saad, I., 2024. A comprehensive review on medicinal plant extracts as antibacterial agents: Factors, mechanism insights and future prospects. *Scientific African*, 26, p.e02395. doi: 10.1016/j.sciaf.2024.e02395.